INFRARED ABSORPTION IN HEATED AIR FROM VIBRATION–ROTATION BANDS OF NITRIC OXIDE

by

D. R. Churchill and S. A. Hagstrom

2-12-64-2 November 1964

Contract No. Nonr 3368 (00) NR 087-133

Lockheed Missiles & Space Company
A Group Division of Lockheed Aircraft Corporation
Sunnyvale, California

FOREWORD

This research was supported by the Office of Naval Research under Contract No. Nonr 3368(00). The work described in this report was performed by members of the Physical Sciences Laboratory of Lockheed Missiles & Space Company at Palo Alto, California, under the direction of Dr. D. H. Holland. The authors wish to acknowledge the valuable suggestions given by Dr. Holland and thank Mrs. C. Chase for her assistance in processing the data.

ABSTRACT

The contribution to the spectral absorption coefficient of heated air arising from the vibration-rotation bands of nitric oxide has been calculated with the aid of the SACHA digital computer programs. These band systems were theoretically reconstructed on a line-by-line basis using experimentally determined constants whenever these were available. A magnetic tape spectral atlas containing the reconstructed spectra was then employed by another computer program to calculate the average transmission of infrared radiation through a slab of heated NO whose occupation numbers were chosen to conform to the appropriate air case. Several parameters were varied in the calculation including the line half-width. Results of the calculations are contained in the form of graphs and tables. Computations were made for temperatures from 1000°K–5000°K and for densities of normal atmospheric to 10^{-4} normal. Frequencies covered were between 1200 cm^{-1} and 10,000 cm^{-1} (λ = 1 μ–8.3 μ).

BLANK PAGE

CONTENTS

ILLUSTRATIONS

TABLES

1. INTRODUCTION

The spectral absorption coefficient of heated air includes, at temperatures of a few thousand degrees, contributions arising both from electronic transitions and from vibration-rotation transitions in diatomic molecules. It is well known [see, for example, Armstrong, Sokoloff, Nicholls, Holland, and Meyerott (Ref. 1, page 159)] that for air heated from 1000°K–3000°K, vibration-rotation transitions in the ground electronic state of nitric oxide (NO) form a major contribution to the absorption coefficient. Since these transitions occur in the frequency region which corresponds to that for which the Planck function is near its maximum at those temperatures, they must be considered as an important emission mechanism.

There have been previous calculations on this band system (Refs. 2–4), frequently referred to as the NO infrared system, but these have utilized simplified models. This report presents the results of recent calculations which have been based on a line by line model where the spectrum has been reconstructed, with the exception of some fine structure, for those lines which will contribute appreciably to the results.

Other band systems which are important in heated air have been treated in a similar fashion and are summarized in other reports (Refs. 5 and 6). For any necessary background information in molecular spectra, the reader is referred to Herzberg (Ref. 7) or to one of the reports (Refs. 5 and 6) mentioned above.

Section 2 and Section 3 discuss the theoretical reconstruction of the line frequencies and intensities for the NO vibration-rotation bands. Section 4 is a brief description of the line atlas for digital computer use. A discussion of an average transmission is given in Section 5. The appropriate line width problem is discussed in Section 6. Since the definition of useful average absorption coefficients arises from basic radiative transfer theory, this is discussed in Section 7. Digital computer results are presented in the form of graphs and tables; these are discussed in Sections 5, 7, and 8.

2. VIBRATION-ROTATION FREQUENCIES OF THE $^2\Pi$ STATE OF NO

The ground electronic state of the NO molecule is a $^2\Pi$ state belonging to a coupling case intermediate between Hund's cases a and b. Actually the coupling more nearly approximates case a, even for fairly large rotational quantum numbers J, since the coupling constant has a relatively large value ($A \sim 124.2\ cm^{-1}$). Two electronic substates arise because of the interaction of the electronic spin with the internal magnetic field of the molecule. These substates are labeled $^2\Pi_{1/2}$ and $^2\Pi_{3/2}$; no transitions occur between them because of spin orthogonality.

A general formula for the term values of a $^2\Pi$ state with coupling intermediate between Hund's cases a and b is given by Hill and Van Vleck (Ref. 8):

$$T_n(v,J) = T_e + G_n(v) + B_v\left[\left(J+\tfrac{1}{2}\right)^2 - 1 + (-1)^n\,\mu(J)\right] - D_v\cdot\begin{cases} J^4 & (n=1) \\ (J+1)^4 & (n=2) \end{cases} \qquad (1)$$

where

$$\mu(J) = \sqrt{\left(J+\tfrac{1}{2}\right)^2 - Y_v + \frac{Y_v^2}{4}} \quad \text{and} \quad Y_v = \frac{A}{B_v}$$

Here v and J are the vibrational and rotational quantum numbers, B_v and D_v are the rotational constants, A is the coupling constant, $G_n(v)$ is the vibrational term, and T_e is the electronic term.* n takes the value 1 for the $^2\Pi_{1/2}$ substate and the value 2 for the $^2\Pi_{3/2}$ substate.

*The word "term" is used to denote an energy expressed in "wave numbers," i.e., cm^{-1}.

A line arising from a transition from the lower vibration-rotation level (v'', J'') to an upper level (v', J') has a frequency in cm^{-1} given by

$$\nu^{(n)} = T_n(v', J') - T_n(v'', J'') \qquad n=1,2 \tag{2}$$

Adopting the notation $F_n(v, J)$ for that part of $T_n(v, J)$ arising from rotation, that is

$$F_n(v, J) = B_v \left[\left(J + \frac{1}{2} \right)^2 - 1 + (-1)^n \mu(J) \right] - D_v \cdot \begin{cases} J^4 & n=1 \\ (J+1)^4 & n=2 \end{cases} \tag{3}$$

the formulas for the R, P, and Q branches are

$$\left.\begin{aligned} \nu_n^R &= \nu^{(n)}_{v', v''} + F_n(v', J''+1) - F_n(v'', J'') \\ \nu_n^Q &= \nu^{(n)}_{v', v''} + F_n(v', J'') - F_n(v'', J'') \\ \nu_n^P &= \nu^{(n)}_{v', v''} + F_n(v', J''-1) - F_n(v'', J'') \end{aligned}\right\} n=1,2 \tag{4}$$

where

$$\nu^{(n)}_{v', v''} = G_n(v') - G_n(v'') \tag{5}$$

Since the intensity of the Q branch falls off as J^{-1} we neglect those lines in our calculation. The values for B_v, D_v, $G_1(v)$, and $G_2(v)$ which were used to compute the spectral line frequencies are given in Table 1.

Table 1

NO MOLECULAR CONSTANTS

State	v	$B_v (cm^{-1})$	$D_v (cm^{-1})$	Y_v	$G_1(v) (cm^{-1})$	$G_2(v) (cm^{-1})$
$X^2\Pi$	0	1.6957	5×10^{-6}	73.24	948.52	948.34
	1	1.6779	5×10^{-6}	74.02	2,824.61	2,824.08
	2	1.6601	5×10^{-6}	74.81	4,672.74	4,671.86
	3	1.6423	5×10^{-6}	75.62	6,492.92	6,491.70
	4	1.6245	5×10^{-6}	76.46	8,285.13	8,283.56
	5	1.6067	5×10^{-6}	77.30	10,049.37	10,047.44
	6	1.5889	5×10^{-6}	78.16	11,785.63	11,783.35
	7	1.5711	5×10^{-6}	79.05	13,493.91	13,491.28
	8	1.5533	5×10^{-6}	79.95	15,174.18	15,171.20
	9	1.5355	5×10^{-6}	80.88	16,926.46	16,823.13
	10	1.5177	5×10^{-6}	81.83	18,450.73	18,447.06
	11	1.4999	5×10^{-6}	82.80	20,047.00	20,042.82
	12	1.4821	5×10^{-6}	83.80	21,615.13	21,610.53
	13	1.4643	5×10^{-6}	84.81	23,154.94	23,149.82
	14	1.4465	5×10^{-6}	85.86	24,666.29	24,660.64
	15	1.4287	5×10^{-6}	86.93	26,148.95	26,142.79
	16	1.4109	5×10^{-6}	88.02	27,602.67	27,595.91

3. SPECTRAL ABSORPTION

The line absorption coefficient for a transition from a lower level (v'', J'') to an upper level (v', J') is given by

$$\mu(\nu) = N_{v'', J''} B_{v'', v', J'', J'} h\nu_{v'', v', J'', J'} F(\nu) \tag{6}$$

where

$\nu_{v'', v', J'', J'}$ is the Bohr frequency of the line in cm^{-1}

$N_{v'', J''}$ is the particle density in the lower level

$B_{v'', v', J'', J'}$ is the Einstein coefficient for absorption

and $F(\nu)$ is a line shape factor such that

$$\int F(\nu)\, d\nu = 1$$

The Einstein coefficient is given by

$$B_{v'', v', J'', J'} = \frac{8\pi^3}{3h^2 c} \frac{\sum_{M'', M'} \left| R^{M'', M'} \right|^2}{2J'' + 1} \tag{7}$$

where

$$R^{M'', M'} = \int \bar{\psi}''_{v'', J'', M''} \vec{R}\, \psi'_{v', J', M'}\, d\tau \tag{8}$$

is the matrix element of the electric moment operator $\vec{R} = \vec{R}_e + \vec{R}_{nuc.}$ of the electrons and nuclei. M'' and M' are azimuthal quantum numbers labeling the spatially degenerate components of the lower and upper rotational states. Assuming the Born-Oppenheimer approximation to be valid we write the wave function

$$\psi = \psi_e \psi_v \psi_r \tag{9}$$

as a product of electronic, vibrational, and rotational wave functions. With this approximation the expression for the matrix element becomes

$$\begin{aligned} R^{M'', M'} &= \int \overline{(\psi_e'' \psi_v'' \psi_r'')} \, \vec{R} \, (\psi_e' \psi_v' \psi_r') \, d\tau \\ &= \int \overline{(\psi_v'' \psi_r'')} \left[\int \psi_e'' \vec{R} \psi_e' \, d\tau_e \right] (\psi_v' \psi_r') \, d\tau_{vr} \\ &= \int \overline{(\psi_v'' \psi_r'')} \, \vec{p} \, (\psi_v' \psi_r') \, d\tau_{vr} \end{aligned} \tag{10}$$

where $\vec{p} = \int \bar{\psi}_e'' \vec{R} \psi_e' \, d\tau_e$ is the electric dipole transition moment with respect to some fixed external coordinate system.

The sum in Eq. (7) may be expressed in the form [c.f., Penner (Ref. 9, p. 129)]

$$\sum_{M'', M'} \left| R^{M'', M'} \right|^2 = (v''|p|v')^2 \, S_{J'', J'} \tag{11}$$

where $p = p(r)$, r being the coordinate along the internuclear axis. $S_{J'', J'}$ is the Hönl-London factor, which contains all the angular dependence. These factors are available in the literature for many types of transitions.

Numerical values of the matrix elements $(v''|p|v')$ must in general be obtained with the aid of experiment, since the electronic wave functions necessary for the determination of p are either not available or are not sufficiently accurate. The usual

method is to expand the dipole moment as a series expansion in the dimensionless change in internuclear distance, i.e.,

$$p(\xi) = p_o + p_1\xi + p_2\xi^2 \tag{12}$$

where

$$\xi = \frac{r - r_o}{r_o}$$

and p_o, p_1, and p_2 are constants.

For a single line the integrated absorption is obtained from Eq. (6):

$$\int_{\text{line}} \mu(\nu)\, d\nu = N_{v'', J''}\, B_{v'', v', J'', J'}\, h\nu_{v'', v', J'', J'} \tag{13}$$

since the line shape factor integrates to unity. Summing over all lines contained in a band (v', v'') and substituting from Eqs. (7) and (11) we obtain*

$$\int_{\text{band}} \mu(\nu)\, d\nu = \frac{8\pi^3}{3hc} \sum_{J''} \sum_{J'} N_{v'', J''}\, \nu_{v'', v', J'', J'}\, (v''|p|v')^2\, \frac{S_{J'', J'}}{2J'' + 1} \tag{14}$$

Assuming an average band frequency $\nu_{v'', v'} = \nu_{v'', v', o, o}$ and utilizing the rotational sum rule $\sum_{J'} S_{J'', J'} = 2J'' + 1$,

$$\int_{\text{band}} \mu(\nu)\, d\nu = \frac{8\pi^3}{3hc}\, \nu_{v'', v'}\, N_{v''}(v''|p|v')^2 \tag{15}$$

---

*In the semiempirical determination of the dipole moment expansion coefficients, the gas sample is assumed to be optically thin.

where $N_{v''} = \sum_{J''} N_{v'',J''}$ is the total population of the v'' level. Taking the expansion (12), the above expression now becomes

$$\int_{\substack{v'',v' \\ \text{band}}} \mu(\nu)\,d\nu = \frac{8\pi^3}{3hc}\,\nu_{v'',v'}\,N_{v''}\left[\int \bar{\psi}''_{v''}\left(p_o + p_1\,\xi + p_2\,\xi^2\right)\psi'_{v'}\,d\tau_v\right]^2 \qquad (16)$$

or

$$\int_{v'',v'} \mu(\nu)\,d\nu = \frac{8\pi^3}{3hc}\,\nu_{v'',v'}\,N_{v''}\left[p_1\int \bar{\psi}''_{v''}\,\xi\,\psi'_{v'}\,d\tau_v + p_2\int \bar{\psi}''_{v''}\,\xi^2\,\psi'_{v'}\,d\tau_v\right]^2 \qquad (17)$$

since the term in p_o drops out due to orthogonality of the vibrational wave functions. Equation 17 may now be used in conjunction with integrated absorption measurements for the fundamental and first overtone bands, giving rise to two equations in two unknowns (p_1 and p_2) provided the requisite wave functions are available for the evaluation of the integrals. To first approximation one might use a single measurement on the fundamental coupled with the use of harmonic oscillator wave functions to evaluate p_1, since the integral in ξ^2 vanishes for those functions. Since we wish to obtain values for some of the overtones, however, this approximation would not be applicable.

Having introduced the electrical anharmonicity through a Taylor expansion of the dipole p, the usual procedure for evaluation of the integrals in (17) is to introduce the mechanical anharmonicity through an expansion of the potential function which is contained in the Schrödinger equation. Perturbed harmonic oscillator wave functions are obtained which are then used to evaluate the integrals.

Following this procedure, Crawford and Dinsmore[10] obtained expressions for p_1 and p_2 in terms of the potential expansion coefficients and the integrated absorption coefficients.

These expressions were in turn used by Breene and Todd[11], who used the potential of Lippincott[12-13] and the integrated absorption measurements of Penner and Weber[14] to calculate the vibrational matrix elements $(v'' \,|p|\, v')$ for the NO vibration-rotation bands for $0 \leq v' \leq 15$, $0 \leq v'' \leq 14$.

A later experiment by Schurin and Clough[15] on the fundamental of this system has yielded a higher value for the integrated absorption coefficient (111 cm^{-1}/cm-atmosphere as compared to 70 obtained by Weber and Penner). Schurin and Clough did not measure the first overtone.

In our calculation, we have used the matrix elements calculated by Breene and Todd uniformly scaled up by $(111/70)^{1/2}$. These are presented in Table 2.

For the X (ground) electronic state of NO, the particle density in the lower level is given by

$$N_{v'',J''} = \frac{N_x (2J'' + 1) \exp(-E_{v'',J''}/kT)}{Q_{vib\text{-}rot}} \tag{18}$$

where N_x is the total particle density for the $x^2\Pi$ state, $E_{v'',J''}$ is the energy of the level referred to the $E_{o,o}$ level, and $Q_{vib\text{-}rot}$ is the vibration-rotation partition function:

$$Q_{vib\text{-}rot} = \sum_{v=o}^{\infty} \exp\left(\frac{-G_o(v)\,hc}{kT}\right) Q_{rot}^{(v)} \tag{19}$$

where

$$Q_{rot}^{(v)} = \int_o^{\infty} (2J + 1) \exp\left(\frac{-F_v(J)\,hc}{kT}\right) dJ \cong \frac{kT}{hc\,B_v} \tag{20}$$

In place of (19) and (20) we have thus far employed an approximate formula which was developed by Bethe[16] and later corrected by Brinkley[17]:

$$Q_{\text{vib-rot}} = \frac{1}{1 - \exp\left(\frac{-1.4388\,\omega_o}{T}\right)} \frac{T}{1.4388\,B_o}\,(1 + \gamma T) \qquad (21)$$

where ω_o and B_o are the vibrational and rotational constants of the $v = 0$ vibrational level and γ is Bethe's correction factor for anharmonicity and non-rigidity. With the appropriate constants inserted for the NO ground state (21) becomes

$$Q_{\text{vib-rot}} = \frac{0.4098\,T(1 + 0.0000119\,T)}{1 - \exp(-2719/T)} \qquad (22)$$

To distinguish between $\Pi_{1/2} - \Pi_{1/2}$ and $\Pi_{3/2} - \Pi_{3/2}$ transitions we again use $n(=1,2)$ as a superscript. If we also let P_x be the fractional population of the $x^2\Pi$ state, we can rewrite equation (6) in the form

$$\mu(\nu) = \left[\frac{N_{\text{Total}}(\text{NO})\,P_x}{L_o\,Q_{\text{vib-rot}}}\right] H^{(n)}_{v'',v',J'',J'} \exp\left(\frac{-E^{(n)}_{v'',J''}}{T}\right) \pi\,F(\nu) \qquad (23)$$

where

$$H^{(n)}_{v'',v',J'',J'} = \frac{4\pi^2 L_o}{3hc}\,\nu^{(n)}_{v'',v',J'',J'}\,(v''|p|v')^2\,S_{J'',J'} \qquad (24)$$

$$E^{(n)}_{v'',J''} = \left(G_o(v'') + F_{v''}(J'')\right)\frac{hc}{k}\quad ,$$

and $L_o = 2.6875 \times 10^{19}$ particles/cm^3 is Loschmidts number. Notice that H and E are characteristics of the isolated molecule, i.e. do not depend on the temperature and density. Since the bracketed term in (23) is dimensionless, H has dimensions cm^{-2}, and $F(\nu)$ has dimensions cm^{-1}, μ has the required dimension cm^{-1}

Although Eq. (23) is valid for arbitrary form factor $F(\nu)$, in our calculations we have assumed a Lorentz line shape

$$F(\nu) = \frac{1}{\pi} \frac{\sigma}{\sigma^2 + (\nu - \nu_{V'',V',J'',J'})^2} \tag{25}$$

where σ, the line half-width at half maximum, is the same for all lines. The absorption coefficient $\mu(\nu)$ at ν due to several contributing (overlapping) lines is given by

$$\mu(\nu) = \sum_{\ell} \mu_{\ell}(\nu) \tag{26}$$

where ℓ labels the lines and the sum runs over all lines whose profiles overlap significantly at ν.

For practical considerations, some suitable criterion must be chosen to limit the calculation to some reasonable number of lines per frequency considered.

Table 2

THE VIBRATIONAL MATRIX ELEMENTS ($M^{v''v'} \times 10^{21}$)

v'' \ v'	1	2	3	4	5	6	7	8
0	72.619	10.138	-1.671	-0.559	-0.157	0.0	0.0	0.0
1	0.0	104.208	17.624	-3.542	-1.148	-0.360	0.0	0.0
2	0.0	0.0	129.520	24.854	-5.924	-2.057	-0.677	0.0
3	0.0	0.0	0.0	151.888	32.134	-8.848	-3.472	-1.143
4	0.0	0.0	0.0	0.0	172.710	39.550	-12.349	-5.535
5	0.0	0.0	0.0	0.0	0.0	192.602	47.124	-16.422
6	0.0	0.0	0.0	0.0	0.0	0.0	211.870	54.827
7	0.0	0.0	0.0	0.0	0.0	0.0	0.0	230.601

v'' \ v'	9	10	11	12	13	14	15	
4	-1.753	0.0	0.0	0.0	0.0	0.0	0.0	
5	-8.311	-2.455	0.0	0.0	0.0	0.0	0.0	
6	-21.008	-11.762	-3.161	0.0	0.0	0.0	0.0	
7	62.595	-26.012	-15.764	-3.755	0.0	0.0	0.0	
8	248.760	70.363	-31.321	-20.138	-4.120	0.0	0.0	
9	0.0	266.290	78.075	-36.832	-24.684	-4.152	0.0	
10	0.0	0.0	283.116	85.702	-42.454	-29.210	-3.759	
11	0.0	0.0	0.0	299.180	93.241	-48.115	-22.540	
12	0.0	0.0	0.0	0.0	314.480	100.710	-53.753	
13	0.0	0.0	0.0	0.0	0.0	329.010	108.160	
14	0.0	0.0	0.0	0.0	0.0	0.0	342.781	

4. CONSTRUCTION AND USE OF THE SPECTRAL ATLAS

A digital computer code has been constructed to write a magnetic tape atlas containing the lines of the NO vibration-rotation spectrum. This code is in Fortran language for use on the IBM 7094 computer. For each line to be included in the calculations, four numbers are written on the tape atlas: (1) the line frequency in cm^{-1}, (2) and (3) the E and H functions described in the preceding section, and (4) the line identification word. Numbers (1) through (3) are written in decimal form while (4) is in octal. The latter is formed of the upper and lower vibrational quantum numbers, the lower rotational quantum number, type of transition (P, Q, R branch), substate indicator (1/2 or 3/2), and a species indicator which is necessary to distinguish the band system when it is merged with other systems (for example in the air problem discussed in other reports[5-6]). There are 25,610 spectral lines contained on the atlas for this system. To compute the absorption coefficient, the atlas must be used in conjunction with the appropriate population numbers and partition function. The population numbers of Gilmore[18] for NO in air have been used in a transmission calculation which will be described next.

5. AN AVERAGE TRANSMISSION CALCULATION

Consider a frequency interval $\Delta\nu$ which is small enough that gross radiation transport features do not change appreciably over the interval, yet is large enough to contain many lines (say ~ 100). Let ν_j denote a fixed frequency point within the interval and let α label a line whose maximum lies within that same interval. A transmission point function may then be defined for an isothermal, homogeneous slab of thickness x :

$$\mathrm{Tr}(\nu_j) = \exp\left\{-\left[\sum_\alpha \mu'_\alpha(\nu_j)\right] x\right\} \tag{27}$$

where $\mu'(\nu_j)$ is the absorption coefficient corrected by the usual factor to account for re-emission

$$\mu'(\nu_j) = \mu(\nu_j)\left[1 - \exp\left(\frac{-h\nu_j}{kT}\right)\right] \tag{28}$$

and the sum is taken over all lines α whose maxima fall within $\Delta\nu$. The reason for a judicious choice of interval is now apparent; it reduces the error which is introduced by omitting contributions to the absorption in $\Delta\nu$ arising from lines whose maxima are outside $\Delta\nu$.

The average transmission through the slab for a frequency interval $\Delta\nu$ centered at frequency ν may then be written

$$\overline{\mathrm{Tr}}^{\Delta\nu} = \frac{1}{\Delta\nu}\int_{\Delta\nu} \exp\left\{-\left[\sum_\alpha \mu'_\alpha(\nu)\right] x\right\} d\nu \tag{29}$$

An approximation to the integral is made by evaluating the argument at many points in $\Delta\nu$ and utilizing the trapezoidal integration scheme.

An average absorption coefficient for the interval may now be defined through the relation

$$e^{-\bar{\mu}(\nu,x)\cdot x} = \overline{Tr}^{\Delta\nu}{}_{(\nu)} \tag{30}$$

Deleting superscripts we obtain

$$\bar{\mu}(\nu,x) = \frac{-\log_e \overline{Tr}}{x} \tag{31}$$

Based on equations (27) through (31) a digital computer code was written to calculate $\overline{Tr}$ and $\bar{\mu}$ for an isothermal, homogeneous slab of heated NO, as a function of slab thickness x.

Results have been obtained for temperatures from 1000°K to 5000°K and for densities corresponding to the NO concentration in air at 1, 10^{-1}, 10^{-2}, 10^{-3}, and 10^{-4} times normal atmospheric density. Frequency intervals were taken centered at the following frequencies: 1200, 1400, 1600, 1800, 2000 cm^{-1}, and every 500 cm^{-1} from 2500 to 9000 cm^{-1}.

From equations (23), (25), and (29) it is clear that the results of the calculation depend on the value of the line half-width, σ, which has been preassigned to all lines. The determination of the effect of choice of σ on the results is an important part of this research. A parameter study has been made to assist in this determination, with the choice of line-widths being guided by estimates which are discussed in the next section.

6. LINE WIDTHS

Rotational line widths for pressure broadened lines in molecules are, in general, not available from experiment for temperatures of 1000°K and above. Furthermore, to our knowledge there are no estimates of such widths based on the better line broadening theories.* The situation concerning our calculations is further complicated by the fact that fine structure due to Λ-type doubling has not been included. At higher temperatures this fine structure produces a pseudo line broadening which will increase with increasing nuclear rotation.

For our purposes, however, a precise line shape for each line considered should not be necessary, since we are concerned with an average absorption coefficient for a frequency interval which contains a large number of lines.

An average half-width to be applied to all lines is a parameter in the calculations described by this report. Because of the general lack of knowledge mentioned above, we now employ simple models to estimate an average half-width for those temperatures and densities of interest here.

The following mechanisms are expected to provide important contributions to the line widths for this study:

1. Pressure (collision) broadening
2. Doppler broadening
3. Pseudo broadening due to neglect of fine structure

*The Anderson theory[19] as expounded by Tsao and Curnutte[20] has been applied to self broadening in linear molecules by Benedict and Herman[21]. However, these calculations are for $T < 500°K$.

Pressure Broadening

An estimate of the optical collision diameter for the NO molecule has been obtained by Weber and Penner[22] for a temperature of 300° K and pressures near 1 atmosphere. Ignoring any temperature or pressure dependence of this collision diameter ($d_{NO} = 4.2$ Å), we assume the collision broadened half-width for NO in air to be given by[23]

$$\sigma_c = \frac{N\bar{v}d^2}{2c} \tag{32}$$

where N is the air particle density, $\bar{v}$ is the mean relative velocity magnitude, and d the optical collision diameter. Since $\bar{v} = |\vec{v}| = (8kT/\pi m)^{1/2}$, where k is Boltzmann's constant and m the mass of the particle,

$$\sigma_c \cong 1.19 \times 10^{-4} \left(\frac{\rho}{\rho_o}\right)_{air} T^{1/2} d^2 \tag{33}$$

Here d is expressed in Angstroms, T in °K and σ_c in cm^{-1}.

Doppler Broadening

The half-width associated with Doppler broadening is given by[9]

$$\sigma_D = \left(\frac{2k\,\ell n\,2}{mc^2}\right)^{1/2} \nu\, T^{1/2} \tag{34}$$

where σ_D and ν are expressed in the same units. Notice that Doppler broadening depends on frequency, while collision broadening does not.

Ratio of Collision Width to Doppler Width for NO

If n = 1, 2, 3, 4 indicates the fundamental, 1st, 2nd, and 3rd overtone respectively; the ratio of collision to Doppler widths is given by

$$\frac{\sigma_c}{\sigma_D} = \frac{17.1}{n} \cdot \frac{\rho}{\rho_o} \tag{35}$$

The ratio σ_c/σ_D is a convenient indicator of the relative importance of each type of broadening. Table 3 displays some results of Eq. 35 which are of interest to our calculation.

Table 3

σ_c/σ_D

	n = 1	n = 2	n = 3	n = 4
$\rho/\rho_o = 1$	17.1	8.55	5.70	4.28
10^{-1}	1.71	0.86	0.57	0.43
10^{-2}	0.17	0.09	0.06	0.04
10^{-3}	0.02	0.01	0.01	–
10^{-4}	Essentially Pure Doppler			

Collision and Doppler Half-widths for NO Vibration Rotation System

Table 4 lists values of collision and Doppler half-widths for NO in air at normal atmospheric density as a function of temperature. The fundamental and 1st overtone bands are included. To obtain collision half-widths at other densities, multiply the tabulated values by ρ/ρ_o.

Table 4

Estimated collision and Doppler half-widths for the fundamental and first overtone bands of the NO vibration-rotation spectrum

T(° K)	$\sigma_c(cm^{-1})$	$\sigma_D^{FUND}(cm^{-1})$	$\sigma_D^{1^{st}O.T.}(cm^{-1})$
300	0.036	0.002	0.004
1000	0.066	0.004	0.008
2000	0.094	0.006	0.011
3000	0.115	0.007	0.013
4000	0.133	0.008	0.016
5000	0.149	0.009	0.017

A Pseudo Line Broadening Effect

Fine structure arising from Λ-type doubling is neglected in the current version of the SACHA programs. Apart from the differences in complexity of the present programs and those which would include Λ-doubling, the reason for neglecting this effect is that (quantitatively) it is not generally well known.

Λ-type doubling is a phenomenon in molecular spectra which occurs when increasing nuclear rotation gives rise to stronger coupling between the nuclear and electronic angular momenta. This is a complicated effect which has been discussed extensively by Van Vleck[24] and by Mulliken and Christy[25].

To first approximation the splitting due to Λ-doubling is given by[7]

$$\nu_{cd} \cong q_o J(J+1) \tag{36}$$

where q_o is a characteristic of a particular vibrational level. Mulliken and Christy give a value of 0.00035 cm^{-1} for the NO $X^2\Pi$ state (for v = 2). Thus for J large enough the line may become resolved.

A partial compensation may be obtained for the neglect of Λ-doubling in the calculation by an appropriate increase in the line width. To more easily visualize such a compensation and to gain an estimate of its limits we consider the following simple pictures:

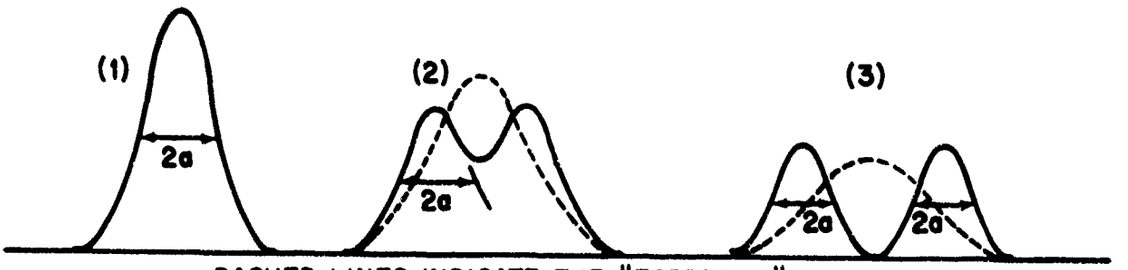

DASHED LINES INDICATE THE "EFFECTIVE" LINE.

In (1) we have an unresolved line with half-width a. As the value of J increases the line starts to resolve (2), where the effective half width is now larger than a. In (3) the line is completely resolved, with each component having a half-width a. It is thus seen that the effect of neglecting Λ-doubling may be compensated for by increasing the average effective line width by a factor of 2 or less.

A Line-Width Parameter Study

Since it is felt that any estimate of an average line half-width has considerable possible error associated with it, the Lorentz half-width associated with the SACHA transmission calculation has been viewed as a calculational parameter, the variation of which will provide information on the sensitivity of the calculation to that parameter.

Accordingly, results were obtained from the machine programs for values of σ = 1.0, 0.1, and 0.01 cm^{-1}. These values were chosen as plausible upper and lower limits with an intermediate value which seems to be a representative collision broadened half-width for normal atmospheric density.

Two Group Absorption Coefficients

The concept of intensity groupings has been discussed in a previous publication.[6] Application of this concept to the transmission problem for heated air has shown the two group approximation to be fairly accurate. Basically, this approximation assumes that after obtaining the transmission through a plane slab of heated gas, one can fit its dependence on the slab thickness x by the expression

$$Tr(x) = \frac{1}{2}\left(e^{-\mu_a' x} + e^{-\mu_b' x}\right)$$

where μ_a' and μ_b' are the two group absorption coefficients. These coefficients are computed for each density, temperature, and frequency for which Tr(x) is computed. Values of μ_a' and μ_b' for the NO vibration-rotation system are listed in Table 5. These were obtained by choosing two values of x which bracket the value of x corresponding to the 0.5 transmission point, then solving the two equations thus determined for μ_a' and μ_b'. This yields a reasonable fit for transmissions greater than about 0.1.

Table 5

TWO GROUP ABSORPTION COEFFICIENTS

$T = 1000°K \quad \sigma = 0.10$

Frequency (cm^{-1})	ρ/ρ_o = 1.0		10^{-1}		10^{-2}		10^{-3}	
	μ_a	μ_b	μ_a	μ_b	μ_a	μ_b	μ_a	μ_b
1200	2.602^{-21}	1.381^{-22}	2.602^{-22}	1.381^{-23}	2.612^{-23}	1.396^{-24}	2.837^{-24}	1.060^{-25}
1400	3.906^{-14}	1.021^{-15}	3.906^{-15}	1.021^{-16}	3.919^{-16}	1.041^{-17}	3.210^{-17}	1.811^{-18}
1600	6.070^{-9}	2.821^{-10}	6.070^{-10}	2.821^{-11}	6.091^{-11}	2.852^{-12}	6.642^{-12}	2.136^{-13}
1800	9.577^{-6}	1.068^{-6}	9.577^{-7}	1.068^{-7}	9.613^{-8}	1.078^{-8}	1.034^{-8}	8.992^{-10}
2000	7.260^{-7}	2.405^{-8}	7.260^{-8}	2.405^{-9}	7.287^{-9}	2.436^{-10}	6.270^{-10}	3.229^{-11}
2500	1.153^{-25}	1.666^{-28}	1.153^{-26}	1.666^{-29}	1.156^{-27}	1.677^{-30}	1.283^{-28}	1.442^{-31}
3000	9.603^{-16}	8.357^{-17}	9.603^{-17}	8.357^{-18}	9.646^{-18}	8.433^{-19}	8.711^{-19}	1.002^{-19}
3300	6.145^{-11}	3.765^{-12}	6.145^{-12}	3.765^{-13}	6.173^{-13}	3.806^{-14}	5.506^{-14}	4.971^{-15}
3500	2.407^{-8}	2.338^{-9}	2.407^{-9}	2.338^{-10}	2.417^{-10}	2.356^{-11}	2.573^{-11}	2.106^{-12}
3700	3.905^{-7}	4.749^{-8}	3.905^{-8}	4.749^{-9}	3.921^{-9}	4.783^{-10}	4.160^{-10}	4.384^{-11}
4000	1.450^{-23}	2.423^{-25}	1.450^{-24}	2.423^{-26}	1.454^{-25}	2.454^{-27}	1.622^{-26}	1.556^{-28}
4500	4.624^{-17}	5.445^{-18}	4.624^{-18}	5.445^{-19}	4.647^{-19}	5.481^{-20}	4.787^{-20}	5.218^{-21}
5000	6.900^{-12}	5.993^{-13}	6.900^{-13}	5.993^{-14}	6.932^{-14}	6.049^{-15}	6.317^{-15}	7.334^{-16}
5500	3.070^{-8}	2.814^{-9}	3.070^{-9}	2.814^{-10}	3.085^{-10}	2.839^{-11}	2.808^{-11}	3.347^{-12}
6000	2.262^{-17}	1.336^{-18}	2.262^{-18}	1.336^{-19}	2.272^{-19}	1.348^{-20}	2.405^{-20}	1.153^{-21}
6500	1.272^{-13}	8.024^{-15}	1.272^{-14}	8.024^{-16}	1.277^{-15}	8.111^{-17}	1.127^{-16}	1.053^{-17}
7000	1.628^{-10}	1.355^{-11}	1.628^{-11}	1.355^{-12}	1.635^{-12}	1.367^{-13}	1.740^{-13}	1.156^{-14}
7500	4.883^{-19}	1.730^{-20}	4.883^{-20}	1.730^{-21}	4.900^{-21}	1.743^{-22}	5.349^{-22}	1.501^{-23}
8000	2.886^{-14}	3.074^{-16}	2.886^{-16}	3.074^{-17}	2.899^{-17}	3.096^{-18}	3.045^{-18}	2.850^{-19}
8500	1.647^{-12}	1.401^{-13}	1.647^{-13}	1.401^{-14}	1.653^{-14}	1.411^{-15}	1.762^{-15}	1.280^{-16}
9000	2.165^{-10}	8.476^{-12}	2.165^{-11}	8.476^{-13}	2.173^{-12}	8.562^{-14}	2.379^{-13}	6.636^{-15}

Table 5 (cont.)

T = 2000°K σ = 0.10

Frequency (cm^{-1})	ρ/ρ_o =							
	1.0		10^{-1}		10^{-2}		10^{-3}	
	μ_a	μ_b	μ_a	μ_b	μ_a	μ_b	μ_a	μ_b
1200	2.539^{-10}	1.597^{-11}	2.539^{-11}	1.597^{-12}	2.539^{-12}	1.597^{-13}	2.294^{-13}	2.014^{-14}
1400	5.886^{-7}	6.851^{-8}	5.886^{-8}	6.851^{-9}	5.886^{-9}	6.851^{-10}	6.120^{-10}	6.240^{-11}
1600	1.464^{-4}	1.734^{-5}	1.464^{-5}	1.734^{-6}	1.464^{-6}	1.734^{-7}	1.525^{-7}	1.567^{-8}
1800	1.994^{-3}	2.723^{-4}	1.994^{-4}	2.723^{-5}	1.994^{-5}	2.723^{-6}	1.795^{-6}	3.164^{-7}
2000	8.594^{-4}	9.229^{-5}	8.594^{-5}	9.229^{-6}	8.594^{-6}	9.229^{-7}	7.768^{-7}	1.136^{-7}
2500	2.218^{-13}	2.896^{-16}	2.218^{-14}	2.896^{-17}	2.218^{-15}	2.896^{-18}	2.474^{-16}	1.719^{-19}
3000	5.821^{-8}	8.776^{-9}	5.821^{-9}	8.776^{-10}	5.821^{-10}	8.776^{-11}	5.608^{-11}	9.207^{-12}
3300	6.435^{-6}	8.733^{-7}	6.435^{-7}	8.733^{-8}	6.435^{-8}	8.733^{-9}	6.124^{-9}	9.550^{-10}
3500	6.339^{-5}	8.910^{-6}	6.339^{-6}	8.910^{-7}	6.339^{-7}	8.910^{-8}	6.529^{-8}	8.233^{-9}
3700	1.329^{-4}	1.079^{-5}	1.329^{-5}	1.079^{-6}	1.329^{-6}	1.079^{-7}	1.202^{-7}	1.308^{-8}
4000	2.223^{-12}	5.610^{-14}	2.223^{-13}	5.610^{-15}	2.223^{-14}	5.610^{-16}	2.441^{-15}	4.804^{-17}
4500	7.758^{-9}	9.138^{-10}	7.758^{-10}	9.138^{-11}	7.758^{-11}	9.138^{-12}	7.326^{-12}	9.947^{-13}
5000	9.645^{-7}	1.487^{-7}	9.645^{-8}	1.487^{-8}	9.645^{-9}	1.487^{-9}	9.837^{-10}	1.411^{-10}
5500	9.925^{-6}	7.583^{-7}	9.925^{-7}	7.583^{-8}	9.925^{-8}	7.583^{-9}	1.040^{-8}	6.534^{-10}
6000	3.228^{-9}	2.631^{-10}	3.228^{-10}	2.631^{-11}	3.228^{-11}	2.631^{-12}	3.403^{-12}	2.406^{-13}
6500	8.624^{-8}	1.045^{-8}	8.624^{-9}	1.045^{-9}	8.624^{-10}	1.045^{-10}	9.036^{-11}	9.618^{-12}
7000	6.336^{-7}	8.503^{-8}	6.336^{-8}	8.503^{-9}	6.336^{-9}	8.503^{-10}	6.544^{-10}	7.991^{-11}
7500	8.358^{-11}	1.789^{-12}	8.358^{-12}	1.789^{-13}	8.358^{-13}	1.789^{-14}	6.817^{-14}	3.339^{-15}
8000	5.920^{-9}	7.741^{-10}	5.920^{-10}	7.741^{-11}	5.920^{-11}	7.741^{-12}	6.136^{-12}	7.356^{-14}
8500	4.090^{-8}	3.122^{-9}	4.090^{-9}	3.122^{-10}	4.090^{-10}	3.122^{-11}	4.308^{-11}	2.686^{-12}
9000	6.028^{-8}	2.695^{-9}	6.028^{-9}	2.695^{-10}	6.028^{-10}	2.695^{-11}	6.684^{-11}	2.217^{-12}

Table 5 (cont.)

T = 3000°K σ = 0.10

Frequency (cm^{-1})	ρ/ρ_o =							
	1.0		10^{-1}		10^{-2}		10^{-3}	
	μ_a	μ_b	μ_a	μ_b	μ_a	μ_b	μ_a	μ_b
1200	6.340^{-7}	5.557^{-8}	6.090^{-8}	5.268^{-9}	5.487^{-9}	4.458^{-10}	3.768^{-10}	3.240^{-11}
1400	1.002^{-4}	1.678^{-5}	9.647^{-6}	1.600^{-6}	8.181^{-7}	1.522^{-7}	5.962^{-8}	9.859^{-9}
1600	2.608^{-3}	5.247^{-4}	2.514^{-4}	5.016^{-5}	2.252^{-5}	4.369^{-6}	1.554^{-6}	3.093^{-7}
1800	8.286^{-3}	1.936^{-3}	7.994^{-4}	1.846^{-4}	7.174^{-5}	1.598^{-5}	4.944^{-6}	1.138^{-6}
2000	6.121^{-3}	1.183^{-3}	5.903^{-4}	1.126^{-4}	4.910^{-5}	1.100^{-5}	3.650^{-6}	6.930^{-7}
2500	1.648^{-9}	1.515^{-12}	1.614^{-10}	1.266^{-13}	1.521^{-11}	4.402^{-15}	1.003^{-12}	7.436^{-16}
3000	1.438^{-5}	2.554^{-6}	1.384^{-6}	2.442^{-7}	1.233^{-7}	2.130^{-8}	8.552^{-9}	1.506^{-9}
3300	2.061^{-4}	4.058^{-5}	1.985^{-5}	3.876^{-6}	1.770^{-6}	3.370^{-7}	1.227^{-7}	2.389^{-8}
3500	6.521^{-4}	1.316^{-4}	6.276^{-5}	1.260^{-5}	5.596^{-6}	1.105^{-6}	3.879^{-7}	7.775^{-8}
3700	7.146^{-4}	5.743^{-5}	6.938^{-5}	5.399^{-6}	6.341^{-6}	4.438^{-7}	4.298^{-7}	3.312^{-8}
4000	8.152^{-9}	1.775^{-10}	7.971^{-10}	1.643^{-11}	7.468^{-11}	1.246^{-12}	4.949^{-12}	1.002^{-13}
4500	2.626^{-6}	4.005^{-7}	2.531^{-7}	3.827^{-8}	2.267^{-8}	3.327^{-9}	1.565^{-9}	2.360^{-10}
5000	3.923^{-5}	6.945^{-6}	3.780^{-6}	6.638^{-7}	3.382^{-7}	5.780^{-8}	2.337^{-8}	4.093^{-9}
5500	5.131^{-5}	4.365^{-6}	4.971^{-6}	4.144^{-7}	4.522^{-7}	3.514^{-8}	3.078^{-8}	2.550^{-9}
6000	1.270^{-6}	1.153^{-7}	1.229^{-7}	1.090^{-8}	1.113^{-8}	9.126^{-10}	7.604^{-10}	6.698^{-11}
6500	5.684^{-6}	8.912^{-7}	5.493^{-7}	8.499^{-8}	4.956^{-8}	7.341^{-9}	3.398^{-9}	5.237^{-10}
7000	8.497^{-6}	1.190^{-6}	8.192^{-7}	1.134^{-7}	7.339^{-8}	9.770^{-9}	5.065^{-9}	6.983^{-10}
7500	2.644^{-8}	1.781^{-9}	2.576^{-9}	1.677^{-10}	2.383^{-10}	1.379^{-11}	1.597^{-11}	1.029^{-12}
8000	5.708^{-7}	7.551^{-8}	5.512^{-8}	7.177^{-9}	4.962^{-9}	6.113^{-10}	3.410^{-10}	4.418^{-11}
8500	8.294^{-7}	7.699^{-8}	8.034^{-8}	7.321^{-9}	7.302^{-9}	6.248^{-10}	4.974^{-10}	4.507^{-11}
9000	3.751^{-7}	7.892^{-9}	3.670^{-8}	6.830^{-10}	2.521^{-9}	1.201^{-10}	2.279^{-10}	4.075^{-12}

Table 5 (cont.)

T = 4000°K σ = 0.10

Frequency (cm^{-1})	ρ/ρ_o =							
	1.0		10^{-1}		10^{-2}		10^{-3}	
	μ_a	μ_b	μ_a	μ_b	μ_a	μ_b	μ_a	μ_b
1200	1.978^{-5}	1.810^{-6}	1.295^{-6}	1.303^{-7}	5.892^{-8}	5.766^{-9}	2.010^{-9}	2.019^{-10}
1400	8.181^{-4}	1.766^{-4}	5.499^{-5}	1.223^{-5}	2.479^{-6}	5.465^{-7}	8.530^{-8}	1.896^{-8}
1600	7.462^{-3}	1.818^{-3}	4.976^{-4}	1.267^{-4}	2.250^{-5}	5.650^{-6}	7.721^{-7}	1.964^{-7}
1800	1.295^{-2}	4.206^{-3}	8.674^{-4}	2.916^{-4}	3.917^{-5}	1.302^{-5}	1.346^{-6}	4.521^{-7}
2000	1.146^{-2}	2.487^{-3}	7.657^{-4}	1.746^{-4}	3.460^{-5}	7.767^{-6}	1.188^{-6}	2.706^{-7}
2500	6.851^{-8}	1.141^{-10}	5.439^{-9}	6.168^{-12}	2.573^{-10}	2.072^{-13}	8.464^{-12}	9.431^{-15}
3000	1.407^{-4}	2.835^{-5}	9.729^{-6}	1.876^{-6}	4.392^{-7}	8.334^{-8}	1.509^{-8}	2.908^{-9}
3300	7.991^{-4}	1.855^{-4}	5.356^{-5}	1.290^{-5}	2.417^{-6}	5.756^{-7}	8.309^{-8}	2.000^{-8}
3500	1.610^{-3}	3.126^{-4}	1.073^{-4}	2.202^{-5}	4.854^{-6}	9.787^{-7}	1.665^{-7}	3.413^{-8}
3700	1.252^{-3}	7.893^{-5}	7.782^{-5}	6.467^{-6}	3.608^{-6}	2.758^{-7}	1.210^{-7}	9.997^{-9}
4000	2.794^{-7}	7.043^{-9}	2.264^{-8}	3.020^{-10}	1.074^{-9}	9.636^{-12}	3.524^{-11}	4.598^{-13}
4500	3.274^{-5}	5.419^{-6}	2.173^{-6}	3.810^{-7}	9.839^{-8}	1.696^{-8}	3.371^{-9}	5.906^{-10}
5000	1.729^{-4}	3.159^{-5}	1.220^{-5}	2.042^{-6}	5.539^{-7}	8.979^{-8}	1.893^{-8}	3.163^{-9}
5500	8.693^{-5}	6.622^{-6}	5.530^{-6}	4.951^{-7}	2.540^{-7}	2.170^{-8}	8.589^{-9}	7.667^{-10}
6000	1.664^{-5}	1.652^{-6}	1.085^{-6}	1.226^{-7}	4.950^{-8}	5.370^{-9}	1.684^{-9}	1.898^{-10}
6500	3.323^{-5}	5.124^{-6}	2.181^{-6}	3.660^{-7}	9.917^{-8}	1.621^{-8}	$3.3[illegible]^{-9}$	5.672^{-10}
7000	2.068^{-5}	3.093^{-6}	1.456^{-6}	1.980^{-7}	6.606^{-8}	8.682^{-9}	2.260^{-9}	3.066^{-10}
7500	3.723^{-7}	2.545^{-8}	2.884^{-8}	1.191^{-9}	1.069^{-9}	8.469^{-11}	4.485^{-11}	1.825^{-12}
8000	3.726^{-6}	4.934^{-7}	2.441^{-7}	3.593^{-8}	1.111^{-8}	1.581^{-9}	3.789^{-10}	5.565^{-11}
8500	2.745^{-6}	2.258^{-7}	2.022^{-7}	1.231^{-8}	8.031^{-9}	7.349^{-10}	2.717^{-10}	2.592^{-11}
9000	4.704^{-7}	1.923^{-8}	3.779^{-8}	8.216^{-10}	1.328^{-9}	6.450^{-11}	5.881^{-11}	1.253^{-12}

Table 5 (cont.)

T = 5000°K σ = 0.10

Frequency (cm^{-1})	ρ/ρ_o =							
	1.0		10^{-1}		10^{-2}		10^{-3}	
	μ_a	μ_b	μ_a	μ_b	μ_a	μ_b	μ_a	μ_b
1200	8.351^{-5}	7.970^{-6}	3.626^{-6}	3.272^{-7}	1.187^{-7}	1.180^{-8}	3.660^{-9}	3.625^{-10}
1400	1.608^{-3}	3.896^{-4}	6.888^{-5}	1.646^{-5}	2.314^{-6}	5.662^{-7}	7.125^{-8}	1.742^{-8}
1600	7.796^{-3}	2.299^{-3}	3.349^{-4}	9.700^{-5}	1.119^{-5}	3.347^{-6}	3.446^{-7}	1.030^{-8}
1800	1.061^{-2}	4.143^{-3}	4.542^{-4}	1.756^{-4}	1.528^{-5}	6.013^{-6}	4.705^{-7}	1.850^{-7}
2000	9.432^{-3}	2.085^{-3}	4.053^{-4}	8.801^{-5}	1.404^{-5}	2.865^{-6}	4.327^{-7}	8.802^{-8}
2500	4.427^{-7}	5.467^{-10}	2.037^{-8}	1.543^{-11}	6.003^{-10}	9.042^{-13}	1.859^{-11}	2.760^{-14}
3000	3.054^{-4}	6.730^{-5}	1.308^{-5}	2.855^{-6}	4.499^{-7}	9.428^{-8}	1.386^{-8}	2.899^{-9}
3300	1.038^{-3}	2.634^{-4}	4.455^{-5}	1.112^{-5}	1.491^{-6}	3.830^{-7}	4.591^{-8}	1.178^{-8}
3500	1.613^{-3}	3.071^{-4}	6.567^{-5}	1.403^{-5}	2.301^{-6}	4.547^{-7}	7.092^{-8}	1.396^{-8}
3700	8.589^{-4}	7.916^{-5}	3.834^{-5}	3.185^{-6}	1.460^{-6}	8.234^{-8}	4.513^{-8}	2.494^{-9}
4000	1.231^{-6}	3.476^{-8}	5.558^{-8}	1.404^{-9}	2.248^{-9}	2.947^{-11}	6.972^{-11}	8.725^{-13}
4500	8.080^{-5}	1.538^{-5}	3.480^{-6}	6.471^{-7}	1.211^{-7}	2.088^{-8}	3.732^{-9}	6.414^{-10}
5000	2.499^{-4}	4.180^{-5}	1.084^{-5}	1.723^{-6}	3.356^{-7}	6.184^{-8}	1.096^{-8}	1.899^{-9}
5500	7.104^{-5}	5.273^{-6}	2.724^{-6}	2.708^{-7}	9.958^{-8}	8.211^{-9}	3.075^{-9}	2.510^{-10}
6000	4.167^{-5}	5.079^{-6}	1.810^{-6}	2.098^{-7}	5.923^{-8}	7.484^{-9}	1.826^{-9}	2.300^{-10}
6500	5.381^{-5}	8.064^{-6}	2.182^{-6}	3.729^{-7}	7.669^{-8}	1.199^{-8}	2.364^{-9}	3.681^{-10}
7000	2.022^{-5}	3.022^{-6}	8.743^{-7}	1.261^{-7}	2.888^{-8}	4.419^{-9}	8.899^{-10}	1.359^{-10}
7500	1.117^{-6}	5.236^{-8}	4.061^{-8}	3.285^{-9}	1.544^{-9}	8.875^{-11}	4.774^{-11}	2.694^{-12}
8000	6.417^{-6}	8.486^{-7}	2.582^{-7}	4.040^{-8}	9.131^{-9}	1.273^{-9}	2.815^{-10}	3.905^{-11}
8500	2.991^{-6}	2.627^{-7}	1.320^{-7}	1.056^{-8}	4.190^{-9}	3.939^{-10}	1.294^{-10}	1.209^{-11}
9000	3.874^{-7}	9.083^{-9}	1.326^{-8}	6.200^{-10}	5.256^{-10}	1.622^{-11}	1.628^{-11}	4.906^{-13}

Table 5 (cont.)

T = 1000°K σ = 0.01

Frequency (cm^{-1})	ρ/ρ_o =							
	10^{-1}		10^{-2}		10^{-3}		10^{-4}	
	μ_a	μ_b	μ_a	μ_b	μ_a	μ_b	μ_a	μ_b
1400	1.263^{-16}	1.207^{-18}	1.266^{-17}	1.222^{-19}	1.452^{-18}	8.239^{-21}	1.095^{-19}	1.436^{-21}
1600	5.310^{-12}	3.790^{-14}	8.461^{-13}	4.536^{-16}	6.105^{-14}	3.269^{-16}	7.096^{-15}	2.277^{-17}
1800	6.069^{-10}	3.970^{-12}	6.084^{-11}	4.008^{-13}	6.934^{-12}	3.039^{-14}	8.035^{-13}	1.252^{-15}
3000	4.571^{-18}	5.459^{-21}	4.579^{-19}	5.667^{-22}	3.313^{-20}	1.404^{-22}	3.841^{-21}	1.127^{-23}
3300	8.030^{-14}	1.233^{-16}	8.042^{-15}	1.263^{-17}	5.842^{-16}	2.251^{-18}	6.742^{-17}	1.952^{-19}
5000	1.085^{-13}	4.095^{-15}	1.089^{-14}	4.125^{-16}	1.179^{-15}	3.706^{-17}	1.294^{-16}	2.983^{-18}
5500	1.752^{-10}	1.070^{-12}	1.756^{-11}	1.078^{-13}	1.999^{-12}	9.389^{-15}	2.311^{-13}	6.954^{-16}
8000	4.914^{-17}	4.385^{-19}	4.927^{-18}	4.468^{-20}	3.984^{-19}	6.853^{-21}	4.357^{-20}	6.192^{-22}
T = 2000°K σ = 0.01								
1400	1.434^{-8}	3.914^{-10}	1.434^{-9}	3.914^{-11}	1.584^{-10}	3.307^{-12}	1.758^{-11}	2.190^{-13}
1600	2.173^{-6}	3.847^{-8}	2.173^{-7}	3.847^{-9}	2.417^{-8}	3.328^{-10}	2.705^{-9}	2.297^{-11}
1800	1.434^{-5}	9.581^{-8}	1.434^{-6}	9.581^{-9}	1.113^{-7}	1.718^{-9}	1.242^{-8}	1.445^{-10}
3000	9.058^{-10}	3.257^{-12}	9.058^{-11}	3.257^{-13}	7.178^{-12}	6.957^{-14}	7.933^{-13}	5.670^{-15}
3300	7.137^{-8}	3.784^{-10}	7.137^{-9}	3.784^{-11}	8.035^{-10}	2.229^{-12}	6.254^{-11}	4.547^{-13}
3500	2.915^{-7}	2.503^{-9}	2.915^{-8}	2.503^{-10}	3.341^{-9}	1.843^{-11}	3.847^{-10}	6.681^{-13}
4500	2.367^{-11}	7.495^{-14}	2.367^{-12}	7.495^{-15}	2.727^{-13}	6.088^{-16}	3.159^{-14}	3.252^{-17}
5000	8.171^{-8}	3.101^{-9}	8.171^{-9}	3.101^{-10}	8.906^{-10}	2.295^{-11}	7.396^{-11}	3.570^{-12}
5500	3.104^{-7}	3.826^{-9}	3.014^{-8}	3.826^{-10}	3.193^{-9}	3.654^{-11}	3.445^{-10}	2.913^{-12}
8000	1.952^{-10}	1.795^{-12}	1.952^{-11}	1.795^{-13}	1.585^{-12}	2.960^{-14}	1.723^{-13}	2.575^{-15}

Table 5 (cont.)

T = 3000°K σ = 0.01

Frequency (cm^{-1})	ρ/ρ_o =							
	10^{-1}		10^{-2}		10^{-3}		10^{-4}	
	μ_a	μ_b	μ_a	μ_b	μ_a	μ_b	μ_a	μ_b
1400	3.611^{-6}	1.385^{-7}	3.332^{-7}	1.175^{-8}	2.239^{-8}	8.526^{-10}	1.143^{-9}	3.233^{-11}
1600	9.185^{-5}	1.737^{-6}	8.614^{-6}	1.178^{-7}	5.704^{-7}	1.051^{-8}	2.191^{-8}	6.838^{-10}
1800	2.037^{-4}	5.960^{-6}	1.902^{-5}	4.715^{-7}	1.264^{-6}	3.647^{-8}	6.625^{-8}	1.045^{-9}
3000	2.553^{-7}	5.683^{-9}	2.368^{-8}	4.796^{-10}	1.584^{-9}	3.497^{-11}	8.216^{-11}	1.273^{-12}
3300	3.758^{-6}	5.564^{-8}	3.510^{-7}	4.346^{-9}	2.333^{-8}	3.403^{-10}	1.226^{-9}	8.723^{-12}
3500	1.382^{-5}	1.603^{-7}	1.298^{-6}	1.102^{-8}	8.585^{-8}	9.709^{-10}	3.295^{-9}	6.045^{-11}
4500	3.240^{-8}	7.482^{-11}	2.194^{-9}	1.409^{-11}	2.013^{-10}	4.371^{-13}	7.583^{-12}	4.119^{-14}
5000	4.999^{-6}	1.475^{-7}	4.651^{-7}	1.059^{-8}	3.102^{-8}	8.952^{-10}	1.213^{-9}	5.571^{-11}
5500	1.990^{-6}	2.853^{-8}	1.833^{-7}	2.363^{-9}	1.233^{-8}	1.754^{-10}	6.285^{-10}	5.688^{-12}
8000	1.639^{-8}	3.258^{-10}	1.516^{-9}	2.767^{-11}	1.016^{-10}	2.006^{-12}	5.246^{-12}	7.391^{-14}
T = 4000°K σ = 0.01								
1400	2.620^{-5}	1.066^{-6}	1.221^{-6}	4.561^{-8}	4.073^{-8}	1.649^{-9}	1.290^{-9}	5.298^{-11}
1600	2.144^{-4}	9.558^{-6}	1.000^{-5}	4.115^{-7}	3.333^{-7}	1.479^{-8}	1.056^{-8}	4.748^{-10}
1800	4.087^{-4}	2.211^{-5}	1.906^{-5}	9.528^{-7}	6.355^{-7}	3.420^{-8}	2.013^{-8}	1.098^{-9}
3000	2.909^{-6}	4.884^{-8}	1.374^{-7}	1.725^{-9}	4.528^{-9}	7.474^{-11}	1.431^{-10}	2.471^{-12}
3300	1.350^{-5}	2.716^{-7}	6.348^{-7}	1.093^{-8}	2.101^{-8}	4.186^{-10}	6.645^{-10}	1.358^{-11}
3500	3.039^{-5}	7.521^{-7}	1.422^{-6}	3.211^{-8}	4.726^{-8}	1.163^{-9}	1.496^{-7}	3.738^{-11}
4500	3.137^{-7}	2.658^{-9}	1.459^{-8}	1.161^{-10}	4.876^{-10}	4.117^{-12}	1.546^{-11}	1.317^{-13}
5000	1.886^{-5}	3.889^{-7}	6.697^{-7}	3.138^{-8}	2.934^{-8}	5.929^{-10}	9.279^{-10}	1.981^{-11}
5500	2.899^{-6}	1.929^{-8}	1.056^{-7}	1.812^{-9}	4.511^{-9}	2.901^{-11}	1.426^{-10}	1.004^{-12}
7000	2.092^{-9}	6.146^{-13}	9.742^{-11}	2.813^{-14}	3.251^{-12}	9.556^{-16}	1.031^{-13}	3.026^{-17}
8000	9.758^{-8}	9.295^{-10}	4.626^{-9}	2.818^{-11}	1.519^{-10}	1.413^{-12}	4.796^{-12}	4.757^{-14}

Table 5 (cont.)

T = 5000°K σ = 0.01

Frequency (cm^{-1})	ρ/ρ_o =							
	10^{-1}		10^{-2}		10^{-3}		10^{-4}	
	μ_a	μ_b	μ_a	μ_b	μ_a	μ_b	μ_a	μ_b
1400	4.043^{-5}	1.122^{-6}	1.220^{-6}	4.948^{-8}	3.776^{-8}	1.512^{-9}	1.090^{-9}	3.842^{-11}
1600	1.856^{-4}	8.339^{-6}	7.299^{-6}	1.874^{-7}	2.260^{-7}	5.604^{-9}	5.055^{-9}	2.563^{-10}
1800	3.360^{-4}	1.873^{-5}	1.315^{-5}	4.195^{-7}	4.071^{-7}	1.256^{-8}	9.140^{-9}	5.814^{-10}
3000	5.152^{-6}	5.853^{-8}	1.519^{-7}	3.639^{-9}	4.707^{-9}	1.102^{-10}	1.373^{-10}	2.553^{-12}
3300	1.266^{-5}	2.801^{-7}	3.821^{-7}	1.123^{-8}	1.182^{-8}	3.442^{-10}	3.409^{-10}	9.048^{-12}
3500	2.485^{-5}	5.138^{-7}	7.433^{-7}	2.141^{-8}	2.301^{-8}	6.558^{-10}	6.661^{-10}	1.702^{-11}
4500	5.797^{-7}	5.559^{-9}	2.256^{-8}	1.323^{-10}	6.989^{-10}	3.938^{-12}	2.032^{-11}	7.045^{-14}
5000	1.354^{-5}	6.134^{-7}	5.356^{-7}	1.591^{-8}	1.659^{-8}	4.809^{-10}	4.821^{-10}	1.095^{-11}
5500	1.441^{-6}	9.880^{-9}	4.307^{-8}	6.242^{-10}	1.333^{-9}	1.894^{-11}	3.865^{-11}	4.419^{-13}
7000	4.401^{-9}	1.280^{-12}	1.717^{-10}	3.907^{-14}	5.324^{-12}	1.167^{-15}	1.562^{-13}	1.961^{-17}
8000	1.019^{-7}	1.231^{-9}	3.022^{-9}	5.643^{-11}	9.356^{-11}	1.724^{-12}	2.718^{-12}	4.366^{-14}

7. RADIATIVE TRANSFER

The spectral flow of radiation from one location to another is described by the equation of radiative transfer

$$\frac{1}{\rho}\frac{dI_\nu(\vec{\Omega})}{ds} \qquad j_\nu(\vec{\Omega}) - \kappa_\nu I_\nu(\vec{\Omega}) \tag{37}$$

where $I_\nu(\vec{\Omega})$ is the spectral intensity in direction $\vec{\Omega}$ and $j_\nu(\vec{\Omega})$ is the spectral source function. Interaction between the radiation and the matter traversed is expressed through κ_ν, the spectral absorption coefficient. s is the coordinate along the ray $\vec{\Omega}$ measured from some convenient origin, and ρ is the matter density. Precise definitions of the above quantities are somewhat involved and will be omitted here. For a good discussion of basic concepts the reader is referred to Ambartsumyan.[26]

j_ν, the source function, denotes the energy radiated by a unit mass of material per unit time, per unit frequency interval about frequency ν, and per unit solid angle in direction $\vec{\Omega}$. Its units are erg sec^{-1} $steradian^{-1}$ gm^{-1} $(sec^{-1})^{-1}$, I_ν is the flux of radiation per unit frequency interval about ν per unit solid angle in direction $\vec{\Omega}$, and per unit area normal to $\vec{\Omega}$. The spectral absorption coefficient κ_ν is expressed in cm^2 gm^{-1} and the density ρ is in units gm cm^{-3}.

When the material is a gas in local thermodynamic equilibrium, j_ν is the sum of a spontaneous and induced emission term:

$$j_\nu = \kappa'_\nu B_\nu(T) + \kappa_\nu I_\nu \exp\left(-\frac{h\nu}{kT}\right) \tag{38}$$

where

$$\kappa'_\nu = \kappa_\nu \left[1 - \exp\left(-\frac{h\nu}{kT}\right)\right] \tag{39}$$

and

$$B_\nu(T) = \frac{2h\nu^3}{c^2}\left[\exp\left(\frac{h\nu}{kT}\right) - 1\right]^{-1} \tag{40}$$

is the Planck distribution function. Since the following discussion is limited to gases in local thermodynamic equilibrium, Eqs. (38) through (40) apply and Eq. (37) becomes

$$\frac{dI_\nu}{ds} = \mu'_\nu(B_\nu - I_\nu) \tag{41}$$

where $\mu'_\nu \equiv \rho\kappa'_\nu$ is the linear spectral absorption coefficient of the gas. The formal solution of Eq. (41) is

$$I_\nu(s, \vec{\Omega}) = I_\nu(0, \vec{\Omega}) \exp\left[-\int_0^s \mu'_\nu(y)\,dy\right] + \int_0^s B_\nu[T(s')]\mu'_\nu(s') \exp\left[-\int_{s'}^s \mu'_\nu(y)\,dy\right] ds' \tag{42}$$

If the material is isothermal and homogeneous, Eq. (42) simplifies greatly since $B_\nu(T)$ and μ'_ν are constant with s. Then

$$I_\nu(s, \vec{\Omega}) = I_\nu(0, \vec{\Omega})\, e^{-\mu'_\nu s} + B_\nu(T)\left[1 - e^{-\mu'_\nu s}\right] \tag{43}$$

If in addition an origin can be picked along $\vec{\Omega}$ such that $I_\nu(0, \vec{\Omega}) = 0$, Eq. (43) reduces to

$$I_\nu(s, \vec{\Omega}) = B_\nu(T)\left[1 - e^{-\mu'_\nu s}\right] \tag{44}$$

To obtain the total spectral intensity at a given point, Eq. (44) must be solved for all rays passing through that point. I_ν will not generally be isotropic because of the geometry of the material. For example consider a slab of gas of thickness x and infinite extent. In this case the coordinate s may be replaced in Eq. (44) by x sec θ where θ is the angle between $\vec{\Omega}$ and the normal to the slab face. The spectral flux leaving one face of the slab is given by

$$F_{\nu+} = \int_{2\pi} I_\nu(x, \Omega) \cos\theta \, d\Omega \tag{45}$$

or

$$F_{\nu+} = 2\pi \int_0^{\pi/2} B_\nu(T)[1 - \exp(-\mu'_\nu x \sec\theta)] \sin\theta \cos\theta \, d\theta \tag{46}$$

Recourse to numerical methods is necessary to evaluate the above integral. Even in this very idealized case a simple solution is not obtained. Furthermore, observed radiation is never strictly monochromatic so integration over some frequency range is always needed for any practical solution. Since the frequency dependence of the absorption coefficient is usually complicated, approximation methods are generally employed to compute the flux. These methods frequently make use of appropriately defined "averages."

Since the flux can always be obtained if the intensity is known, we prefer to treat the latter quantity in the averaging process. An average over a small frequency interval $\Delta\nu$ may be defined

$$\overline{I(s)}^{\Delta\nu} \equiv \frac{1}{\Delta\nu} \int_{\Delta\nu} I_\nu(s) \, d\nu \tag{47}$$

and under conditions for which Eq. (44) is valid

$$\overline{I(s)}^{\Delta\nu} = \frac{1}{\Delta\nu}\int_{\Delta\nu} B_\nu(T)\left[1 - e^{-\mu'_\nu s}\right] d\nu$$

$$= \frac{1}{\Delta\nu}\int_{\Delta\nu} B_\nu(T)\, d\nu - \frac{1}{\Delta\nu}\int_{\Delta\nu} B_\nu(T)\, e^{-\mu'_\nu s}\, d\nu$$

$$= \overline{B(T)}^{\Delta\nu} - \frac{1}{\Delta\nu}\int_{\Delta\nu} B_\nu(T)\, e^{-\mu'_\nu s}\, d\nu \qquad (48)$$

If the frequency interval is taken small enough so that $B_\nu(T)$ varies little over that interval then we may approximate:

$$\overline{I(s)}^{\Delta\nu} \cong B_\nu(T)\left[1 - \frac{1}{\Delta\nu}\int_{\Delta\nu} e^{-\mu'_\nu s}\, d\nu\right] \qquad (49)$$

Following Elsasser[27] we define the average transmission

$$\overline{Tr(s)}^{\Delta\nu} \equiv \frac{1}{\Delta\nu}\int_{\Delta\nu} e^{-\mu'_\nu s}\, d\nu \qquad (50)$$

and rewrite Eq. (49):

$$\overline{I(s)}^{\Delta\nu} \cong B_\nu(T)\left[1 - \overline{Tr(s)}^{\Delta\nu}\right] \qquad (51)$$

A corresponding average absorption coefficient may also be defined, viz.:

$$\overline{\mu(s)}^{\Delta\nu} = \frac{-\ln \overline{Tr(s)}^{\Delta\nu}}{s} \qquad (52)$$

Expressions (50) and (52) have already been utilized in Section 5.

The ordinary Planck mean absorption coefficient is defined by

$$\overline{\mu_e} \equiv \frac{\int_0^\infty B_\nu(T)\mu'_\nu \, d\nu}{\int_0^\infty B_\nu(T) \, d\nu} \tag{53}$$

One can also define the contribution to the Planck mean over a frequency interval $\Delta\nu$:

$$\overline{\mu_e}^{\Delta\nu} \equiv \frac{\int_{\Delta\nu} B_\nu(T)\mu'_\nu \, d\nu}{\int_0^\infty B_\nu(T) \, d\nu} \tag{54}$$

Now for the optically thin case each monochromatic transmission function may be expanded and second-order terms neglected

$$e^{-\mu'_\nu s} \cong 1 - \mu'_\nu s \tag{55}$$

in which case Eq. (48) leads to

$$\overline{I_\nu(s)}^{\Delta\nu} = \left[\frac{1}{\Delta\nu}\int_{\Delta\nu} B_\nu(T)\mu'_\nu(s) \, d\nu\right] s$$

$$= \frac{\sigma T^4}{\pi} \overline{\mu_e}^{\Delta\nu} s \tag{56}$$

Just as the total intensity may be calculated from Eqs. (54) and (56) in the optically thin case by summing over all those intervals $\Delta\nu$ which contribute appreciably to the total, so may the total intensity be estimated for other optical cases by use of Eq. (51) and the results of the SACHA calculation for the average transmission. While this is true in principle, the actual carrying out of such computations should be guided by the proposed application of the results. We have chosen to present in Table 6 the results of the Planck mean calculation since this currently offers the best comparison with other calculations.

Table 6

The contribution to the Planck mean absorption coefficient of air, $\overline{\mu_e}$, from the vibration-rotation bands of NO. Values of $\overline{\mu_e}$ are in cm^{-1}.

T (°K)	(ρ/ρ_o) of Air				
	1.0	10^{-1}	10^{-2}	10^{-3}	10^{-4}
1000	1.0×10^{-6}	1.0×10^{-7}	1.0×10^{-8}	1.0×10^{-9}	1.0×10^{-10}
2000	7.1×10^{-5}	7.1×10^{-6}	7.1×10^{-7}	7.1×10^{-8}	7.1×10^{-9}
3000	2.4×10^{-4}	2.3×10^{-5}	2.1×10^{-6}	1.4×10^{-7}	6.3×10^{-9}
4000	2.3×10^{-4}	1.5×10^{-5}	6.9×10^{-7}	2.4×10^{-8}	7.7×10^{-10}
5000	1.1×10^{-4}	4.7×10^{-6}	1.6×10^{-7}	4.9×10^{-9}	1.4×10^{-10}

8. DISCUSSION OF RESULTS

The results of the average transmission calculation are presented in the appendix of this report in the form of graphs. Two types of graphs are presented: average transmission plotted (1) as a function of slab thickness and (2) as a function of frequency for a particular slab thickness. Results are grouped according to line half-width, density, and temperature.

Care must be exercised in comparing curves which correspond to different line half-widths since the sample frequency interval $\Delta\nu$ is also different. (As the line width is decreased more frequency subdivisions within $\Delta\nu$ are required to give adequate line shape detail, hence the size of $\Delta\nu$ must be decreased to keep the number of such frequency points within the limits specified in the machine program.) The differences occurring where the optically thin case applies are of this type. For example, for half-widths of 1.0 cm^{-1} and 0.1 cm^{-1} frequency intervals of $\Delta\nu$ = 100 cm^{-1} and 50 cm^{-1}, respectively, were used. For a line half-width of 0.01 cm^{-1}, however, it was necessary to further decrease the frequency interval to $\Delta\nu$ = 6 cm^{-1} which is small enough so that there is considerable variation in the number of lines contained within the interval for different central frequencies. Thus, at 1800 cm^{-1} there are 62 lines in $\Delta\nu$ compared to 9 at 2000 cm^{-1}, 13 at 3700 cm^{-1}, and 28 at 3500 cm^{-1}. Variation in line strength is also a factor which may cause different curve shape when the number of lines included in an interval is small.

Some of the curves (e.g., ν = 2000 cm^{-1}) display an apparently anomalous behavior which is caused by the absence of lines in a particular region. For example, no lines are contained on the atlas in the frequency region from 2022.06 cm^{-1} to 2368.11 cm^{-1} since this is a "window" between the $\Delta\nu$ = 1 and $\Delta\nu$ = 2 band sequences. When the curves for σ = 1.0 cm^{-1} are calculated, the frequency interval is taken to be

$\Delta\nu$ = 100 cm^{-1}; and when this is centered at 2000 cm^{-1}, approximately one quarter of the interval is "pure window" which establishes an effective minimum average transmission for the interval. For σ 0.1 cm^{-1}, $\Delta\nu$ is decreased to 50 cm^{-1} so that none of the "window" falls within the sample interval.

The plots of average transmission versus frequency presented here, therefore, cannot be considered precise in their detail since the number of frequency intervals, and sizes of the intervals in the case of very narrow lines, is probably marginal.

It is nevertheless clear from the transmission curves that line half-width is of crucial importance to the radiation transport problem, especially at low densities where the line widths are essentially pure Doppler (see Tables 3 and 4). The dependence on line shape is probably more critical than the present calculation would indicate on two counts. First, the use of a single unresolved line with an effective half-width for lines which are actually Λ-doubled loses most of its meaning as soon as the splitting becomes comparable to the true width of one of the component lines (see figure on p. 64). Equation (36) shows that for J values as small as 10 the Λ-doubling is several times the Doppler width and is comparable to the collision line widths at normal atmospheric densities. Since Λ-type splitting increases like J^2, under certain ρ/ρ_0 conditions the splitting can easily exceed the Doppler line widths by an order of magnitude. Under these conditions the lumping together of the two Λ-components has little meaning and further leads to average transmissions that are too high. The plots of average transmission versus slab thickness for σ = 0.01 cm^{-1} are therefore probably all too high (but see below).

Second, the use of a Lorentz line profile under conditions where Doppler broadening predominates leads to average transmissions that are too low, since the fall-off in the wings of a pure Doppler broadened line is actually exponential. Clearly, a line shape factor that is Lorentzian about the line center yet Doppler in the wings would be much more realistic.

It would .ppear that a better understanding of line profile effects in NO infrared radiation will come only through a much more detailed calculation with Λ-type doubling included throughout and using a more realistic and flexible line shape factor along with a complete parametric study of the latter.

9. REFERENCES

1. B. H. Armstrong, J. Sokoloff, R. W. Nicholls, D. H. Holland, and R. E. Meyerott, J.Q.S.R.T. 1, 143 (1961)
2. B. Kivel and K. Bailey, Tables of Radiation from High Temperature Air, AVCO Research Report No. 21 (1957)
3. M. C. Nardone, R. G. Breene, S. S. Zeldin, and T. R. Riethof, Radiance of Species in High Temperature Air, General Electric Space Sciences Laboratory Report R63SD3 (June 1963)
4. R. G. Breene, Jr., J. Chem Phys. 29, 512 (1958)
5. D. R. Churchill, S. A. Hagstrom, J. D. Weisner, and B. H. Armstrong, The Spectral Absorption Coefficient of Heated Air, Lockheed Missiles & Space Company, DASA Report Control No. 1348, Nov 1962
6. D. R. Churchill, S. A. Hagstrom, and R. K. M. Landshoff, The Calculations of Spectral Absorption in Heated Air, Lockheed Missiles & Space Company, DASA Report Control No. 1465, Dec 1963. See also D. R. Churchill, S. A. Hagstrom, and R. K. M. Landshoff, J. Quant. Spectrosc. Radiat. Transfer 4, 291 (1964)
7. G. Herzberg, Spectra of Diatomic Molecules, Van Nostrand, New York (1950)
8. E. Hill and J. H. Van Vleck, Phys. Rev. 32, 250 (1928)
9. S. S. Penner, Quantitative Molecular Spectroscopy and Gas Emissivities, Addison-Wesley, Reading, Massachusetts (1959)
10. B. L. Crawford, Jr., and H. L. Dinsmore, J. Chem. Phys. 18. 983 (1950)
11. R. G. Breene, Jr., and M. N. Todd, Jr., J. Chem. Phys. 28, 11 (1958)
12. E. R. Lippincott, J. Chem. Phys. 21, 2070 (1953)

13. E. R. Lippincott, J. Chem. Phys. 23, 603 (1955)

14. S. S. Penner and D. Weber, J. Chem. Phys. 21, 649 (1953)

15. B. Schurin and S. A. Clough, J. Chem. Phys. 38, 1855 (1963)

16. H. A. Bethe, The Specific Heat of Air up to 25,000°C, OSRD Report 369 (1942)

17. S. R. Brinkley, Jr., J. G. Kirkwood, and J. M. Richardson, Tables of the Properties of Air Along the Hugoniot Curve and the Adiabatic Terminating in the Hugoniot, OSRD Report 3550 (1944).

18. F. R. Gilmore, Equilibrium Composition and Thermodynamic Properties of Air to 24,000°K, Rand Corporation RM-1543, Santa Monica, Calif. (1955)

19. P. W. Anderson, Phys. Rev. 76, 647 (1949)

20. C. J. Tsao and B. Curnutte, J. Quant. Spectrosc. Radiat. Transfer 2, 41 (1962)

21. W. S. Benedict and R. Herman, J. Quant. Spectrosc. Radiat. Transfer 3, 265 (1963)

22. D. Weber and S. S. Penner, J. Chem. Phys. 21, 1503 (1953)

23. H. E. White, Introduction to Atomic Spectra, McGraw-Hill, New York (1934)

24. J. H. Van Vleck, Phys. Rev. 33, 467 (1929)

25. R. S. Mulliken and A. Christy, Phys. Rev. 38, 87 (1931)

26. V. A. Ambartsumyan, Theoretical Astrophysics, Pergamon Press, New York (1958)

27. W. M. Elsasser, Heat Transfer by Infrared Radiation in the Atmosphere, Harvard Meteorological Studies #6, Harvard University Printing Office, Cambridge, Mass. (1942)

Appendix A

AVERAGE TRANSMISSION PLOTS

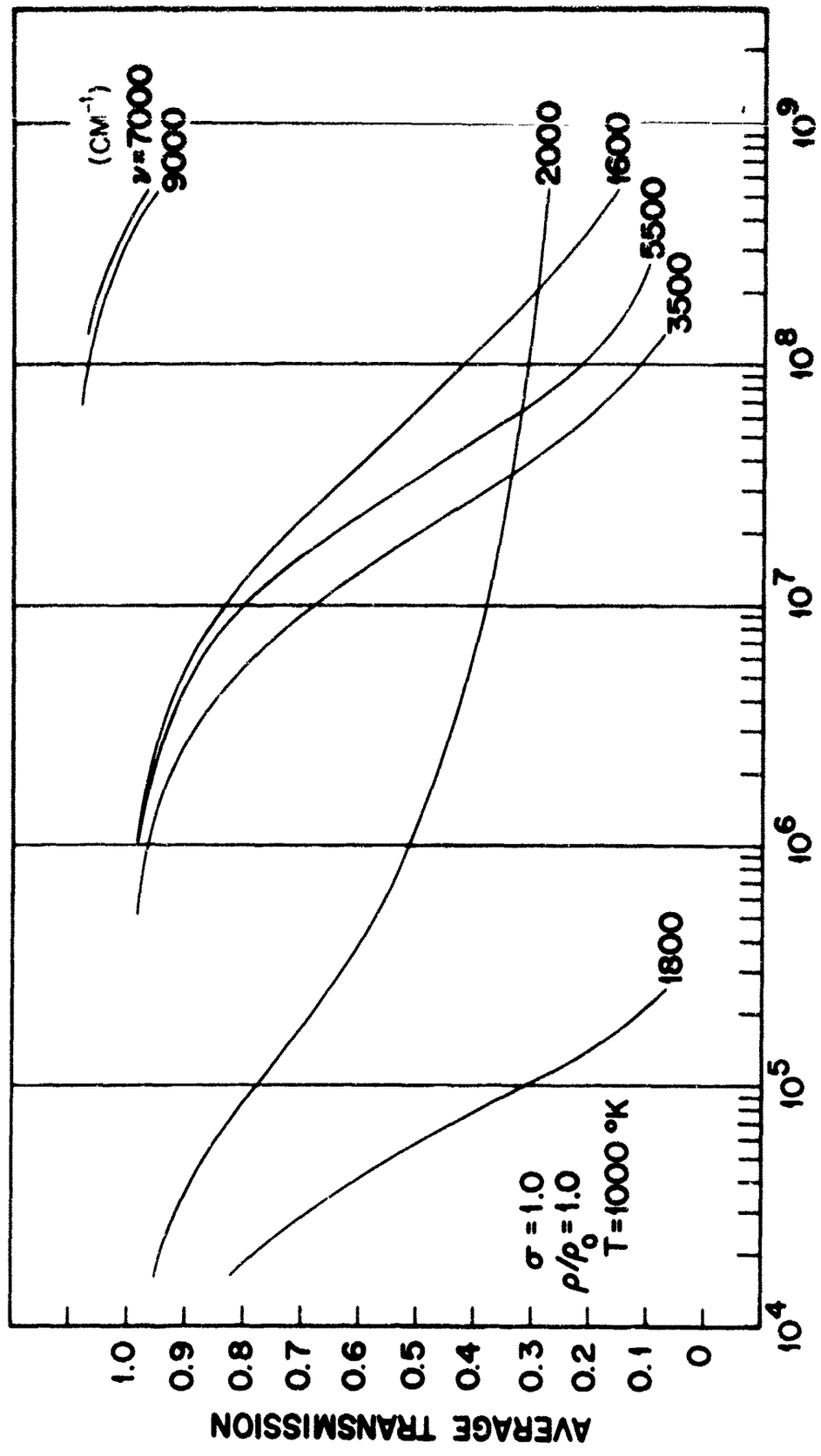

Fig. 1 Average transmission of optical radiation through a slab of heated air as a function of optical path length: contribution from vibration-rotation bands of nitric oxide.

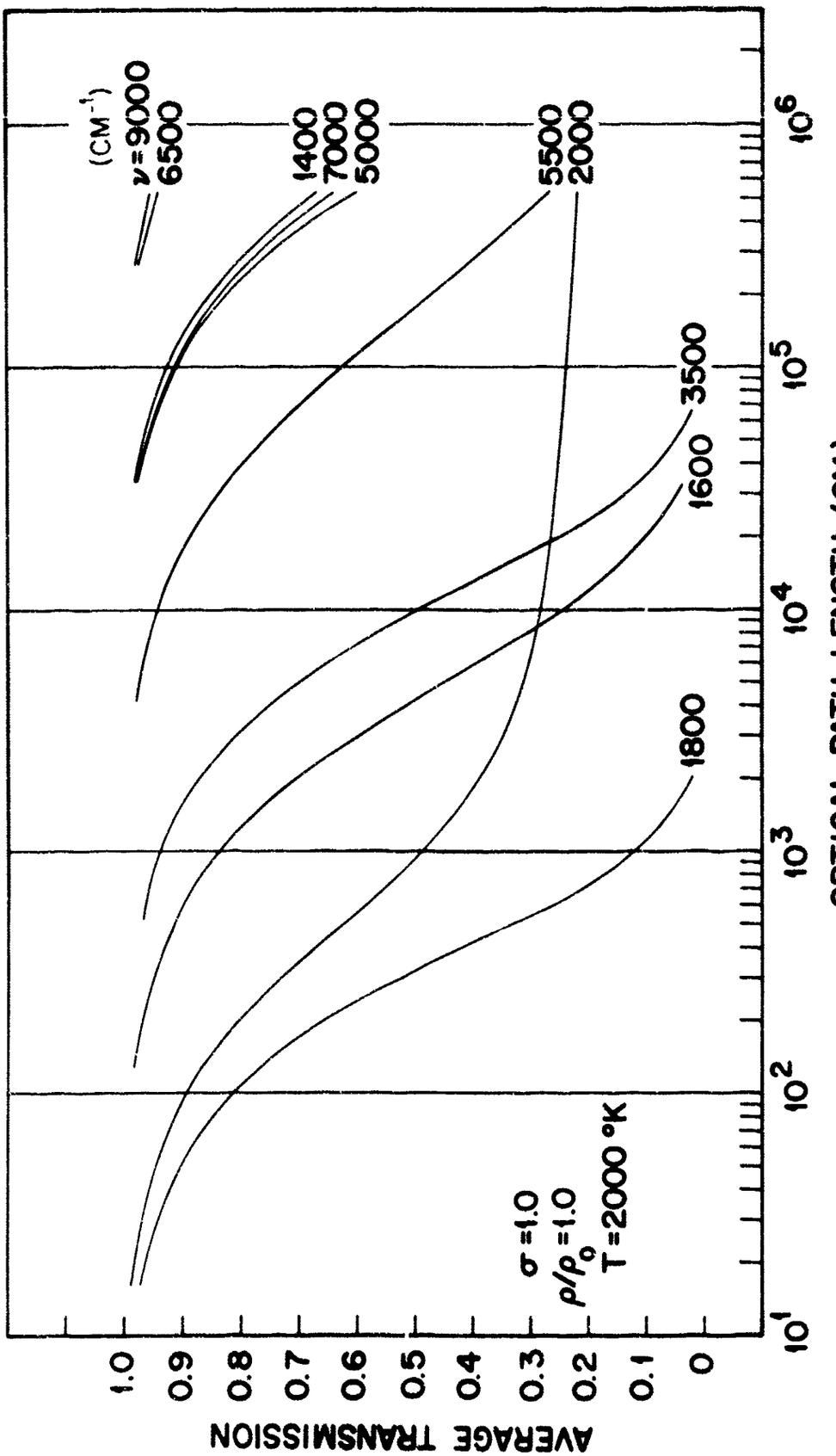

Fig. 2 Average transmission of optical radiation through a slab of heated air as a function of optical path length: contribution from vibration-rotation bands of nitric oxide.

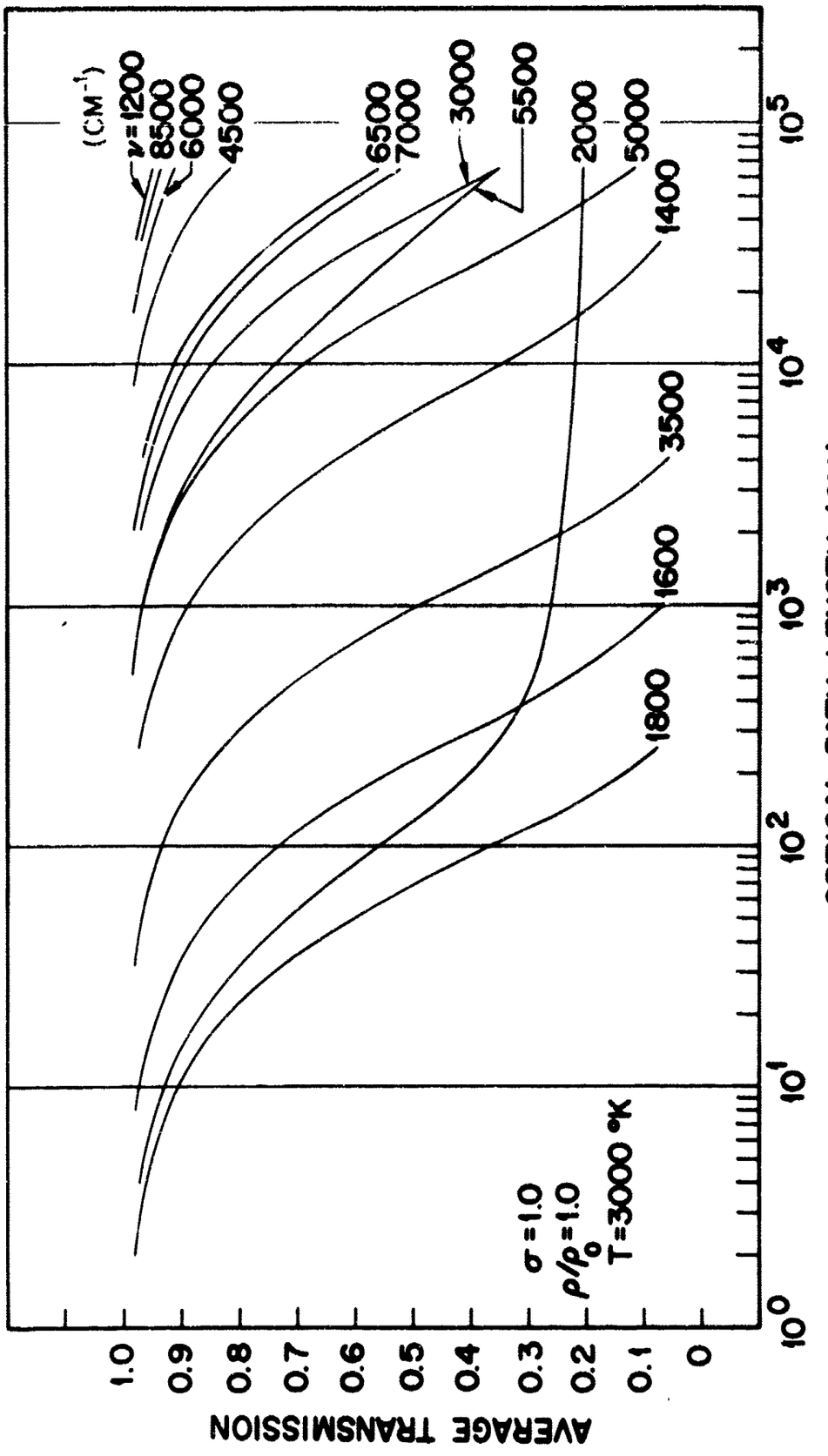

Fig. 3 Average transmission of optical radiation through a slab of heated air as a function of optical path length: contribution from vibration-rotation bands of nitric oxide.

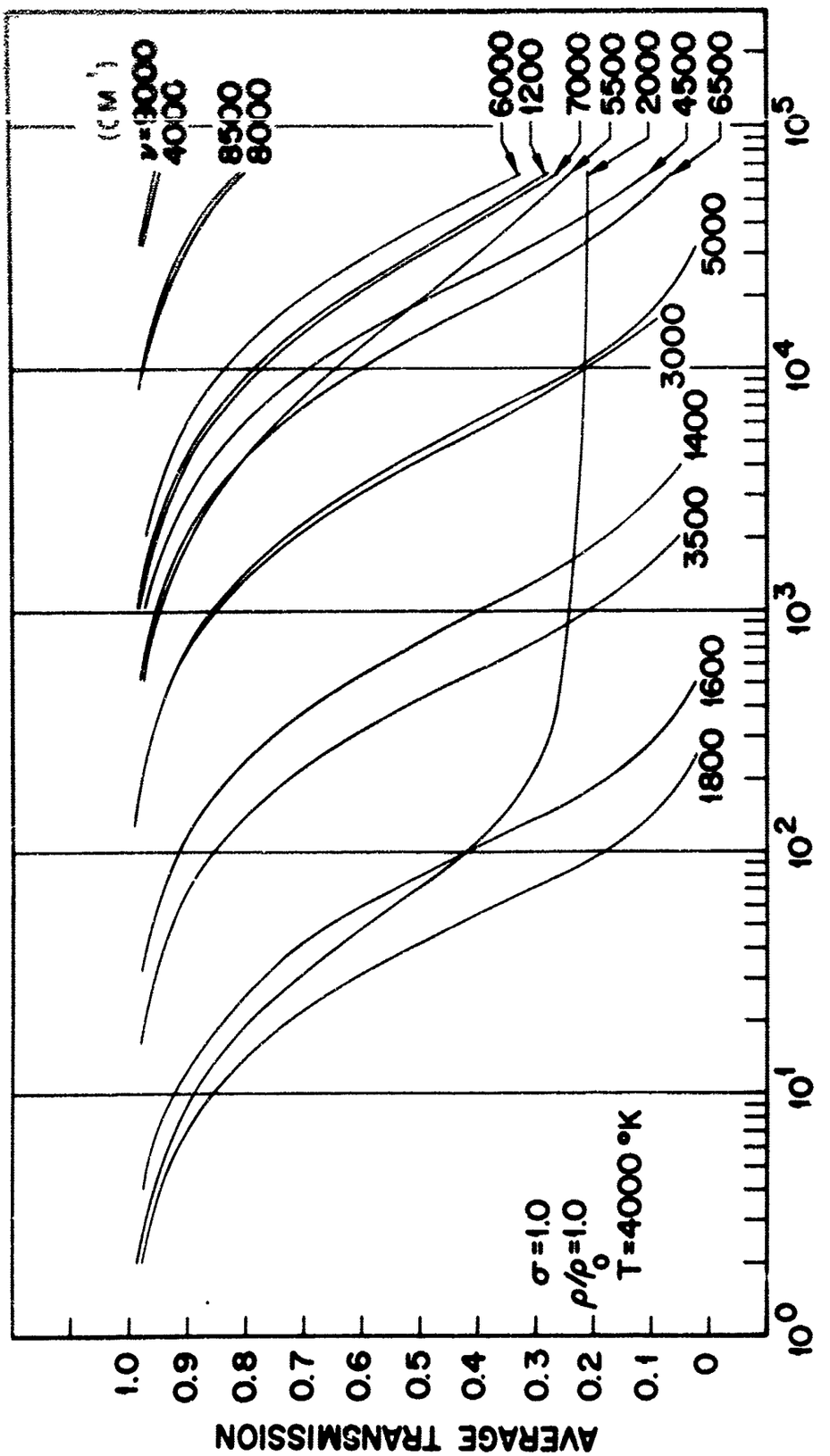

Fig. 4 Average transmission of optical radiation through a slab of heated air as a function of optical path length: contribution from vibration-rotation bands of nitric oxide.

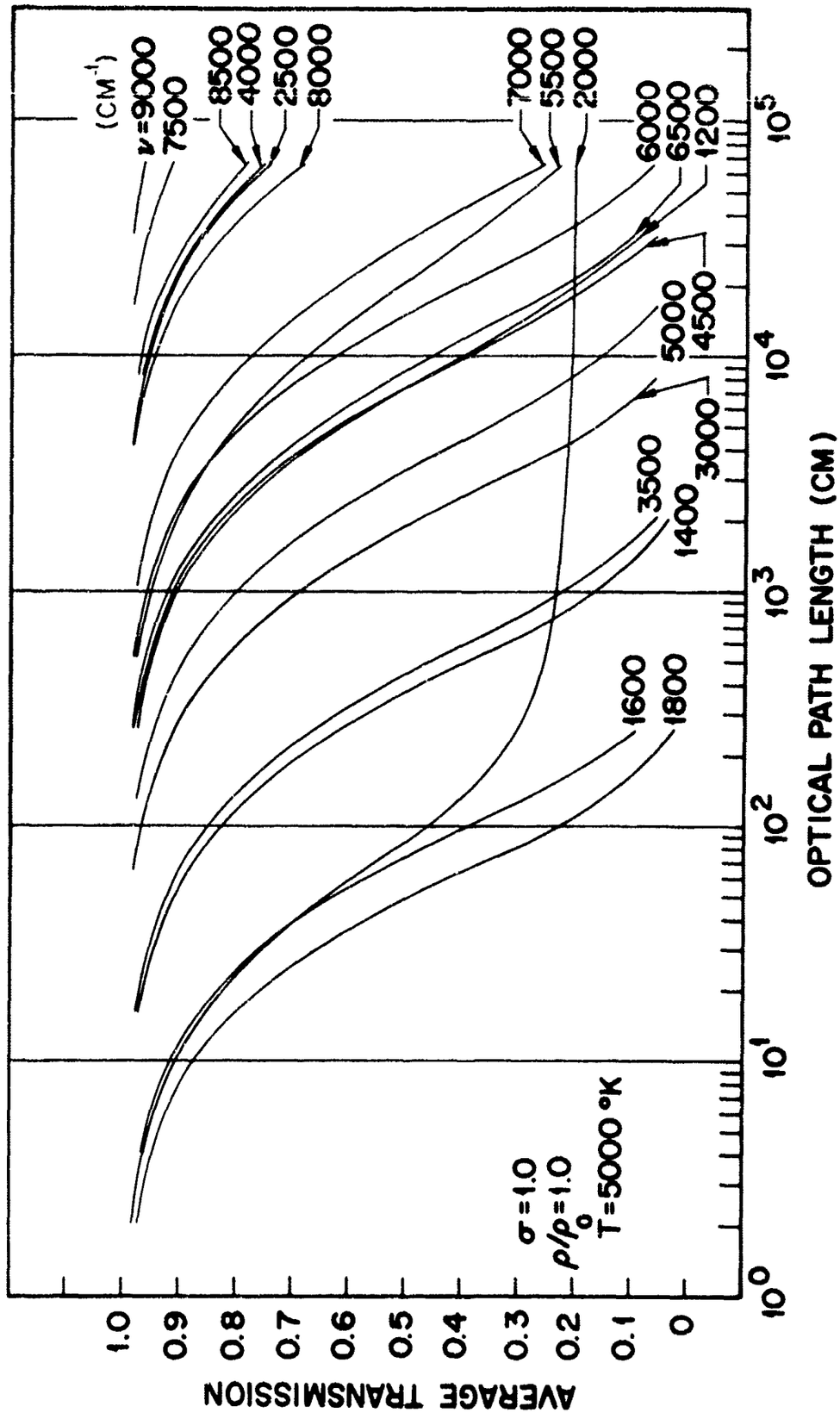

Fig. 5 Average transmission of optical radiation through a slab of heated air as a function of optical path length: contribution from vibration-rotation bands of nitric oxide.

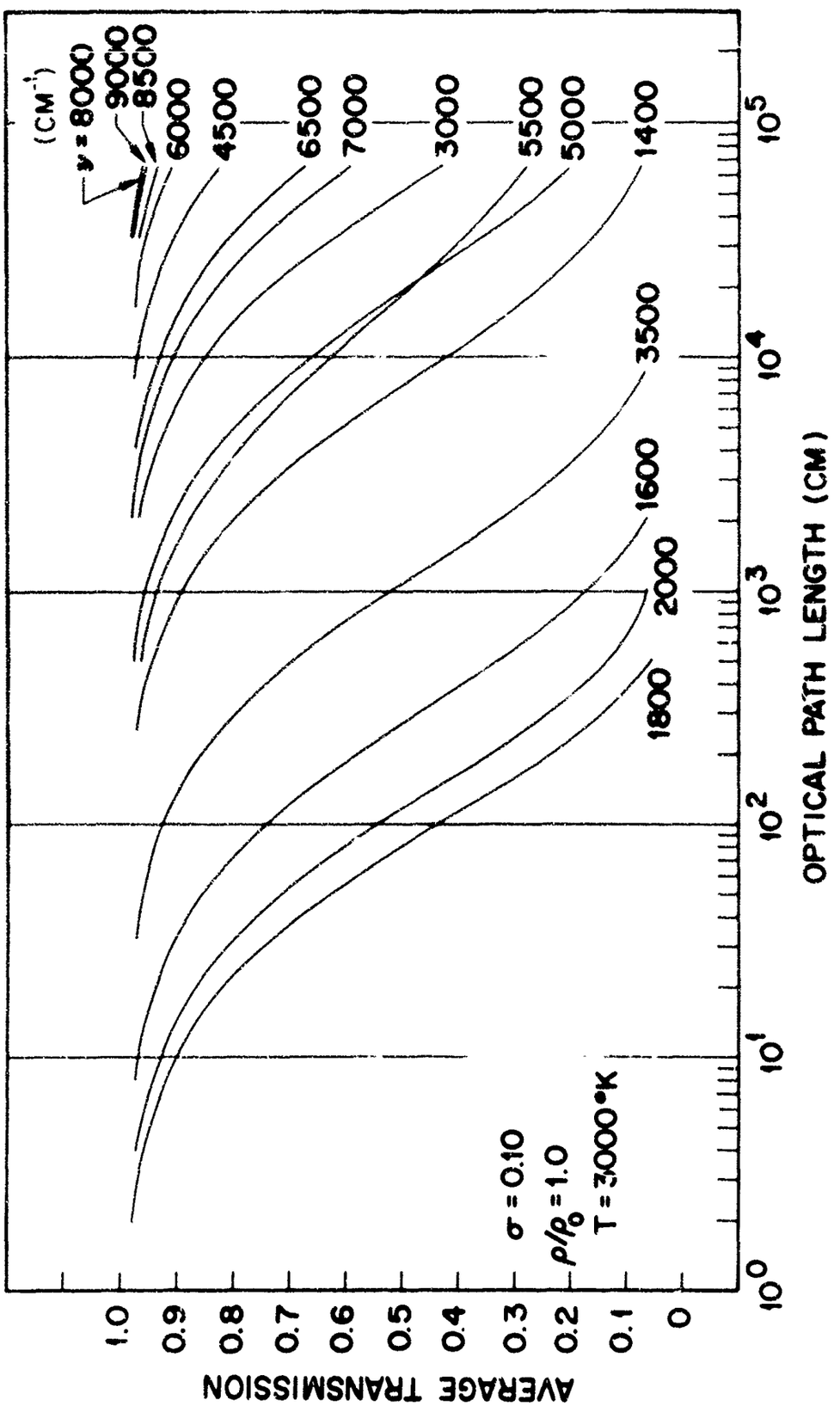

Fig. 6 Average transmission of optical radiation through a slab of heated air as a function of optical path length: contribution from vibration-rotation bands of nitric oxide.

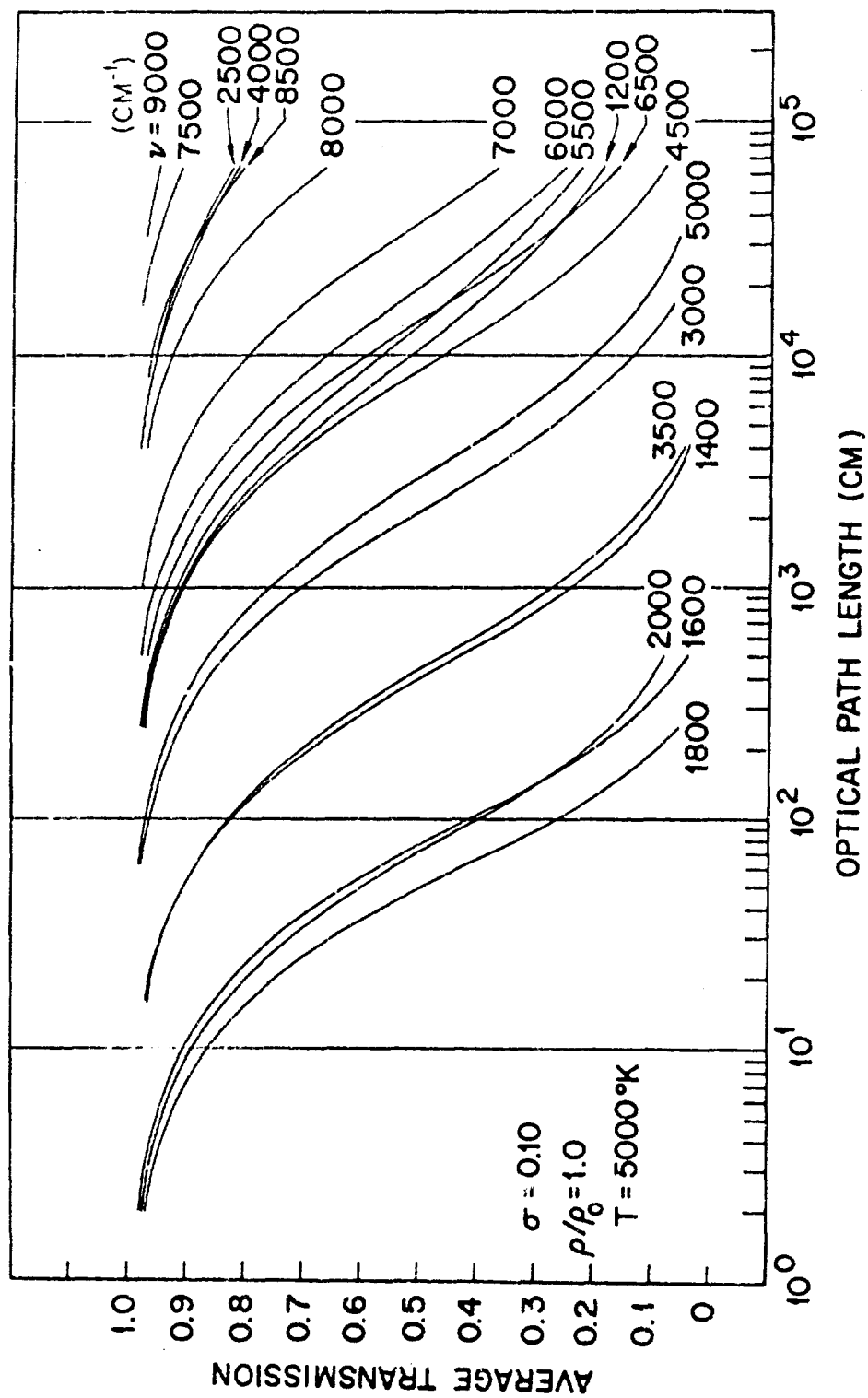

Fig. 7 Average transmission of optical radiation through a slab of heated air as a function of optical path length: contribution from vibration-rotation bands of nitric oxide.

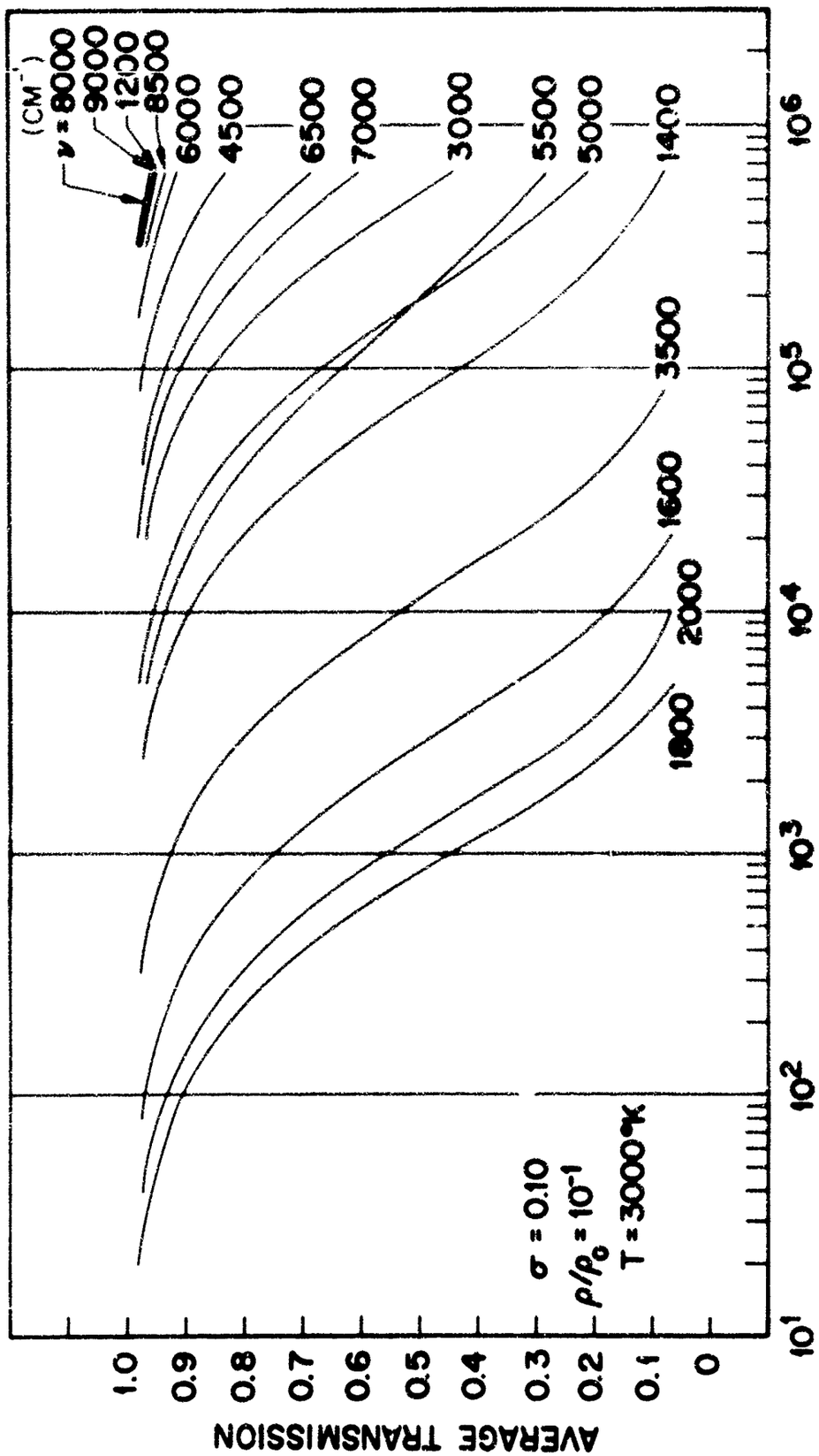

Fig. 8 Average transmission of optical radiation through a slab of heated air as a function of optical path length: contribution from vibration-rotation bands of nitric oxide.

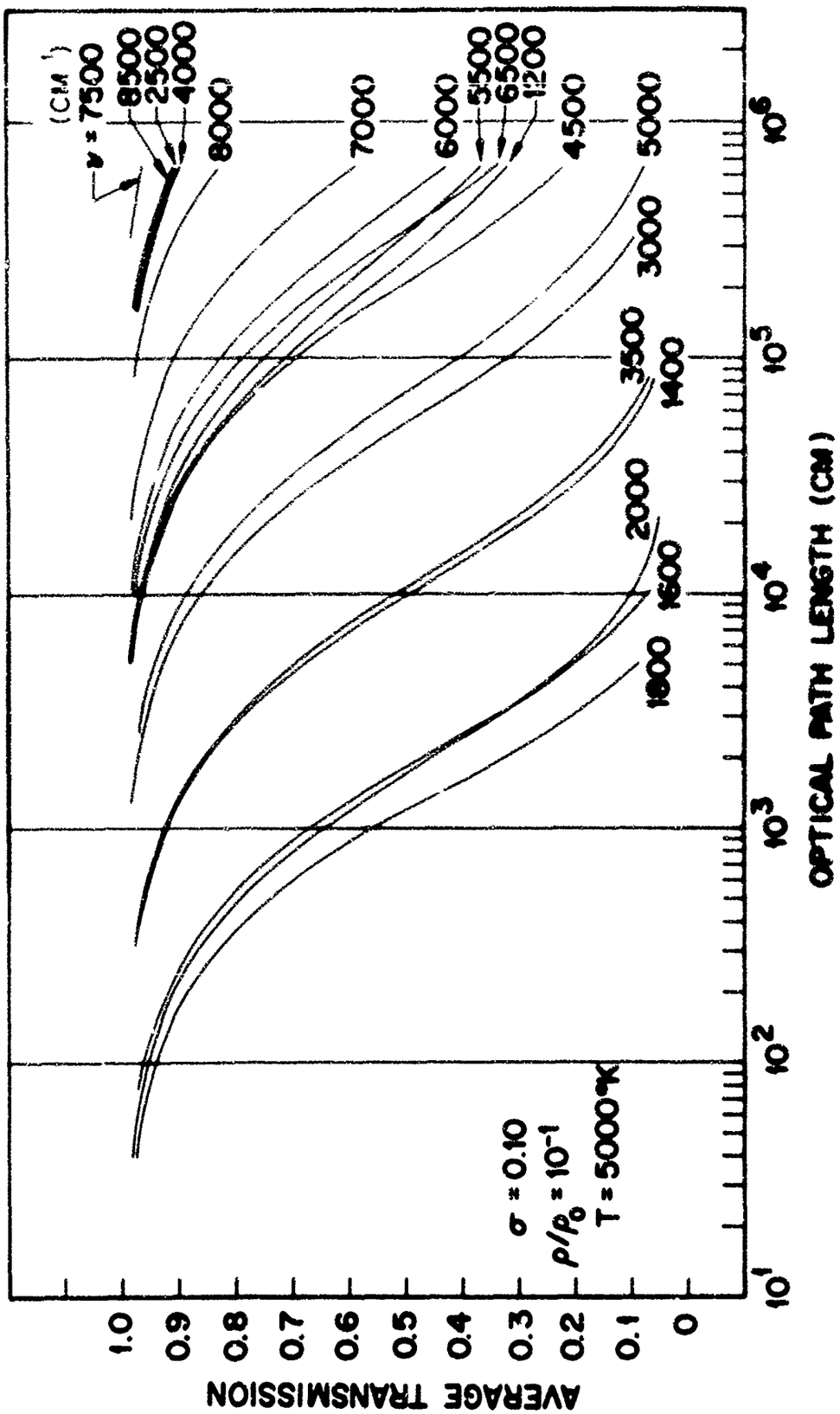

Fig. 9 Average transmission of optical radiation through a slab of heated air as a function of optical path length: contribution from vibration-rotation bands of nitric oxide.

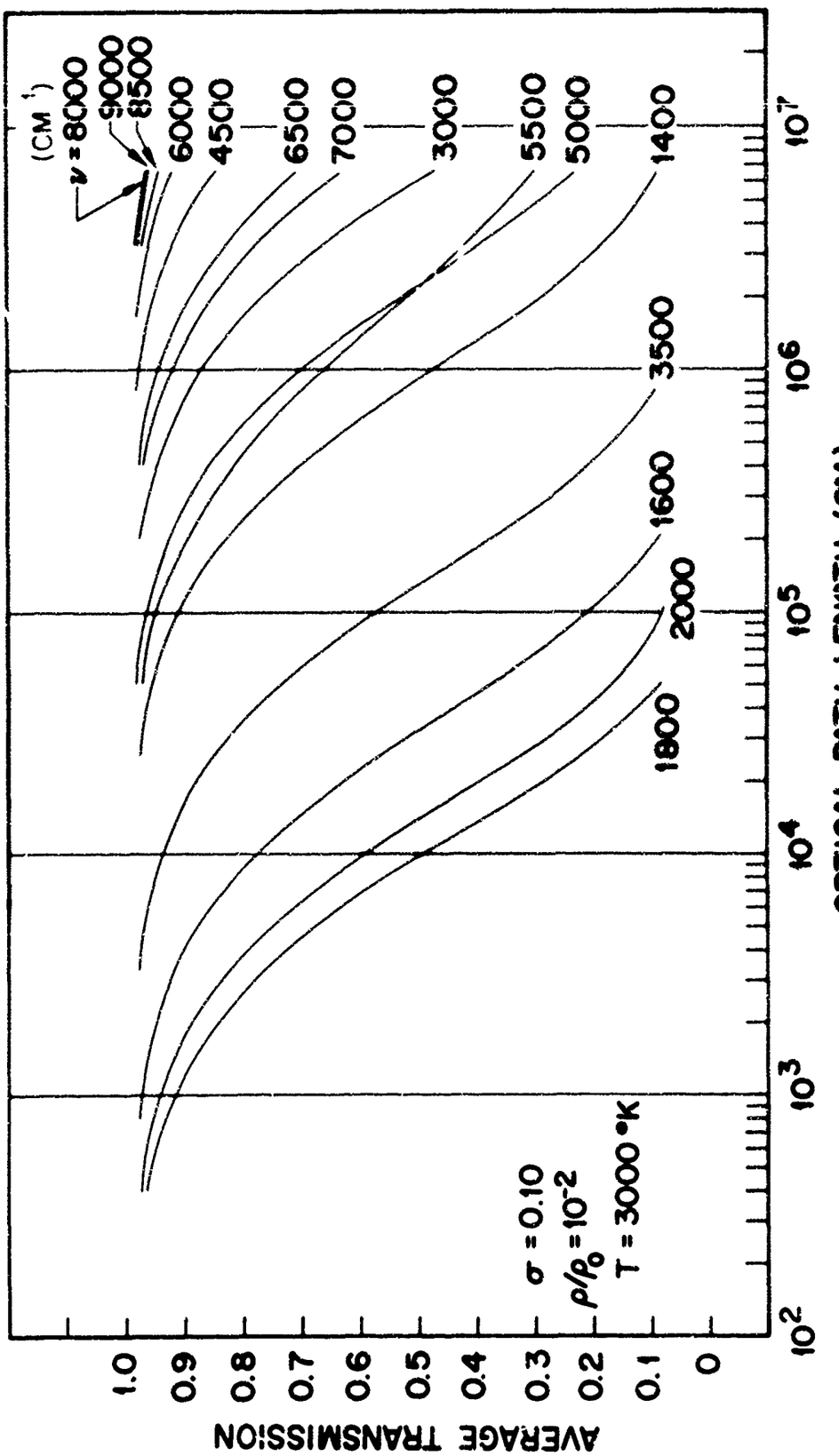

Fig. 10 Average transmission of optical radiation through a slab of heated air as a function of optical path length: contribution from vibration-rotation bands of nitric oxide.

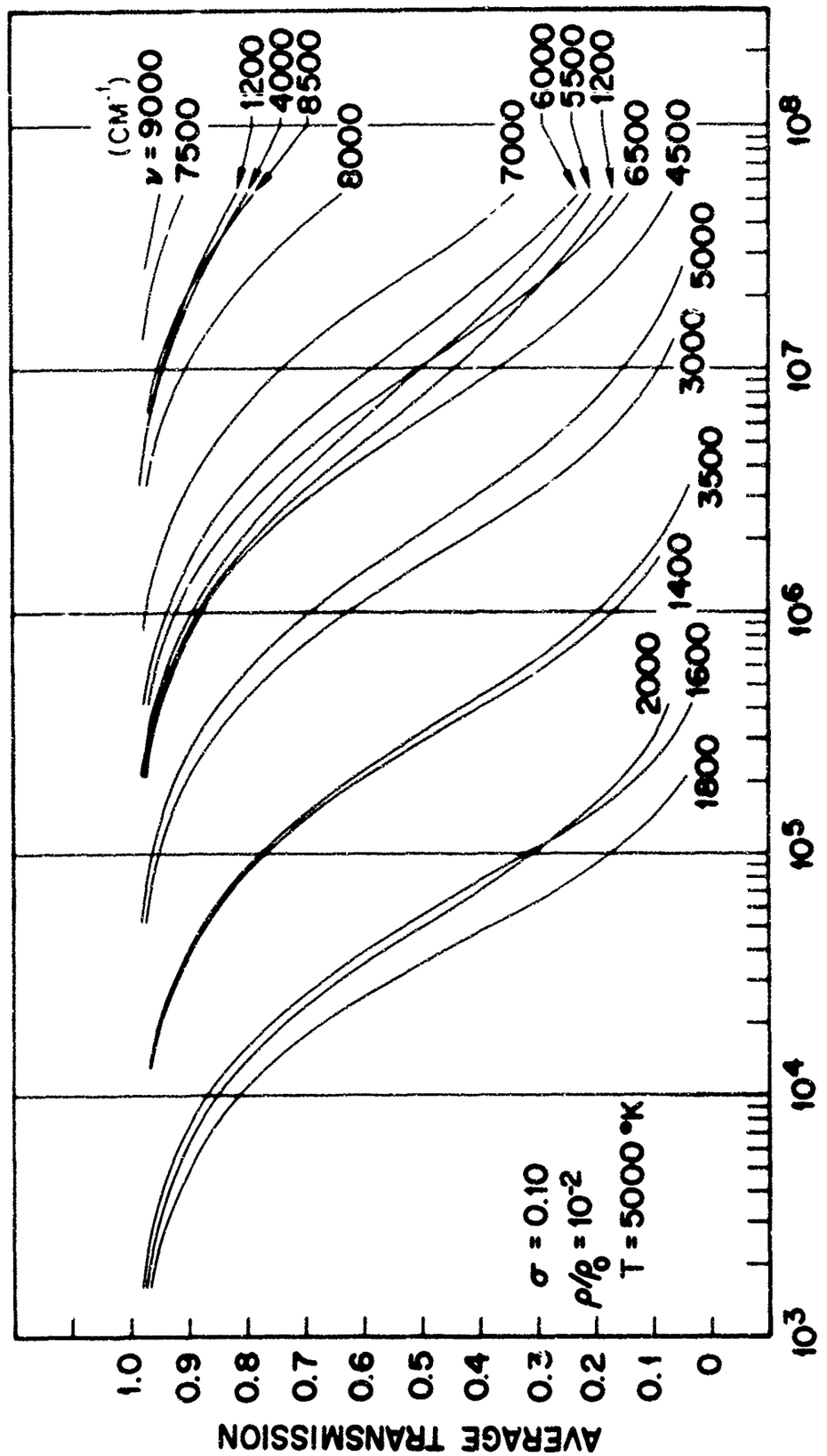

Fig. 11 Average transmission of optical radiation through a slab of heated air as a function of optical path length: contribution from vibration-rotation bands of nitric oxide.

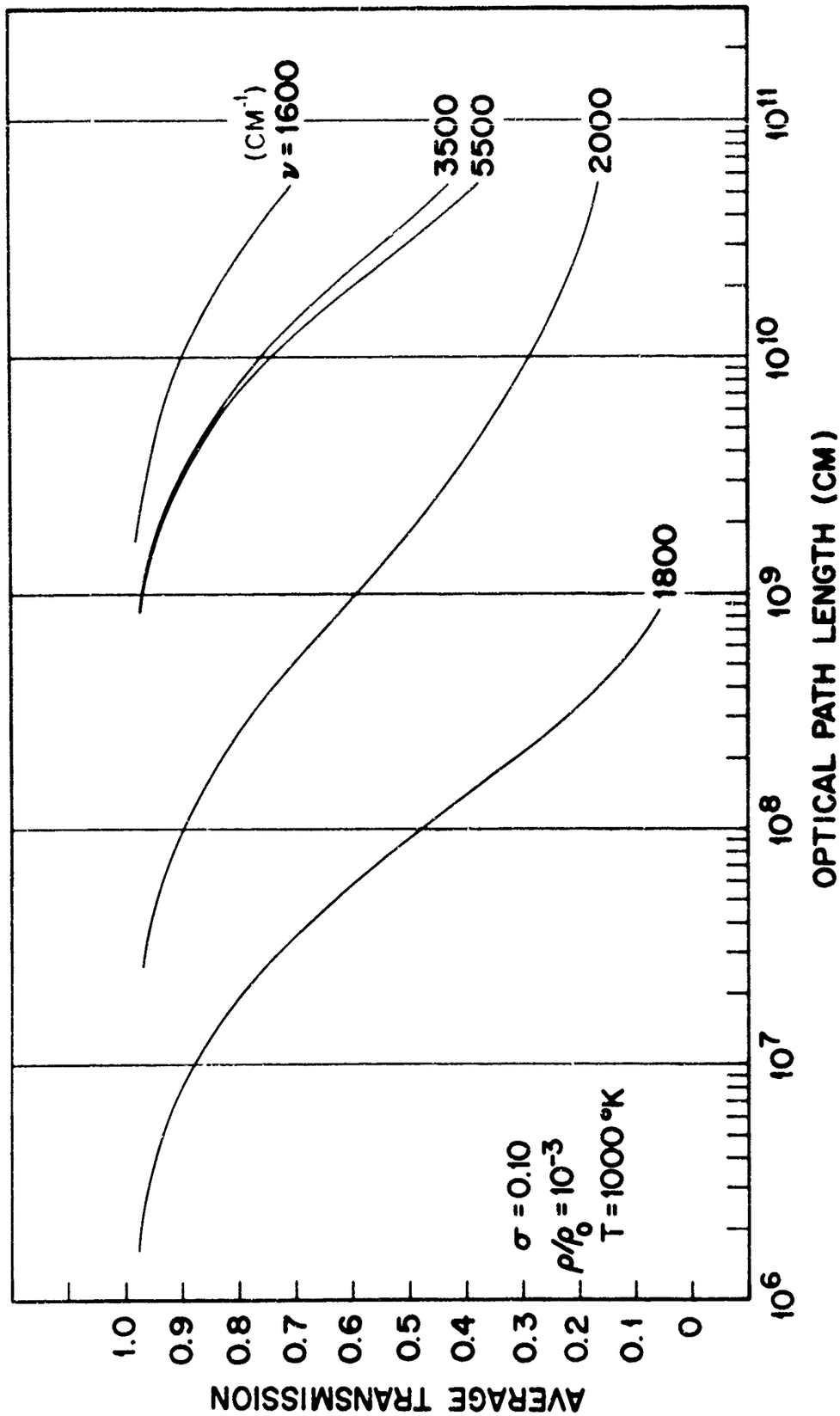

Fig. 12 Average transmission of optical radiation through a slab of heated air as a function of optical path length: contribution from vibration-rotation bands of nitric oxide.

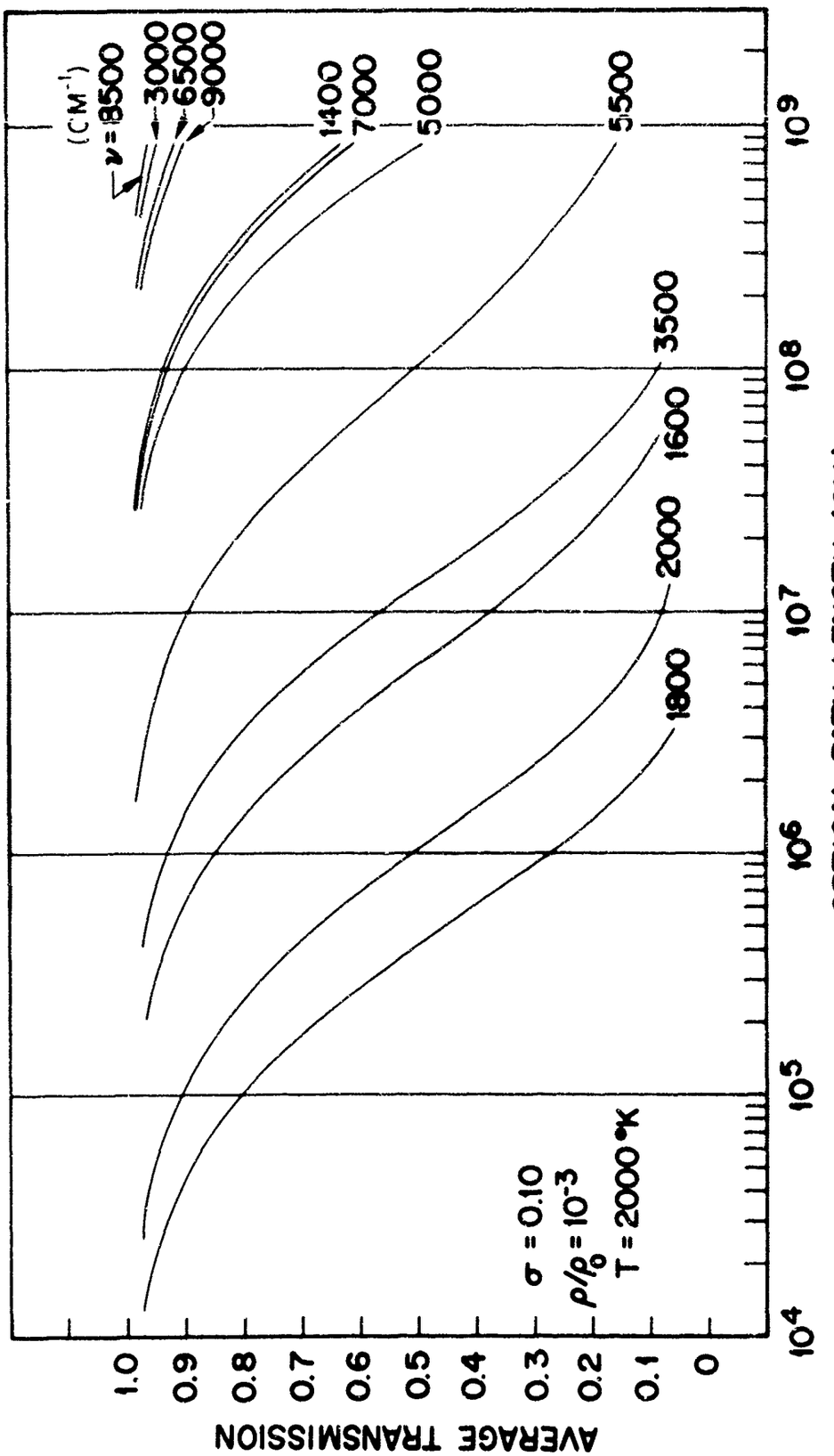

Fig. 13 Average transmission of optical radiation through a slab of heated air as a function of optical path length: contribution from vibration-rotation bands of nitric oxide.

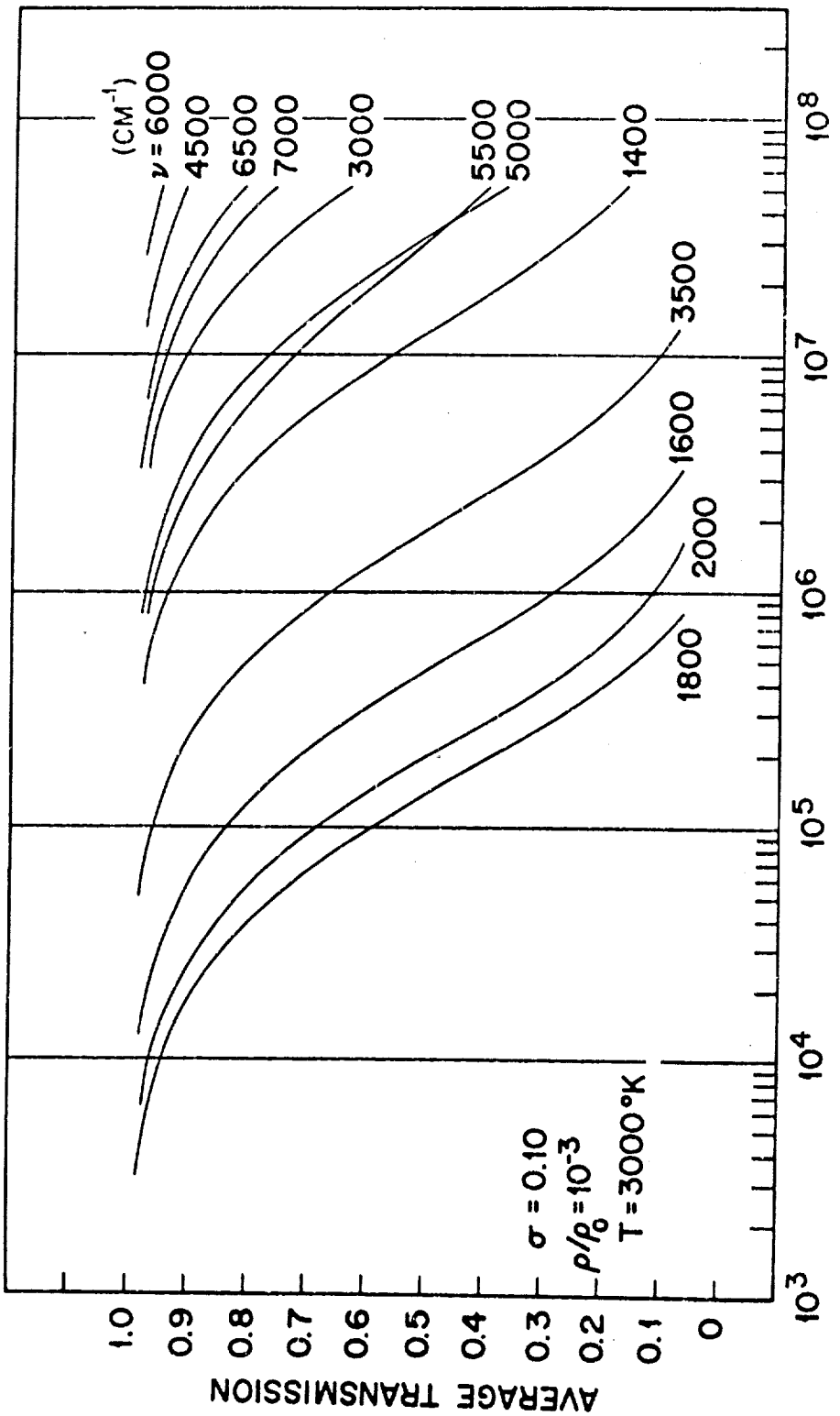

Fig. 14 Average transmission of optical radiation through a slab of heated air as a function of optical path length: contribution from vibration-rotation bands of nitric oxide.

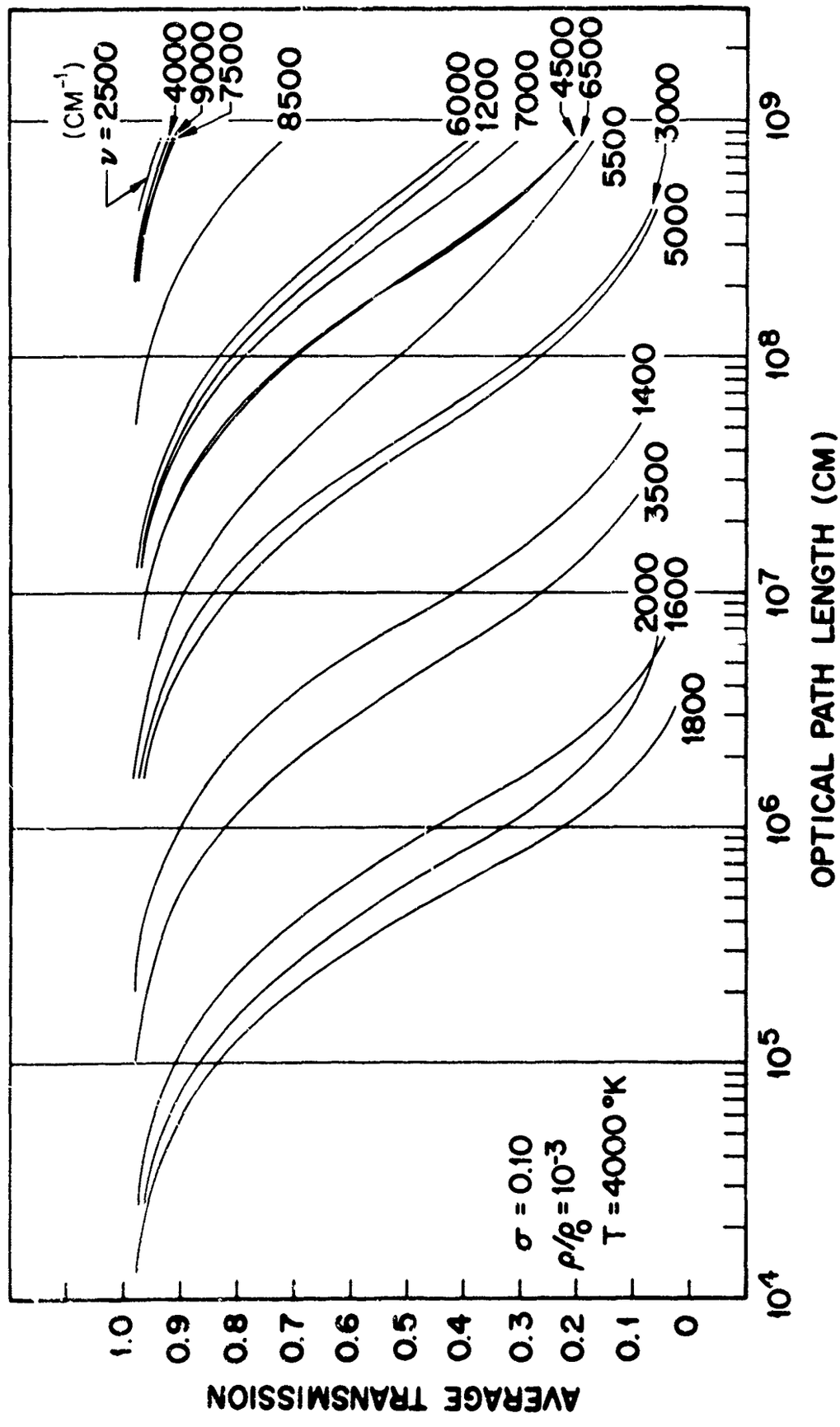

Fig. 15 Average transmission of optical radiation through a slab of heated air as a function of optical path length: contribution from vibration-rotation bands of nitric oxide.

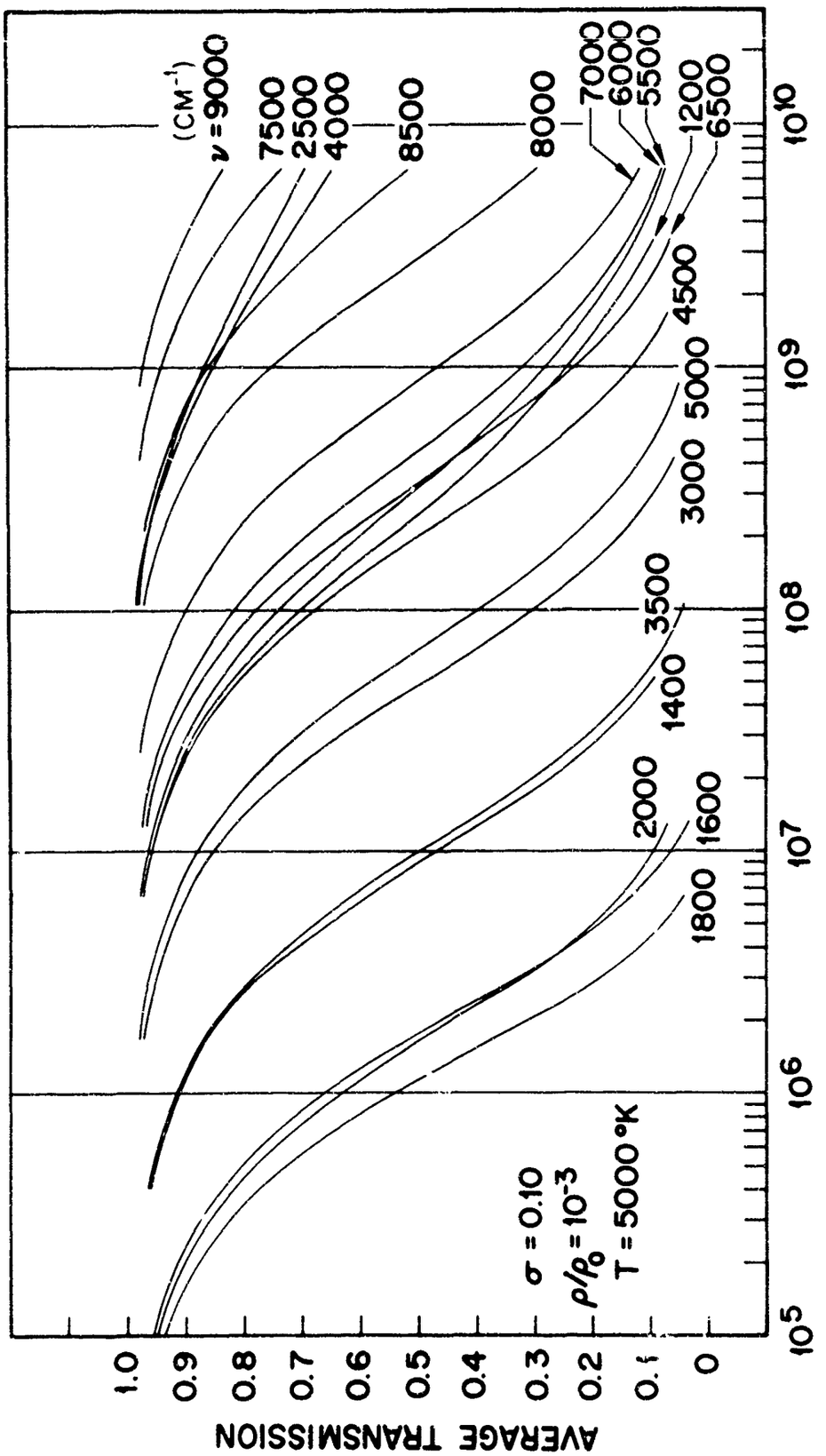

Fig. 16 Average transmission of optical radiation through a slab of heated air as a function of optical path length: contribution from vibration-rotation bands of nitric oxide.

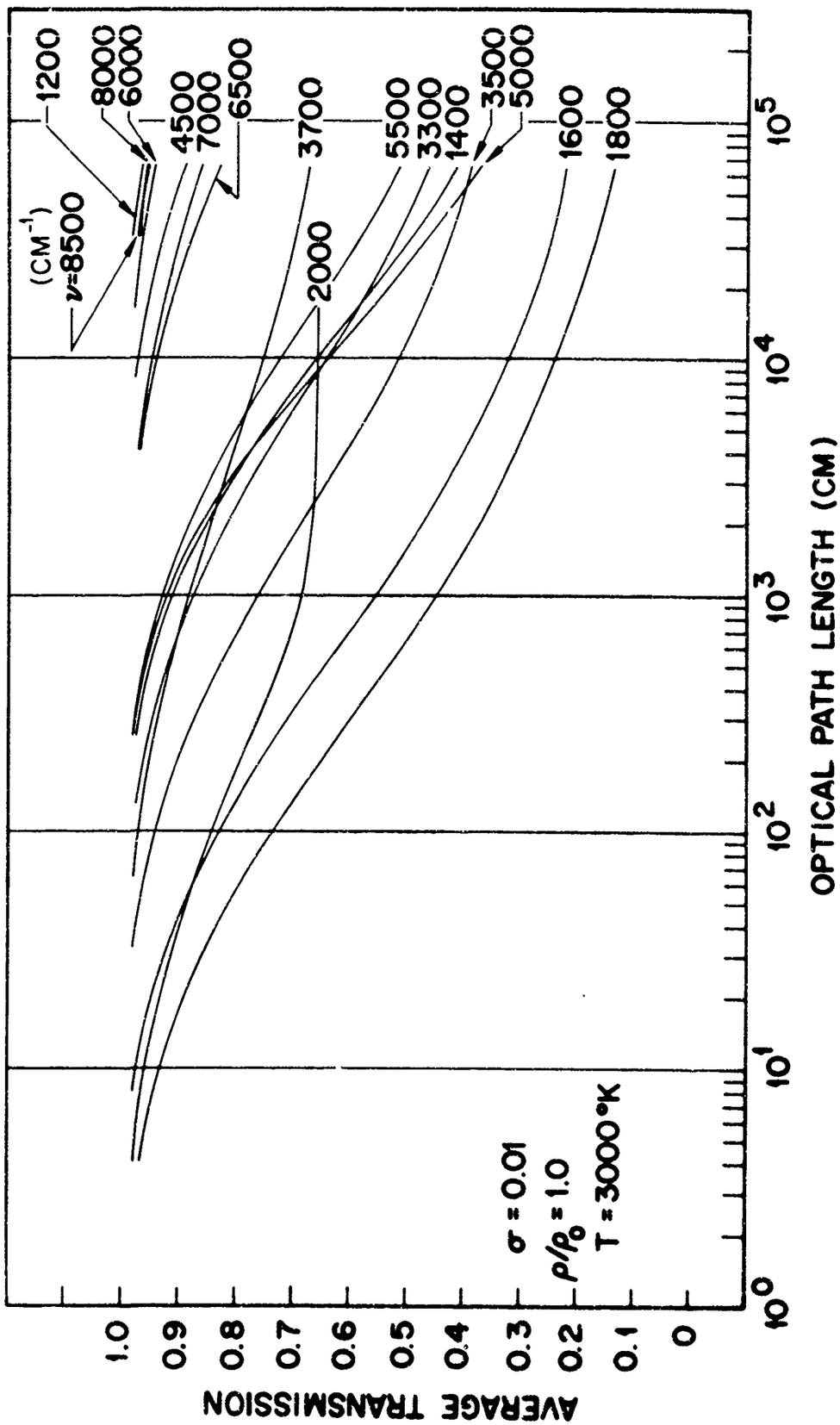

Fig. 17 Average transmission of optical radiation through a slab of heated air as a function of optical path length: contribution from vibration-rotation bands of nitric oxide.

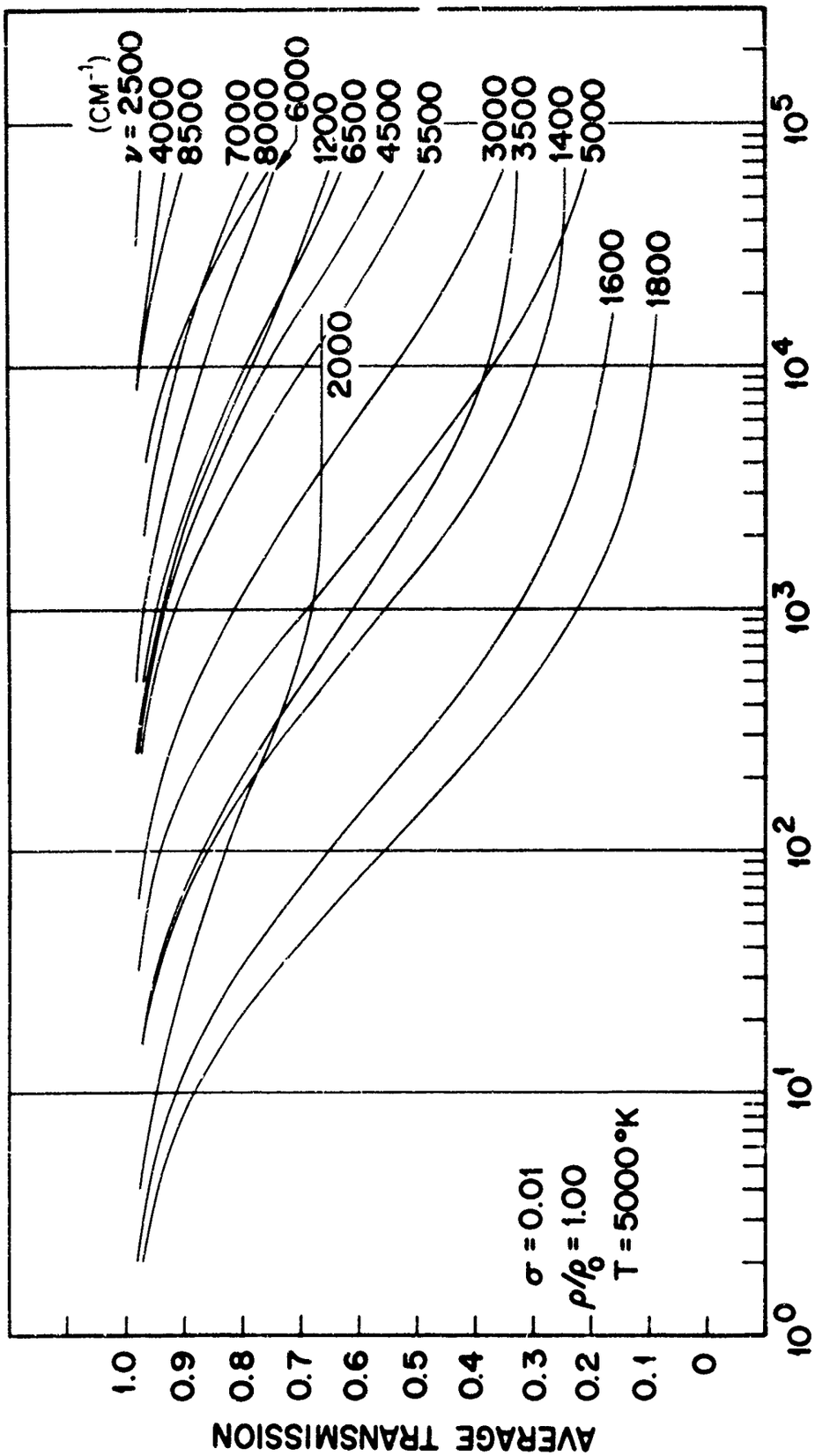

Fig. 18 Average transmission of optical radiation through a slab of heated air as a function of optical path length: contribution from vibration-rotation bands of nitric oxide.

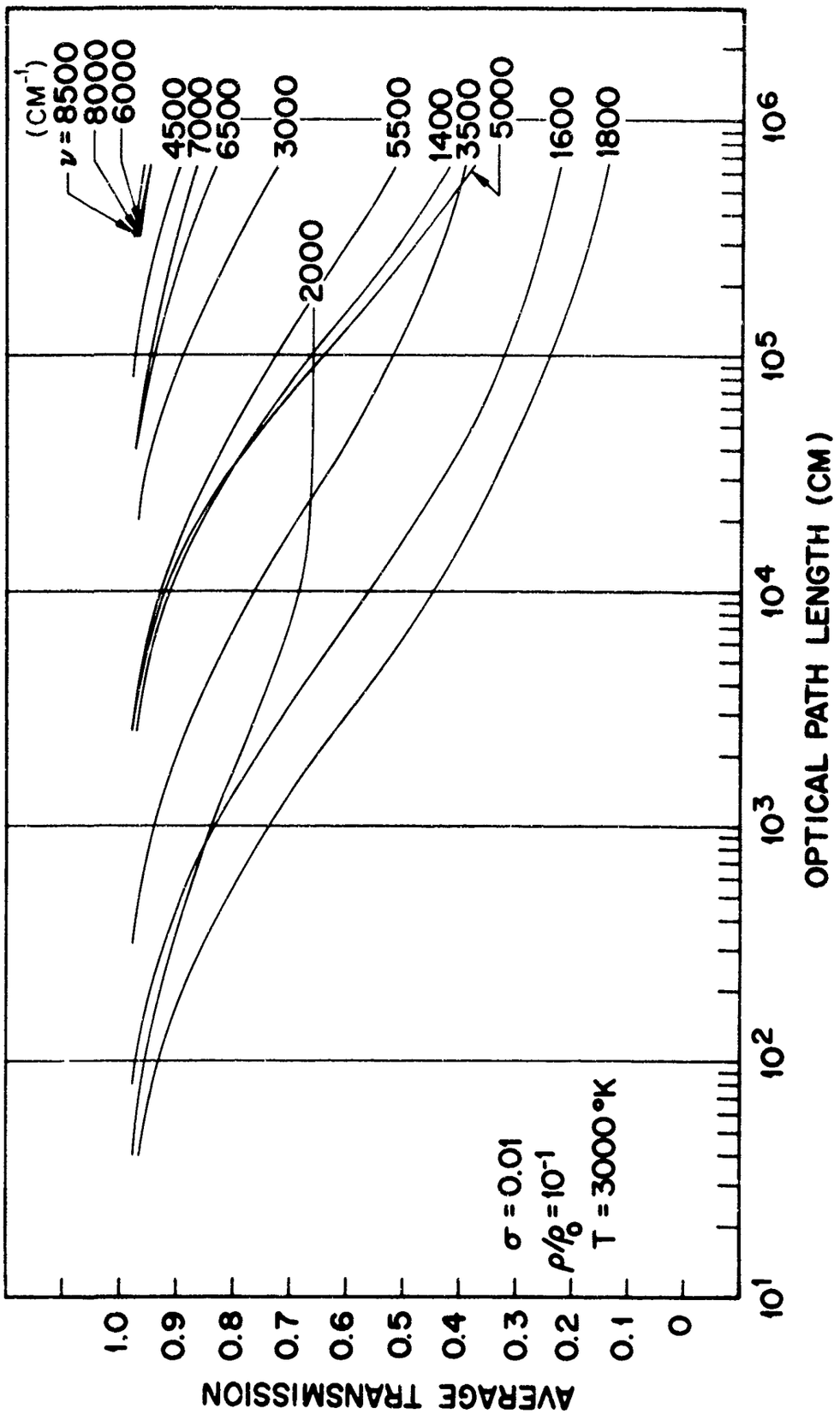

Fig. 19 Average transmission of optical radiation through a slab of heated air as a function of optical path length: contribution from vibration-rotation bands of nitric oxide.

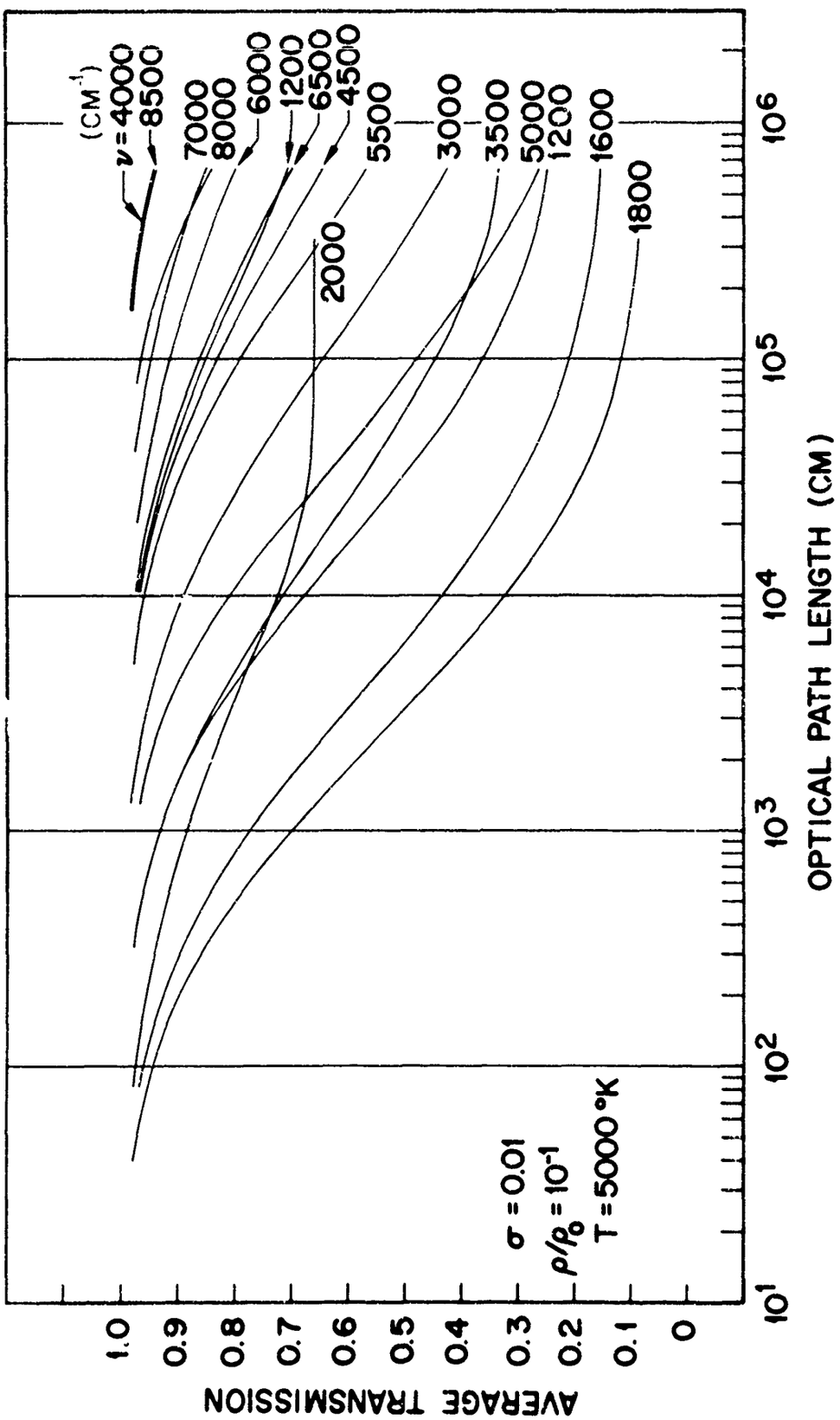

Fig. 20 Average transmission of optical radiation through a slab of heated air as a function of optical path length: contribution from vibration-rotation bands of nitric oxide.

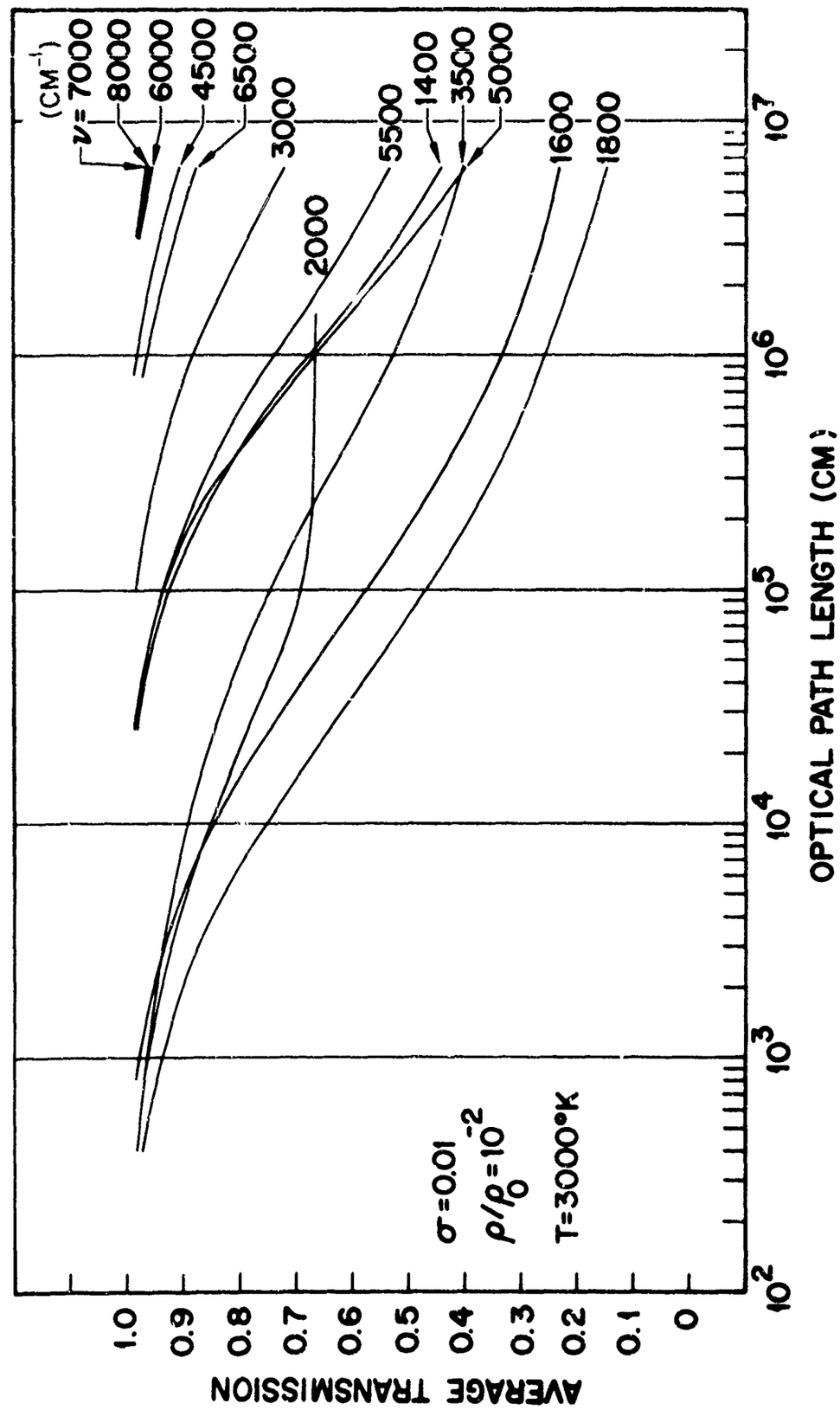

Fig. 21 Average transmission of optical radiation through a slab of heated air as a function of optical path length: contribution from vibration-rotation bands of nitric oxide.

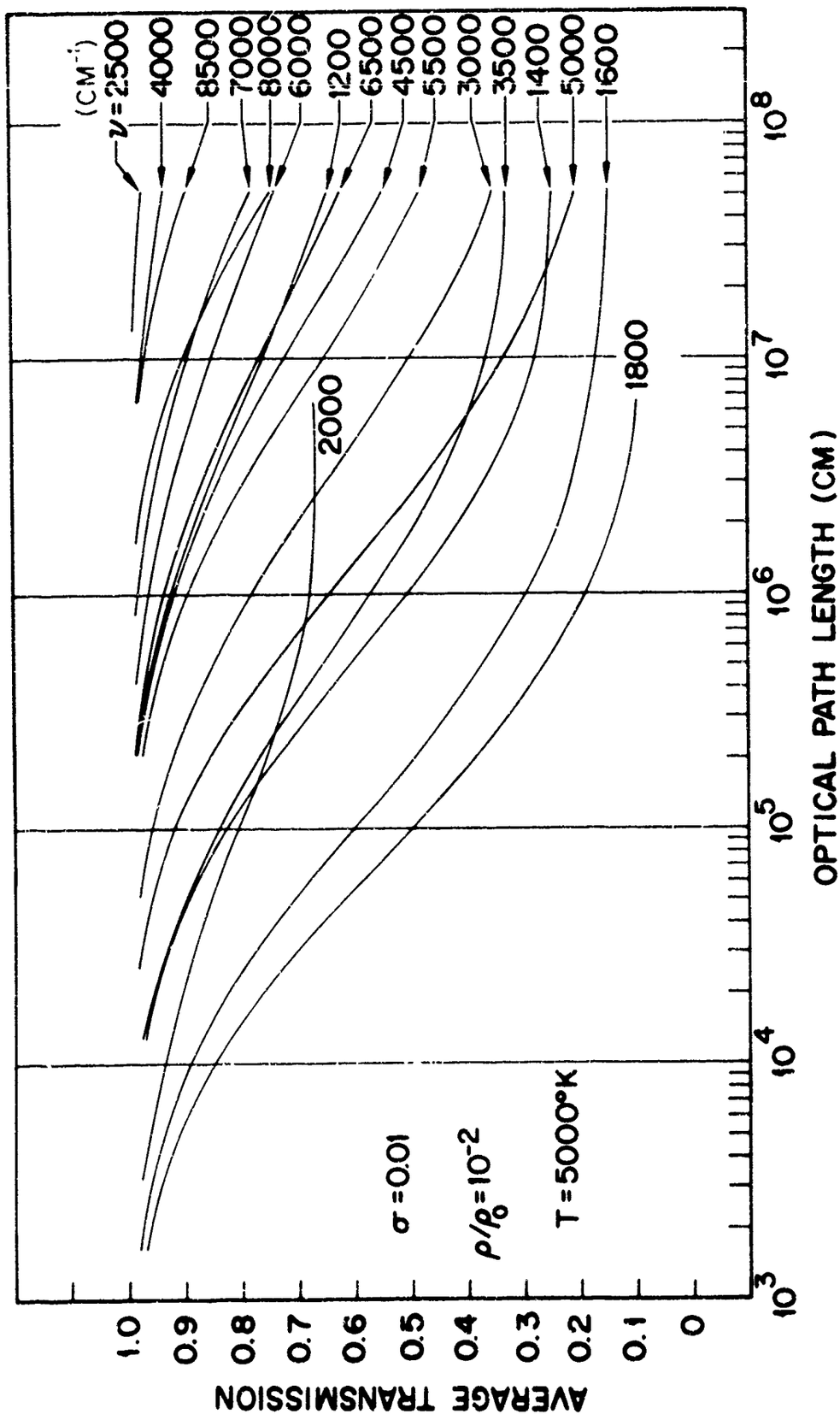

Fig. 22 Average transmission of optical radiation through a slab of heated air as a function of optical path length: contribution from vibration-rotation bands of nitric oxide.

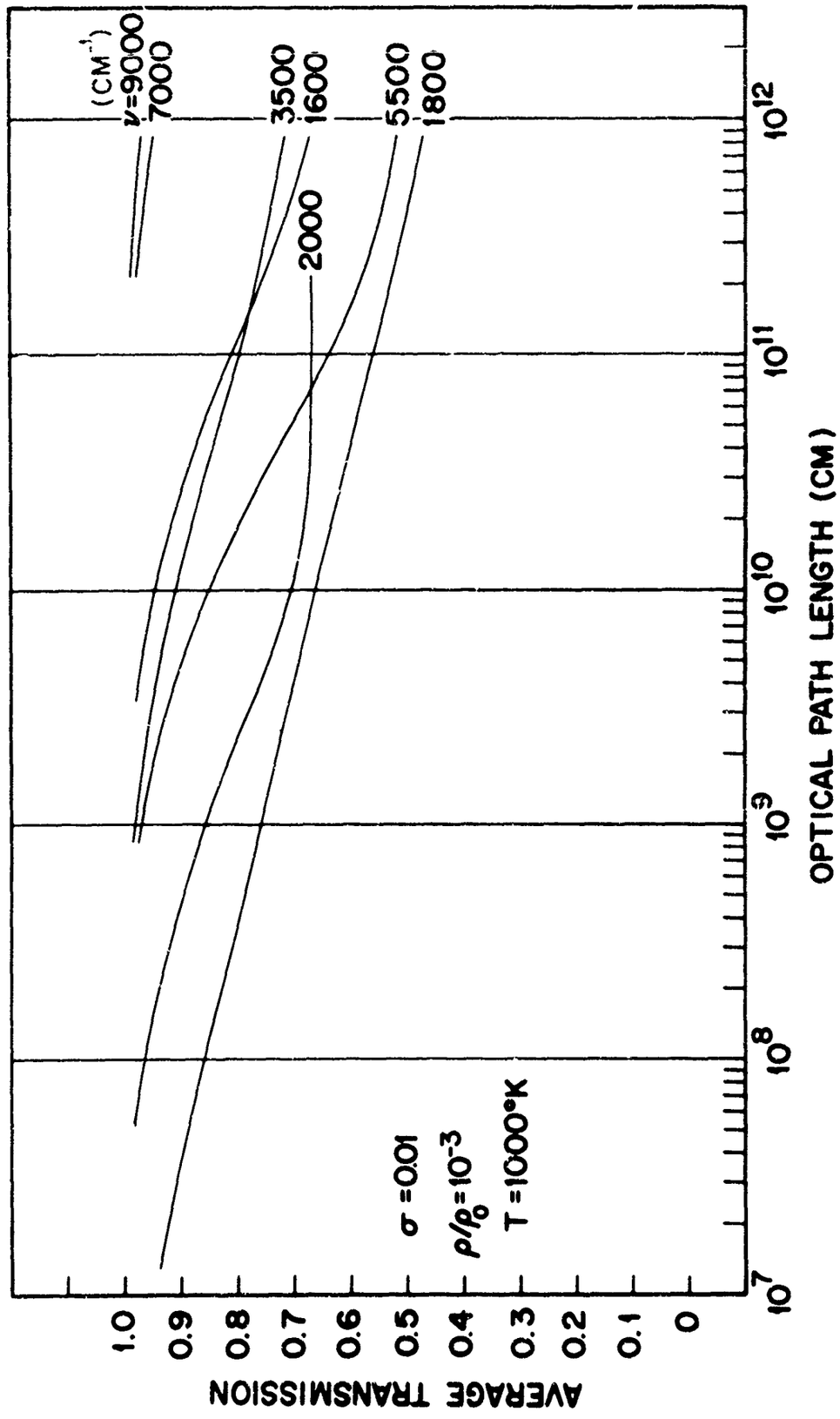

Fig. 23 Average transmission of optical radiation through a slab of heated air as a function of optical path length: contribution from vibration-rotation bands of nitric oxide.

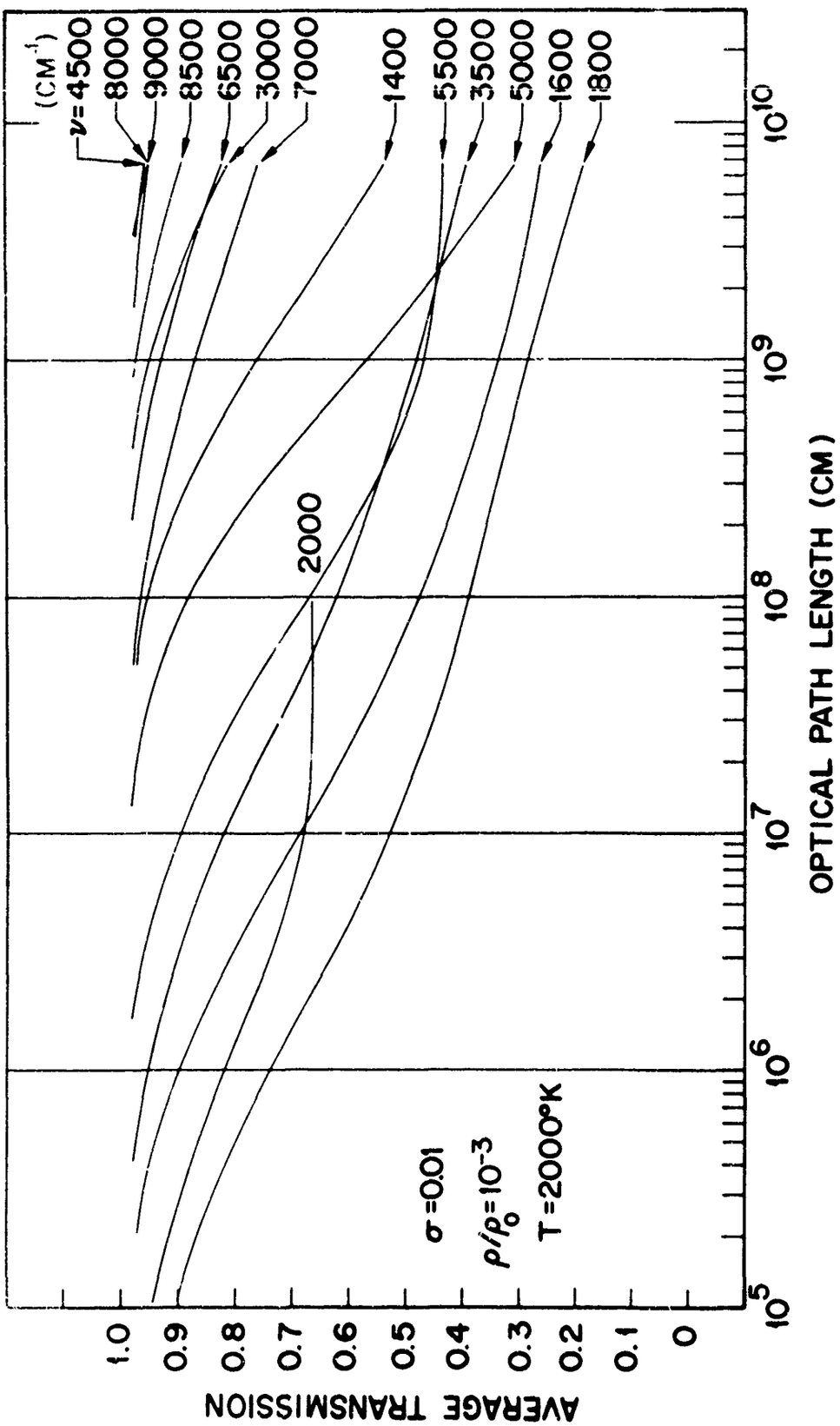

Fig. 24 Average transmission of optical radiation through a slab of heated air as a function of optical path length: contribution from vibration-rotation bands of nitric oxide.

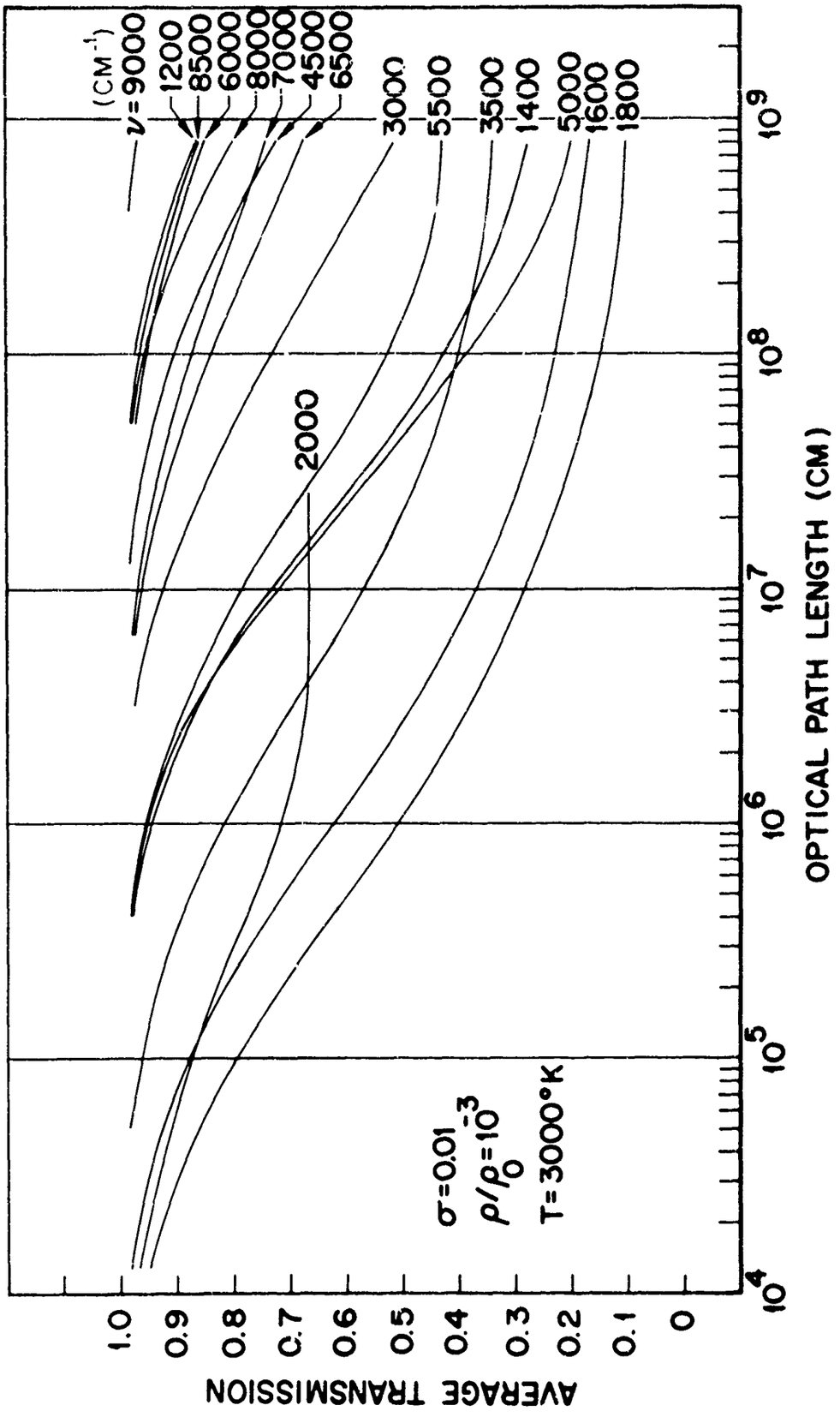

Fig. 25 Average transmission of optical radiation through a slab of heated air as a function of optical path length: contribution from vibration-rotation bands of nitric oxide.

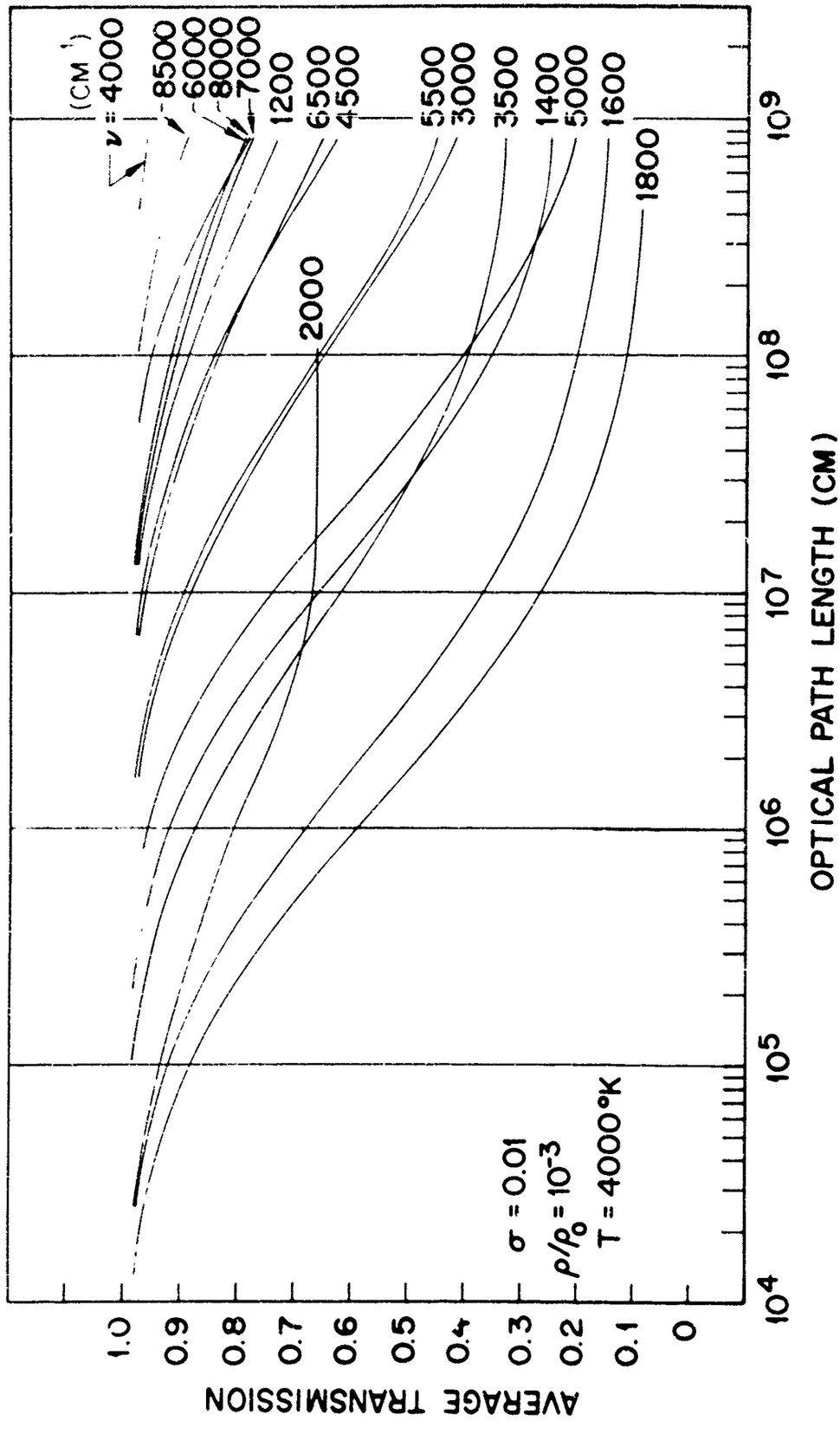

Fig. 26 Average transmission of optical radiation through a slab of heated air as a function of optical path length: contribution from vibration-rotation bands of nitric oxide.

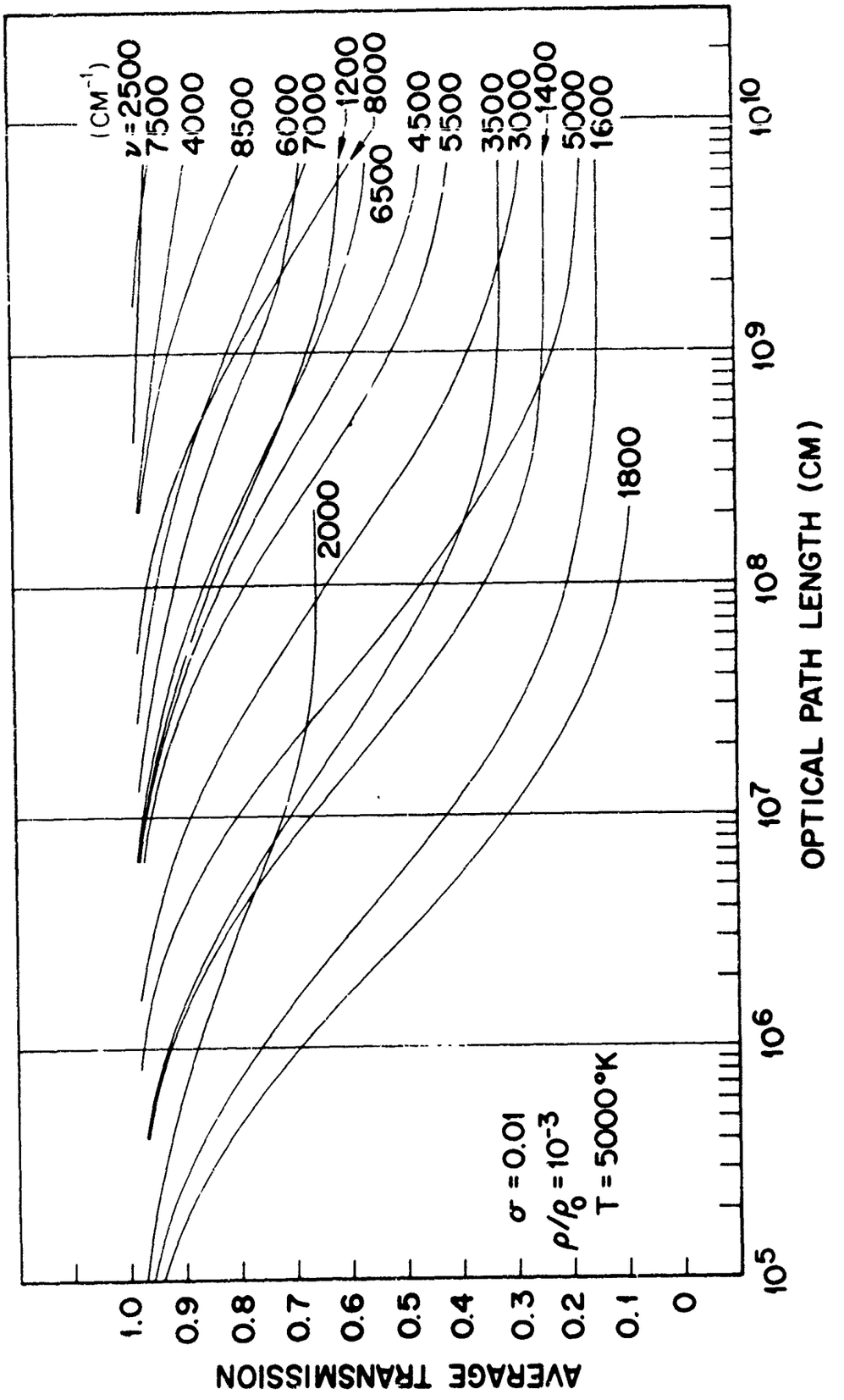

Fig. 27 Average transmission of optical radiation through a slab of heated air as a function of optical path length: contribution from vibration-rotation bands of nitric oxide.

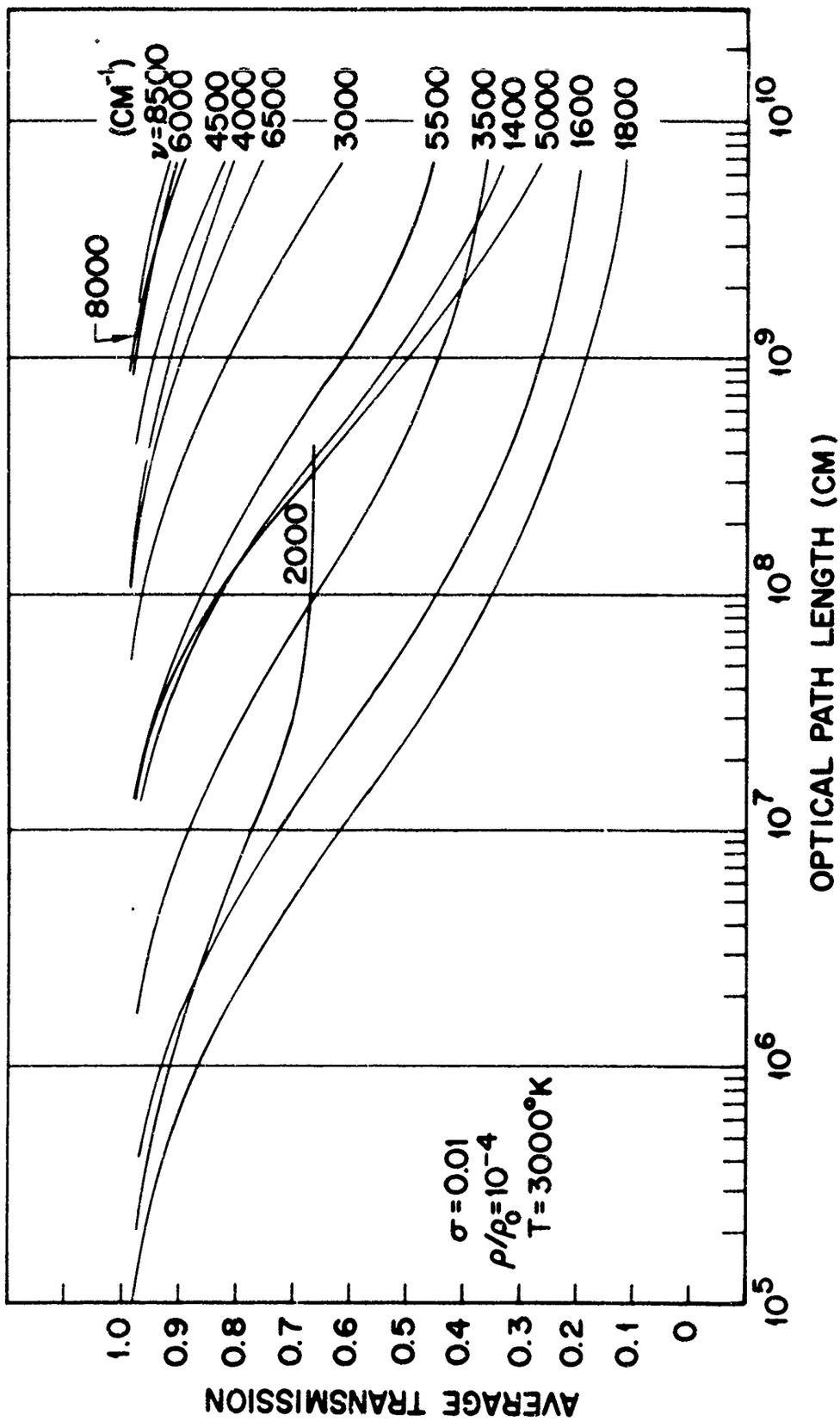

Fig. 28 Average transmission of optical radiation through a slab of heated air as a function of optical path length: contribution from vibration-rotation bands of nitric oxide.

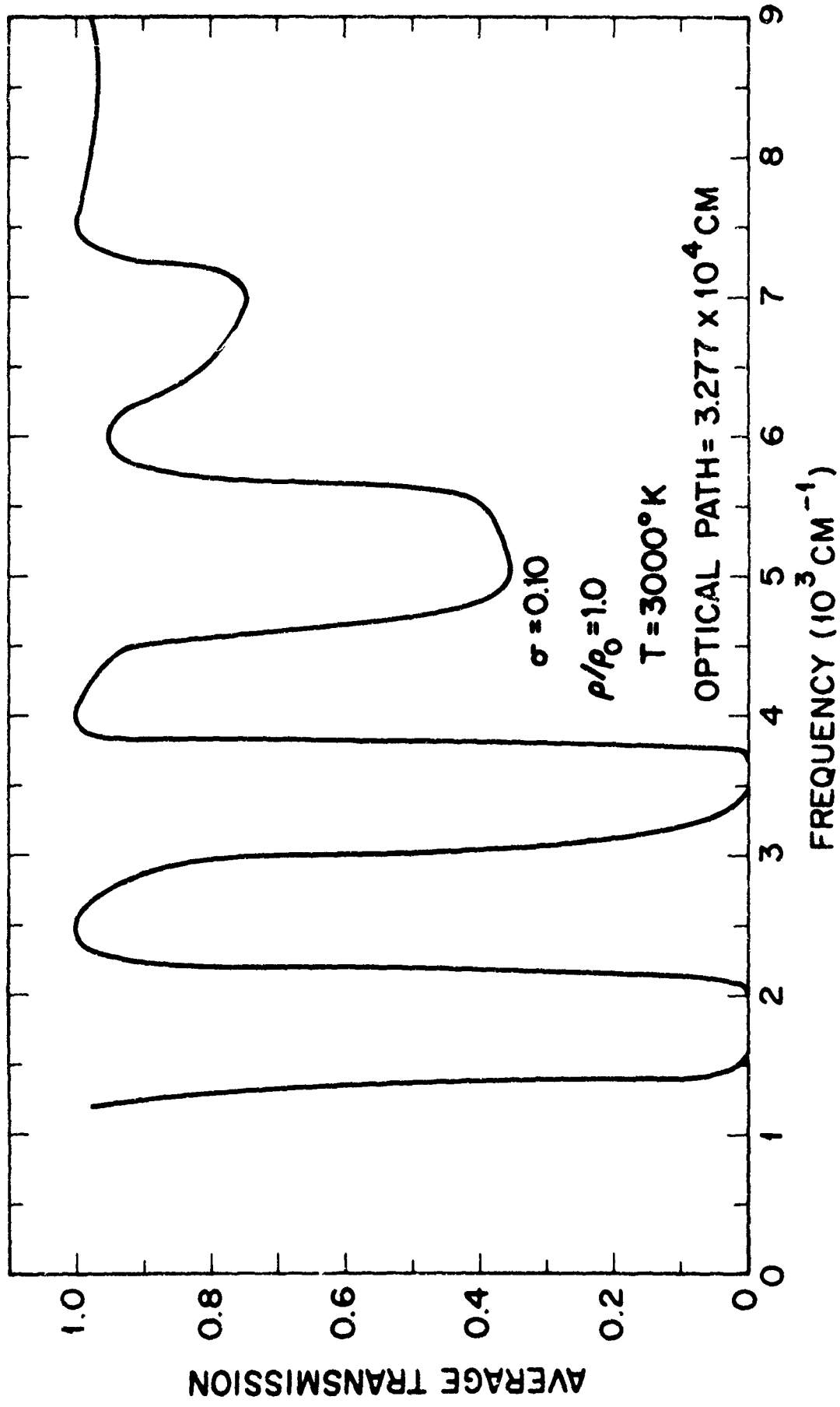

Fig. 29 Average transmission of optical radiation through a slab of heated air as a function of frequency: contribution from vibration-rotation bands of nitric oxide. The temperature and optical path length are given in the figure.

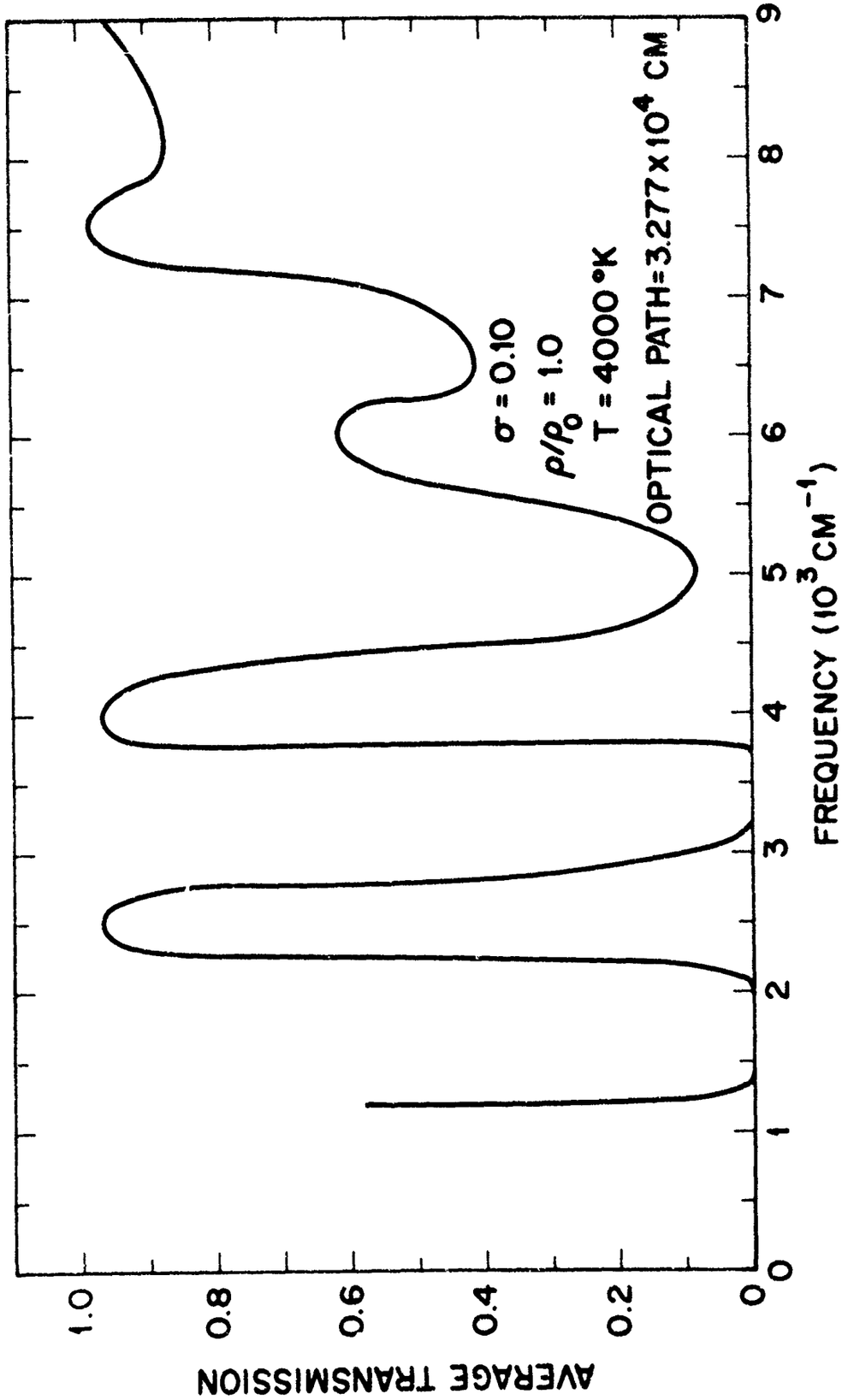

Fig. 30 Average transmission of optical radiation through a slab of heated air as a function of frequency: contribution from vibration-rotation bands of nitric oxide. The temperature and optical path length are given in the figure.

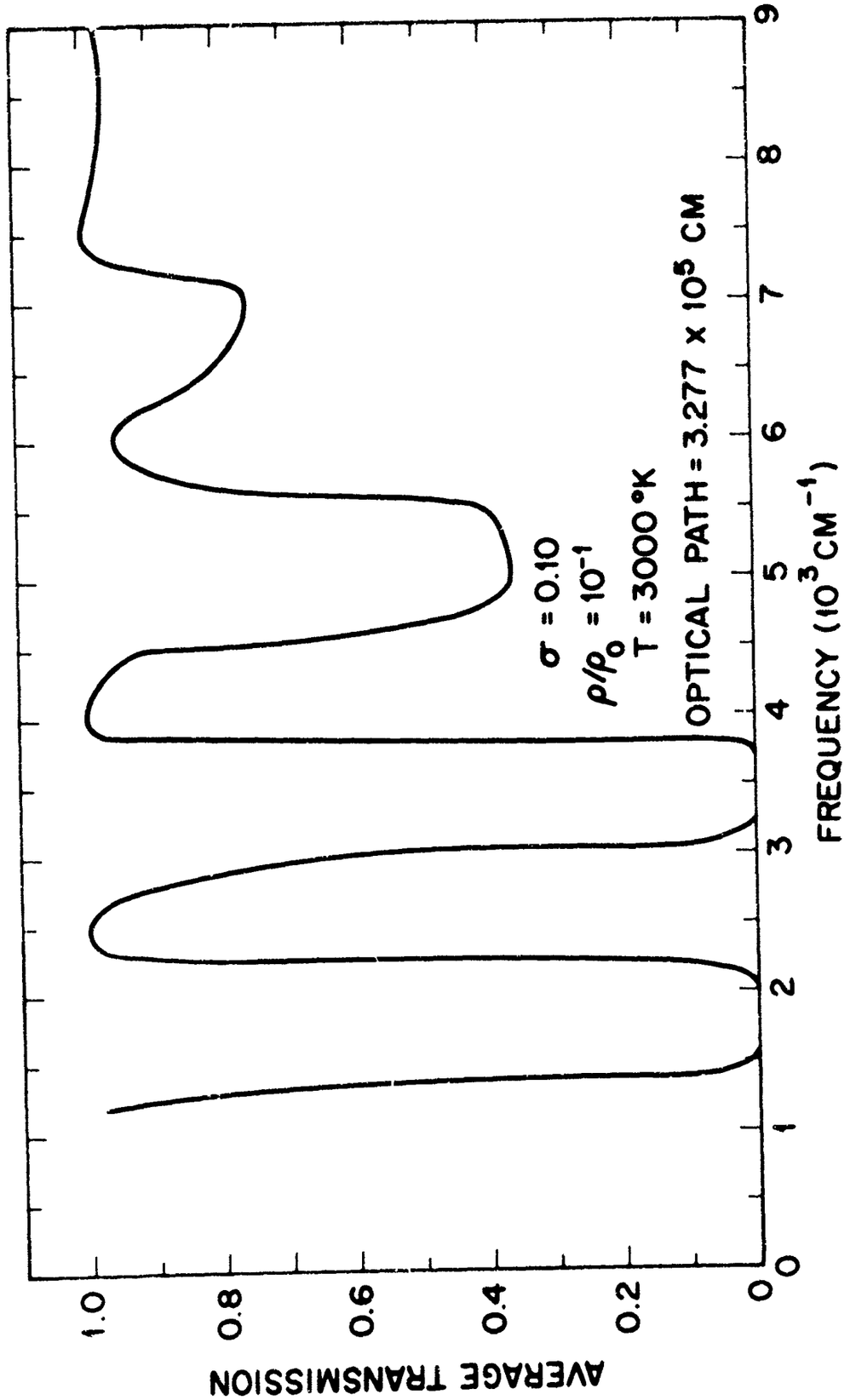

Fig. 31 Average transmission of optical radiation through a slab of heated air as a function of frequency: contribution from vibration-rotation bands of nitric oxide. The temperature and optical path length are given in the figure.

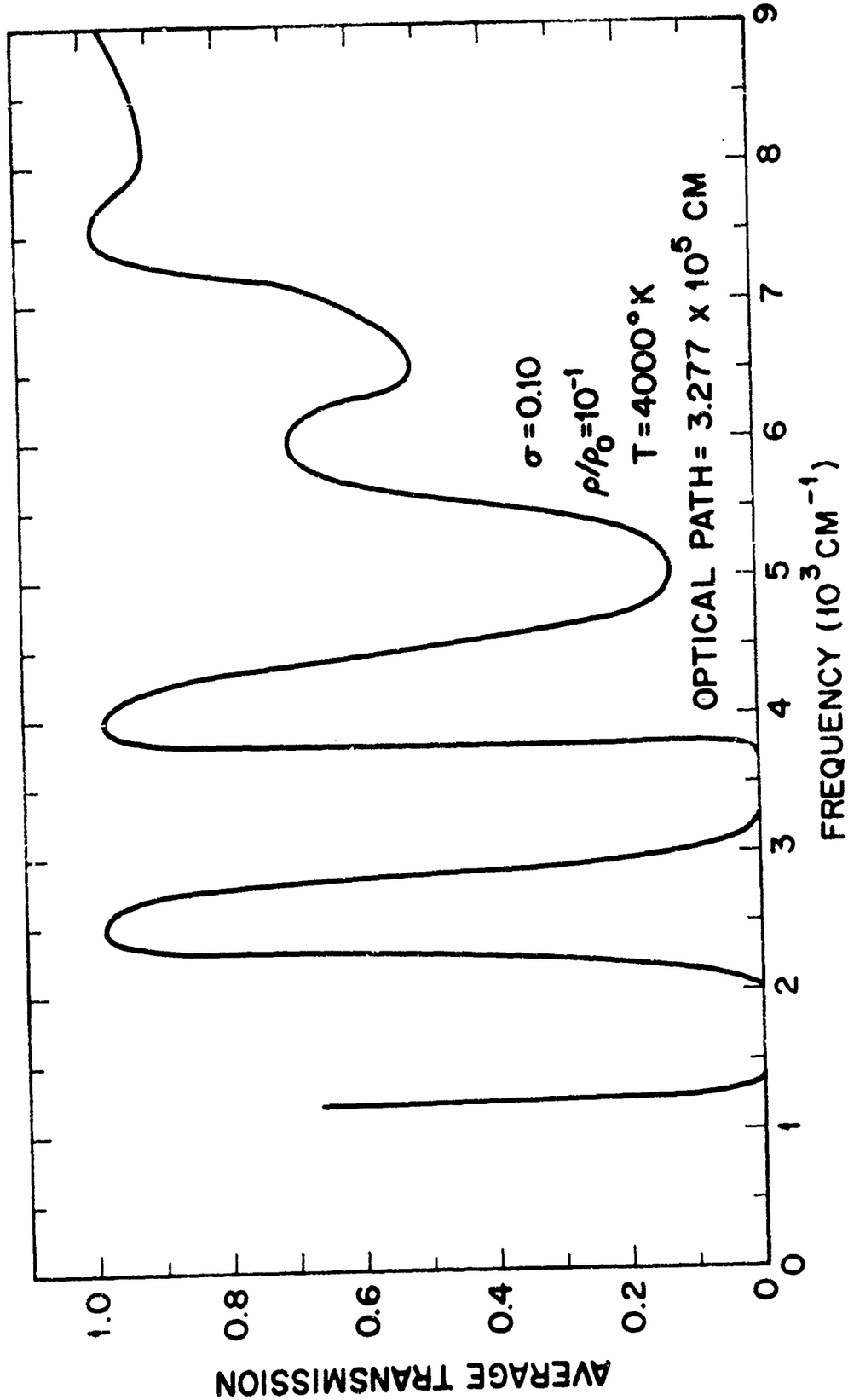

Fig. 32 Average transmission of optical radiation through a slab of heated air as a function of frequency: contribution from vibration-rotation bands of nitric oxide. The temperature and optical path length are given in the figure.

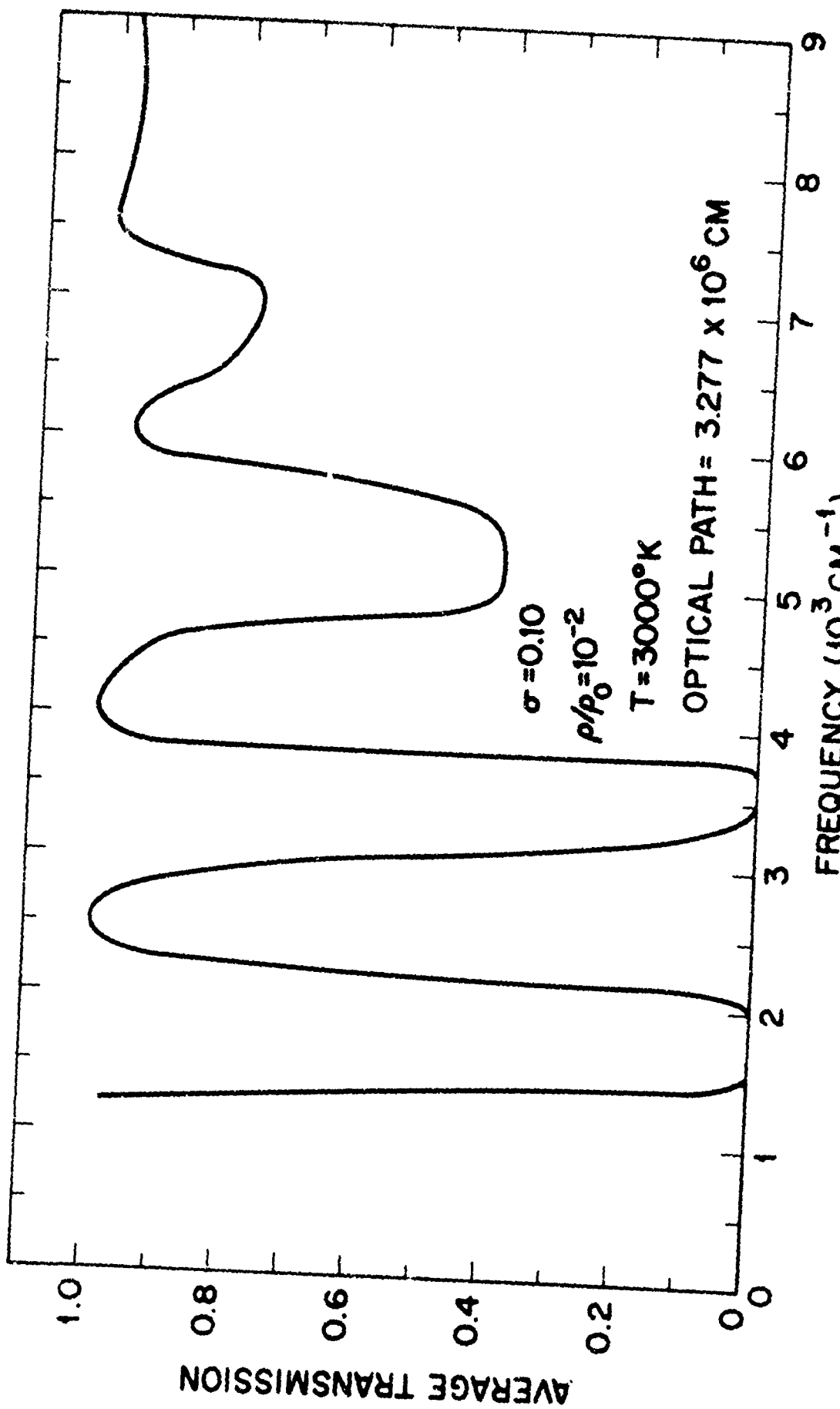

Fig. 33 Average transmission of optical radiation through a slab of heated air as a function of frequency: contribution from vibration-rotation bands of nitric oxide. The temperature and optical path length are given in the figure.

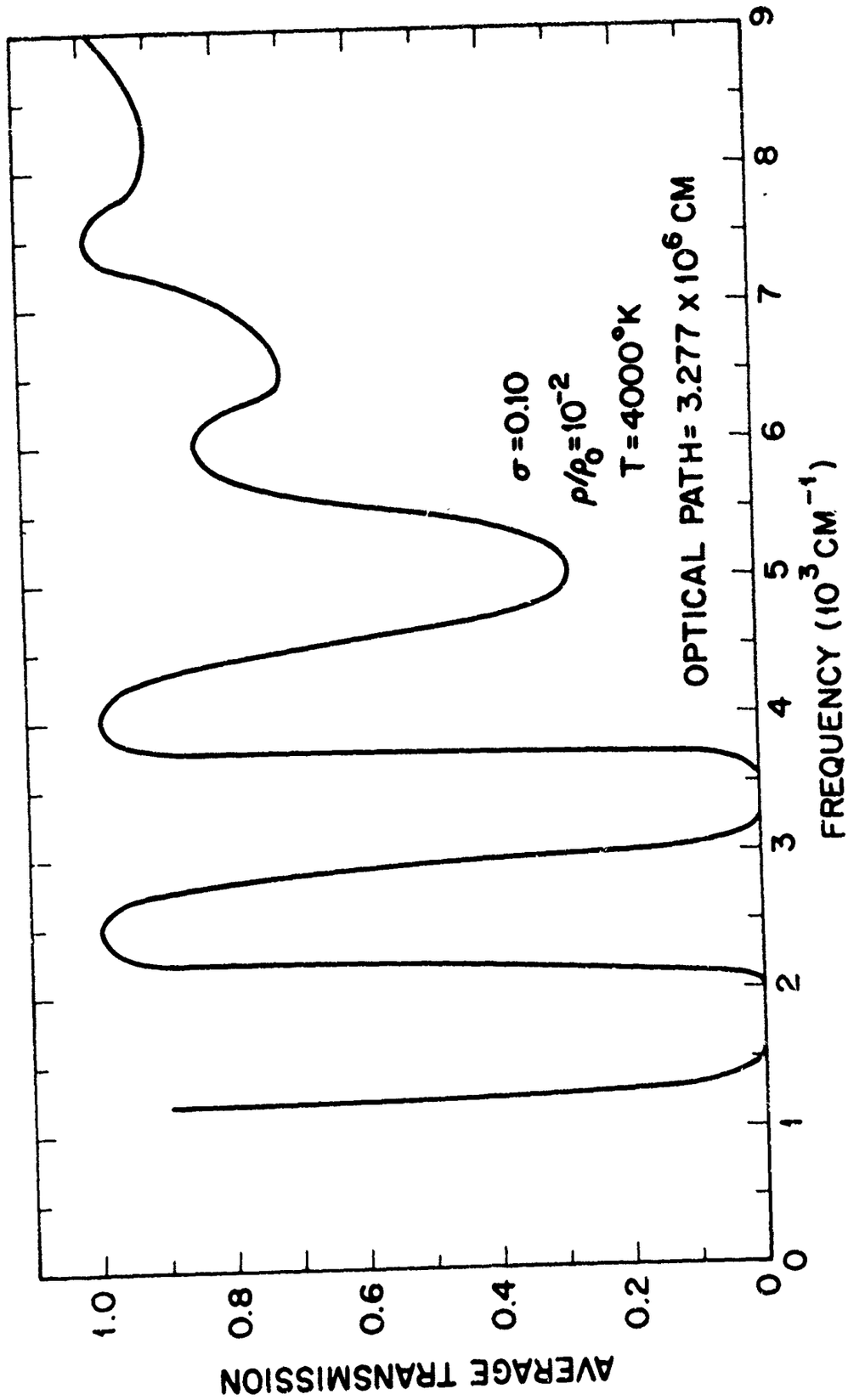

Fig. 34 Average transmission of optical radiation through a slab of heated air as a function of frequency: contribution from vibration-rotation bands of nitric oxide. The temperature and optical path length are given in the figure.

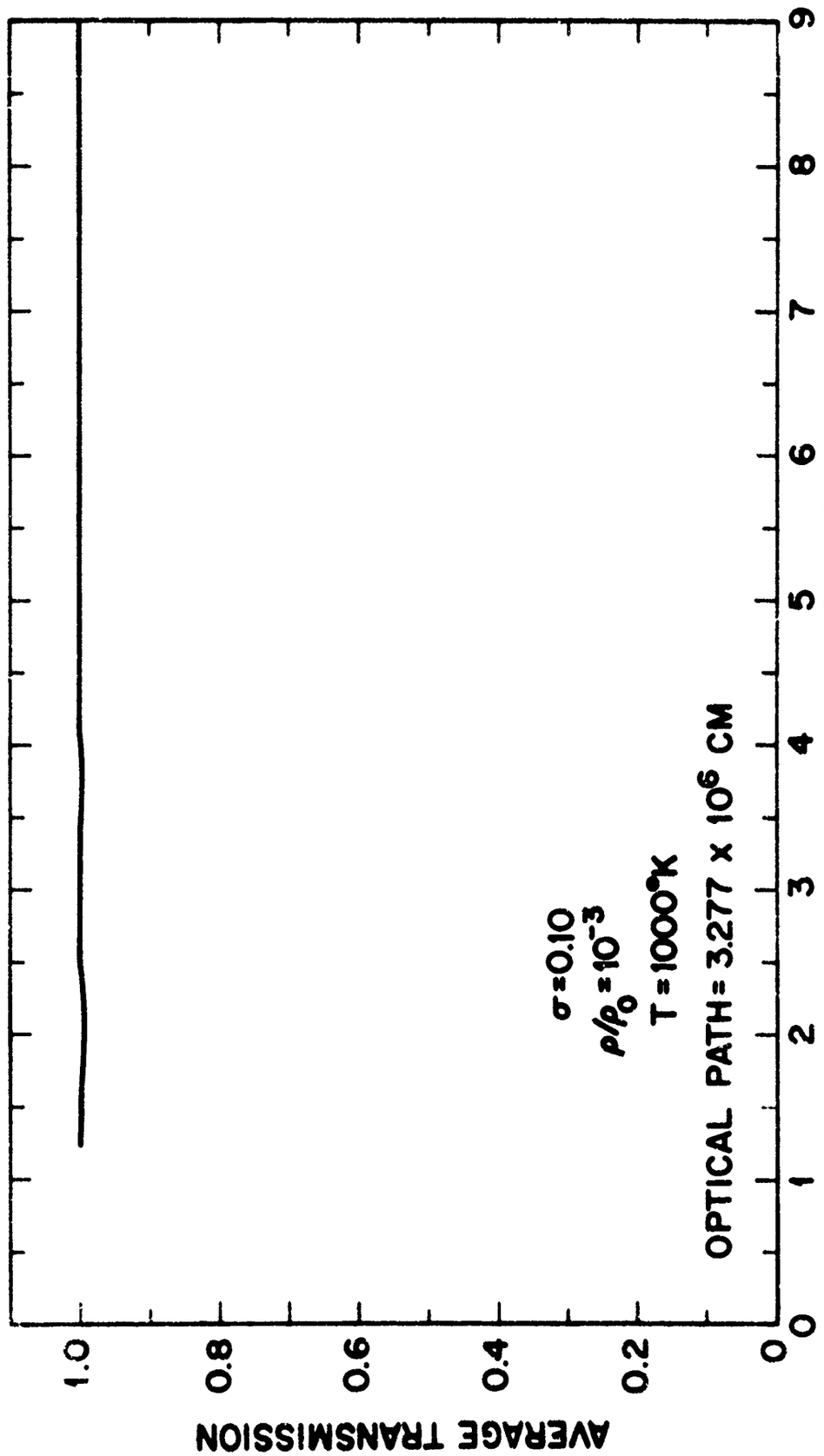

Fig. 35 **Average transmission of optical radiation through a slab of heated air as a function of frequency: contribution from vibration-rotation bands of nitric oxide. The temperature and optical path length are given in the figure.**

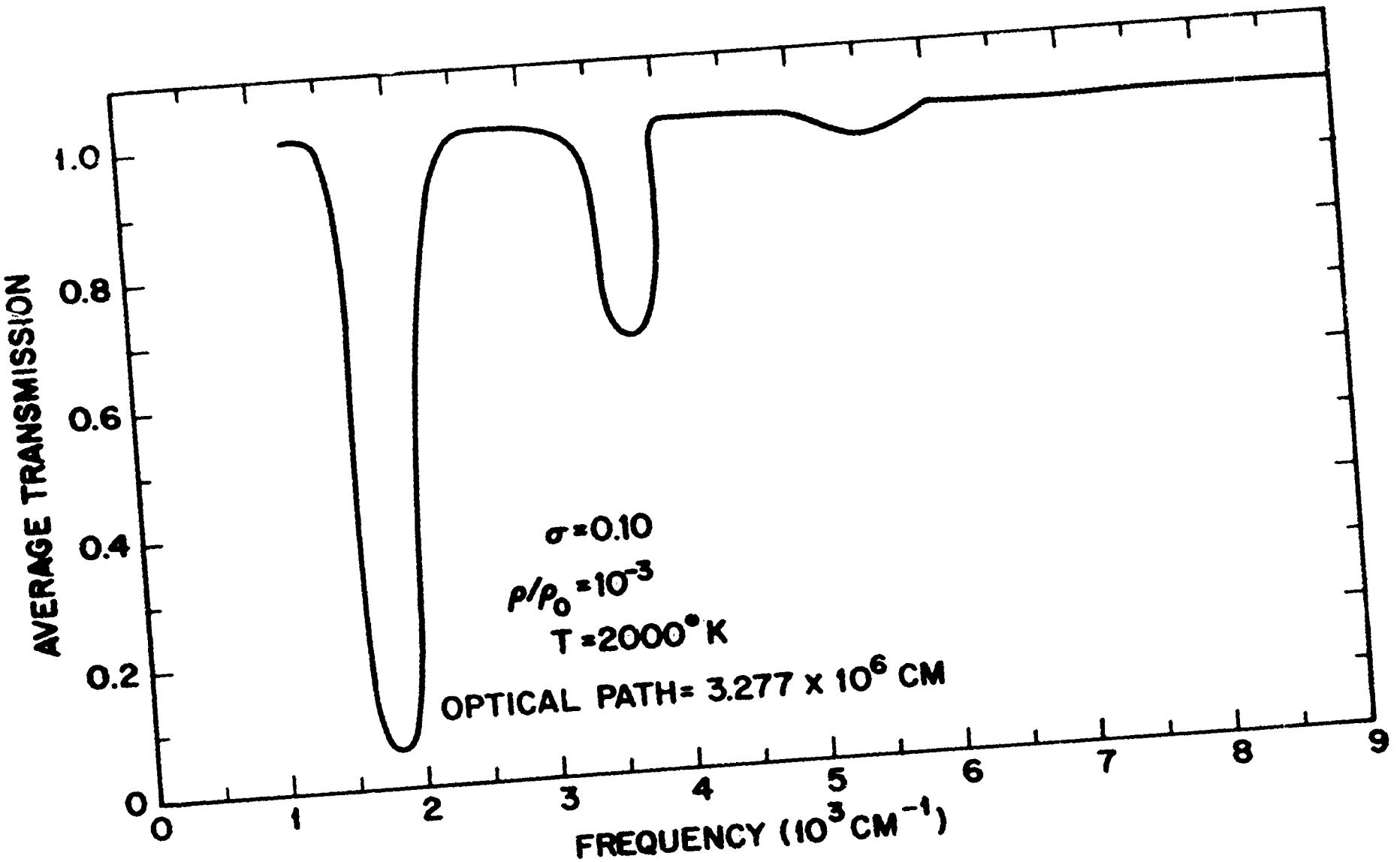

Fig. 36 Average transmission of optical radiation through a slab of heated air as a function of frequency: contribution from vibration-rotation bands of nitric oxide. The temperature and optical path length are given in the figure.

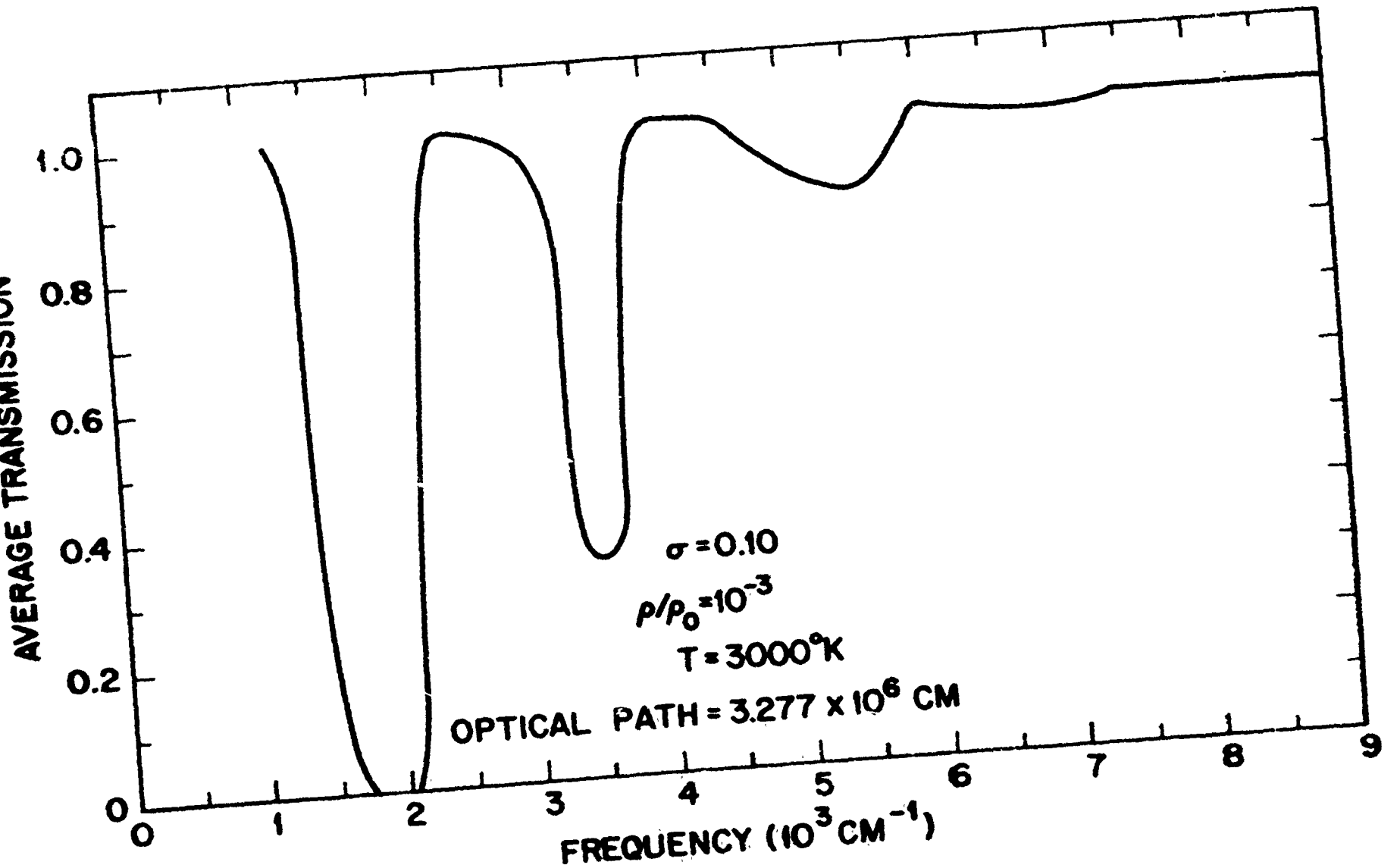

Fig. 37 Average transmission of optical radiation through a slab of heated air as a function of frequency: contribution from vibration-rotation bands of nitric oxide. The temperature and optical path length are given in the figure.

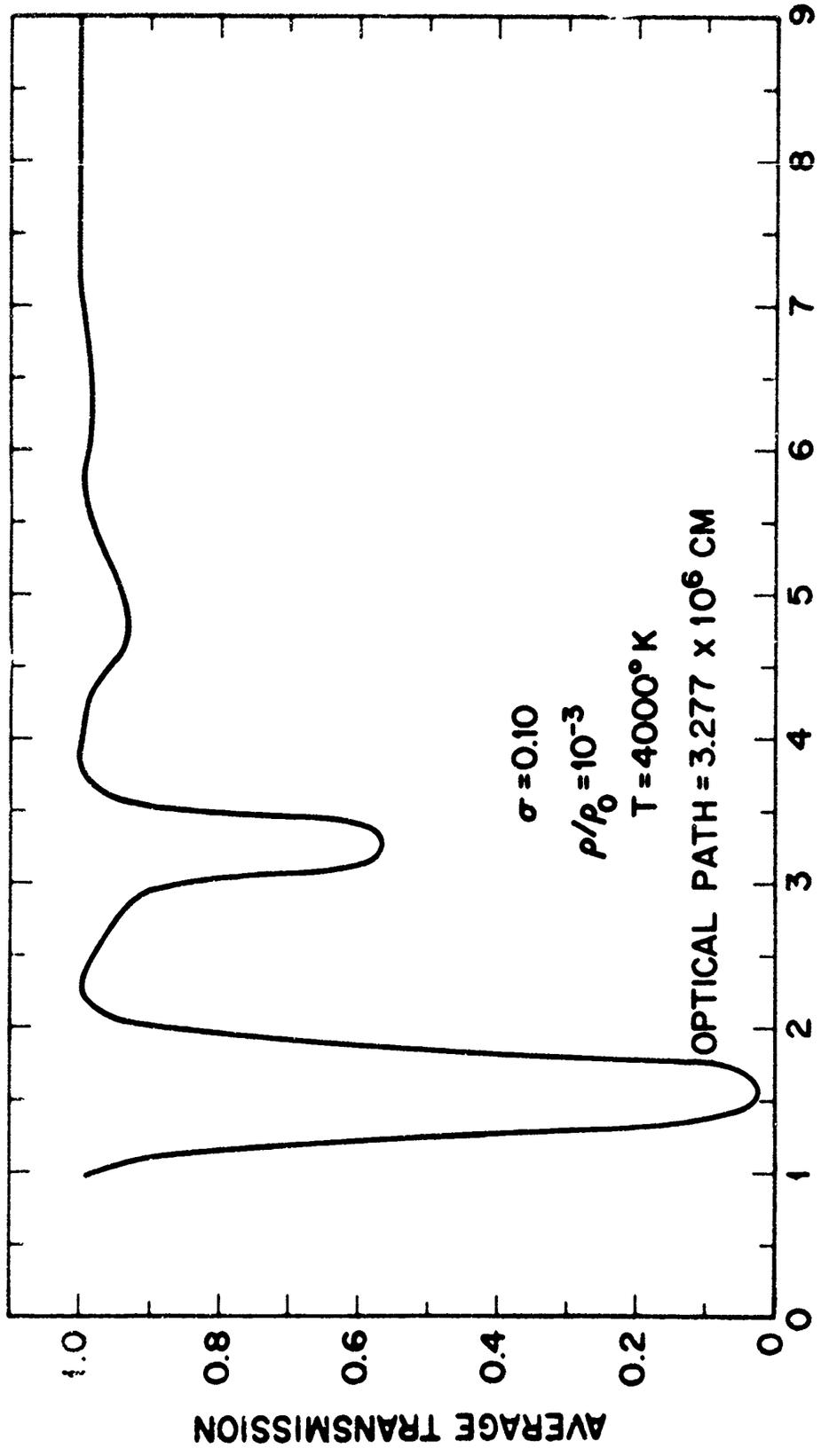

Fig. 38 Average transmission of optical radiation through a slab of heated air as a function of frequency: contribution from vibration-rotation bands of nitric oxide. The temperature and optical path length are given in the figure.

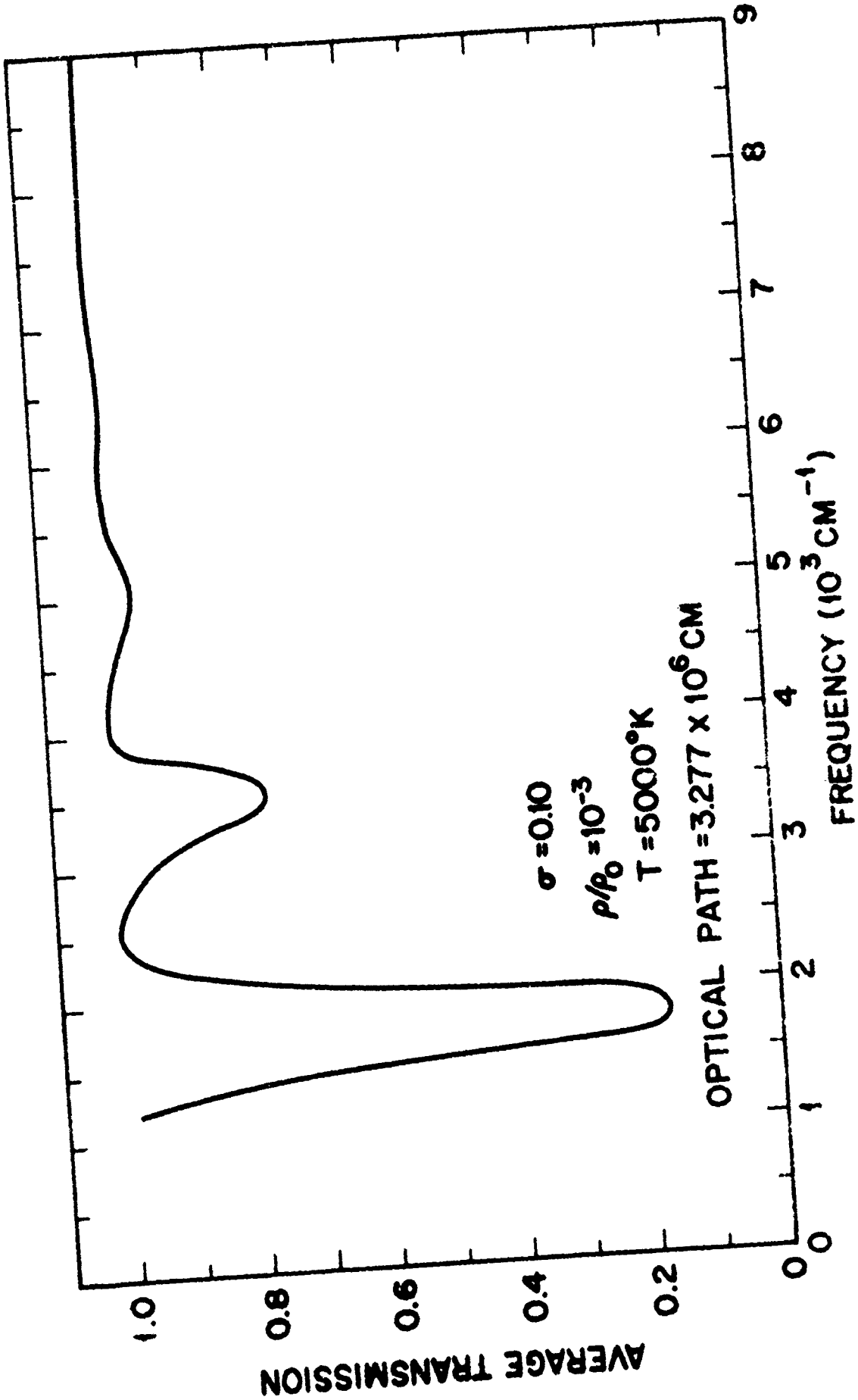

Fig. 39 Average transmission of optical radiation through a slab of heated air as a function of frequency: contribution from vibration-rotation bands of nitric oxide. The temperature and optical path length are given in the figure.

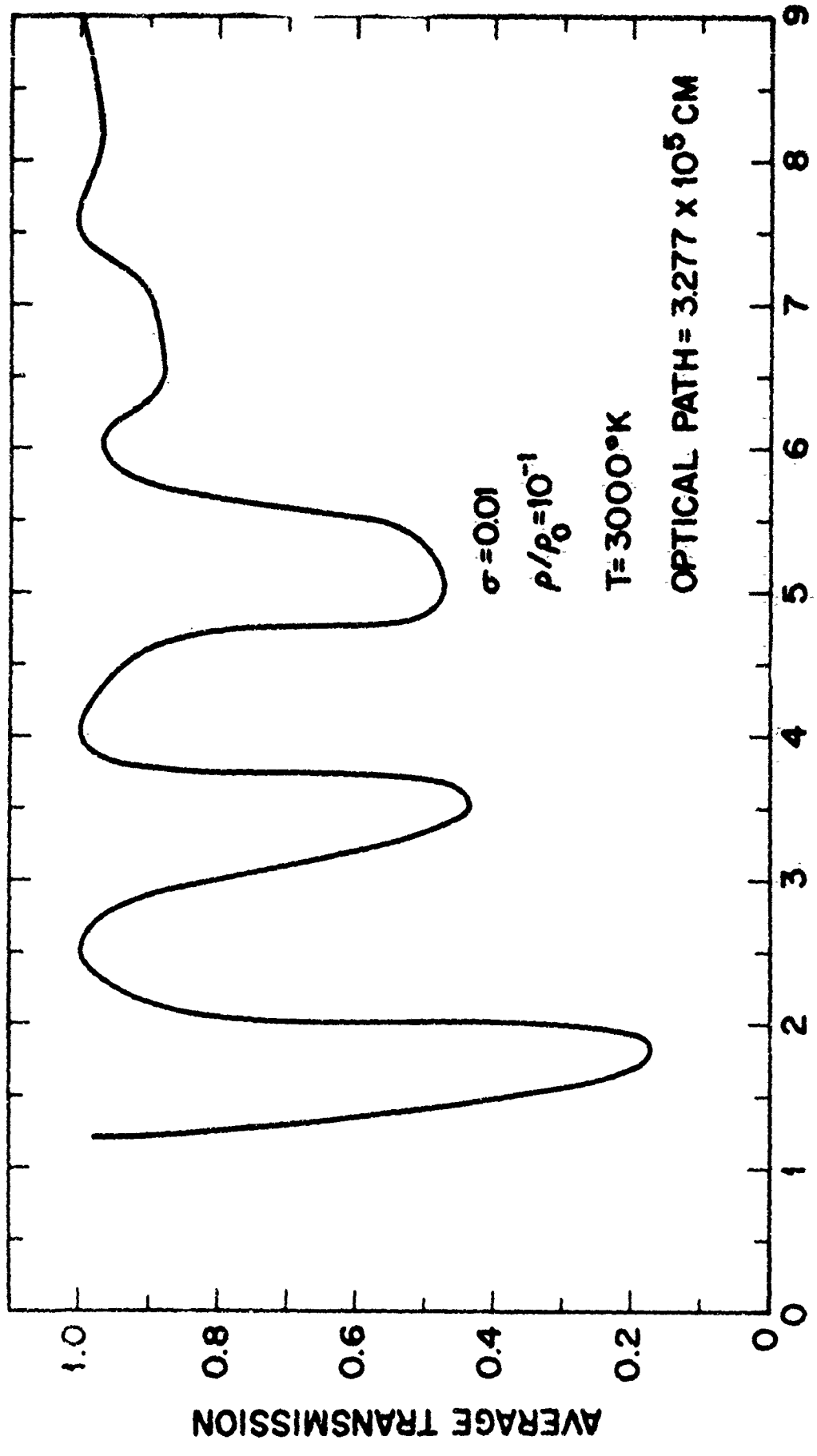

Fig. 40 Average transmission of optical radiation through a slab of heated air as a function of frequency: contribution from vibration-rotation bands of nitric oxide. The temperature and optical path length are given in the figure.

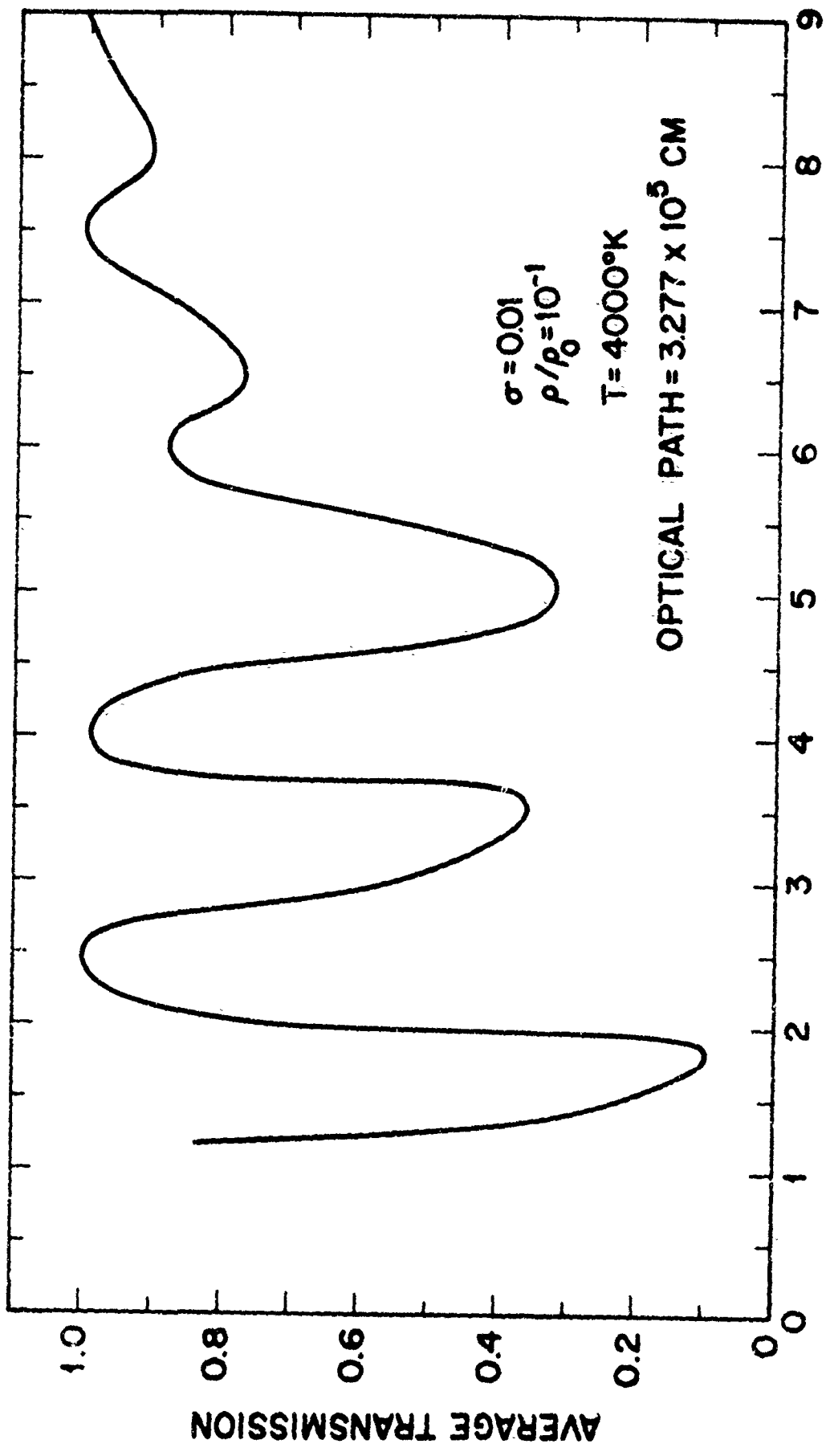

Fig. 41 Average transmission of optical radiation through a slab of heated air as a function of frequency: contribution from vibration-rotation bands of nitric oxide. The temperature and optical path length are given in the figure.

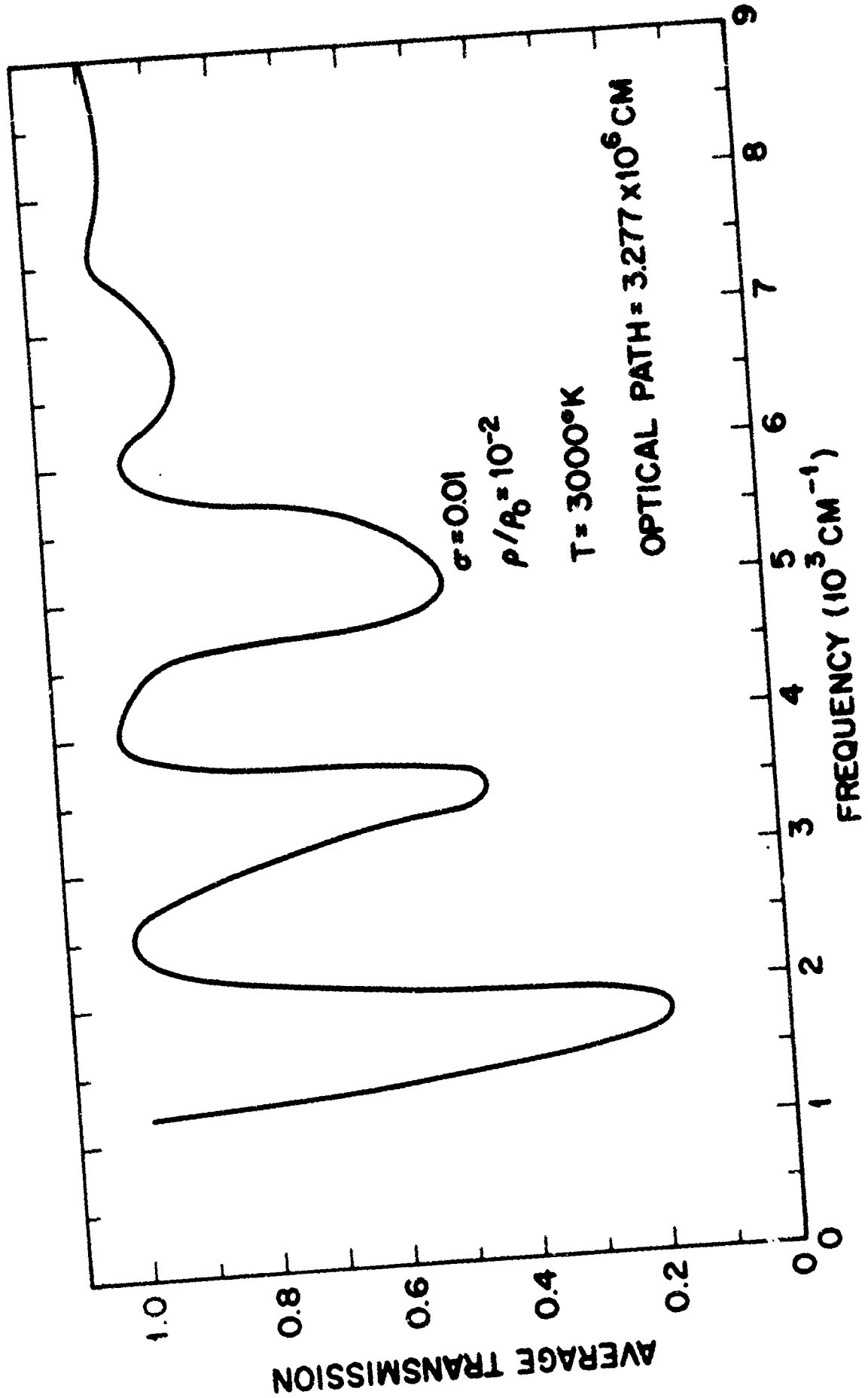

Fig. 42 Average transmission of optical radiation through a slab of heated air as a function of frequency: contribution from vibration-rotation bands of nitric oxide. The temperature and optical path length are given in the figure.

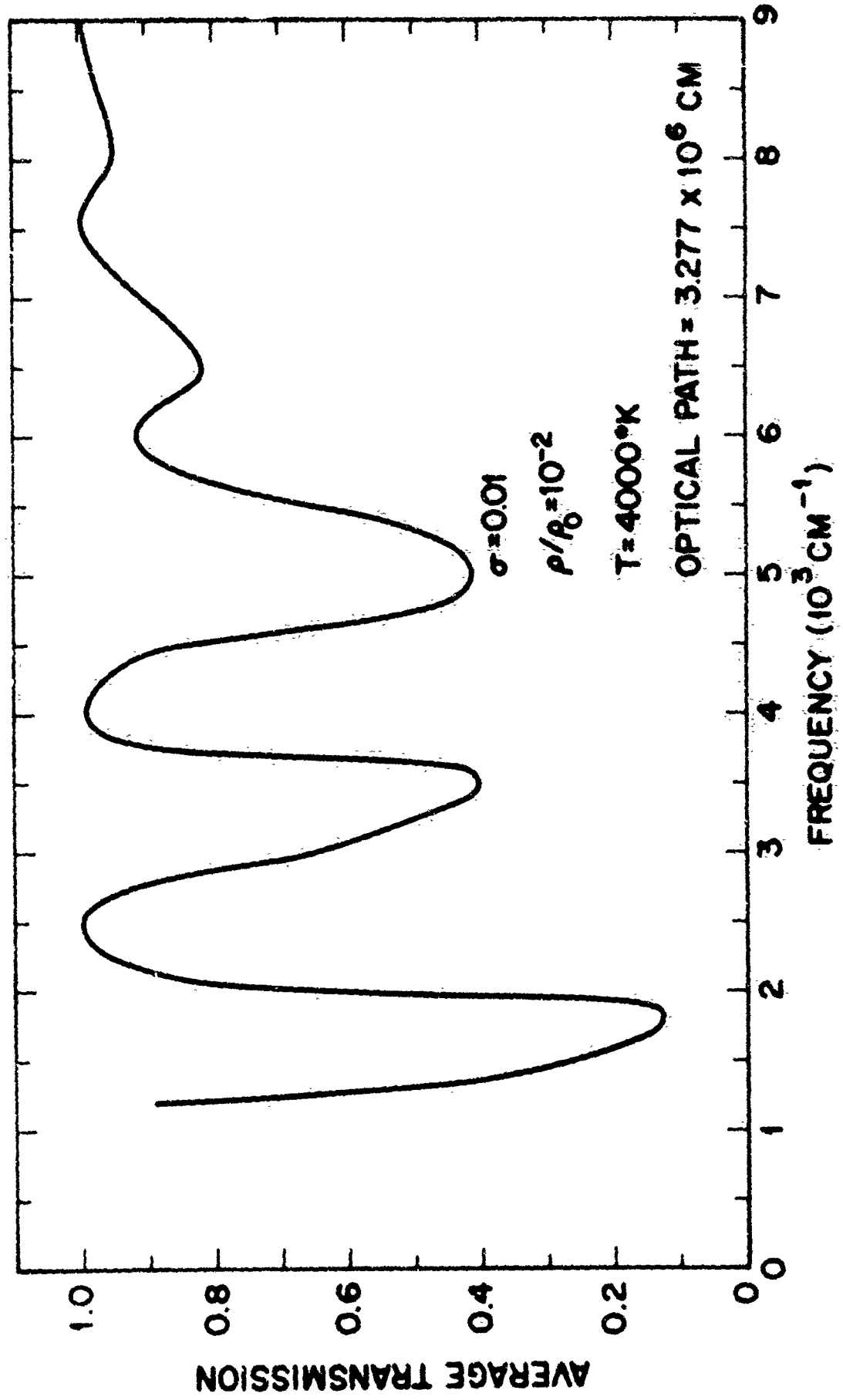

Fig. 43 Average transmission of optical radiation through a slab of heated air as a function of frequency: contribution from vibration-rotation bands of nitric oxide. The temperature and optical path length are given in the figure.

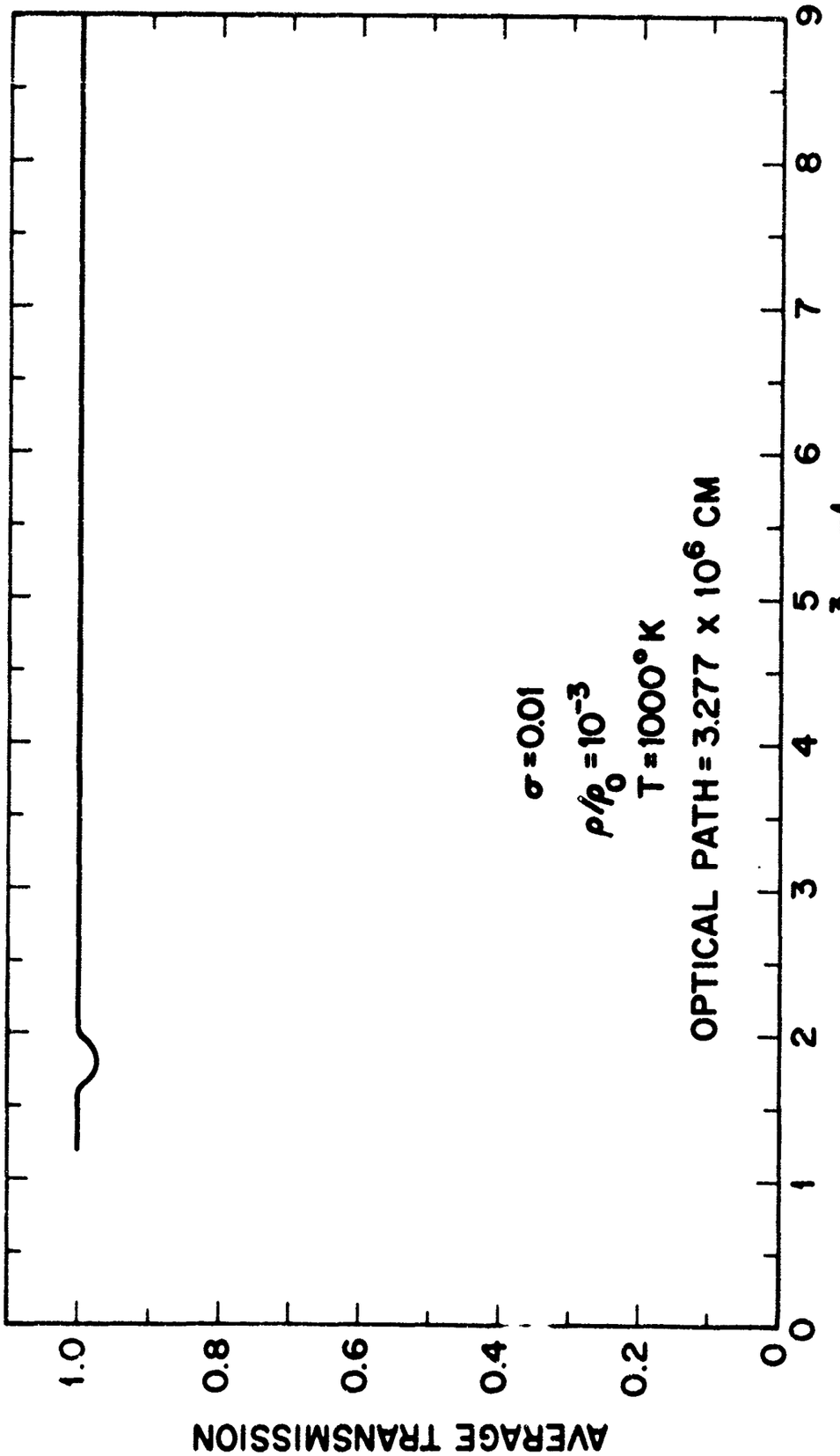

Fig. 44 Average transmission of optical radiation through a slab of heated air as a function of frequency: contribution from vibration-rotation bands of nitric oxide. The temperature and optical path length are given in the figure.

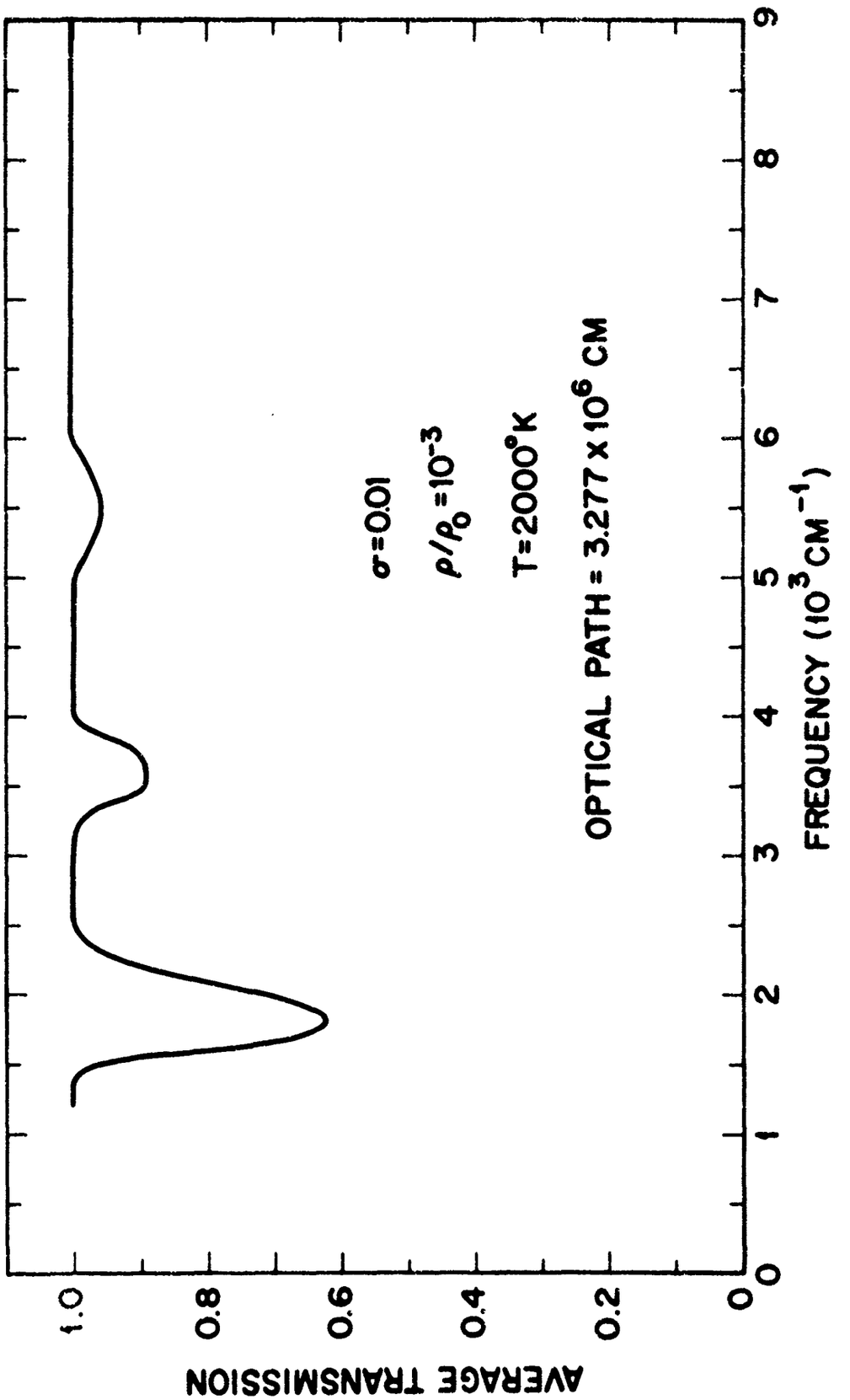

Fig. 45 Average transmission of optical radiation through a slab of heated air as a function of frequency: contribution from vibration-rotation bands of nitric oxide. The temperature and optical path length are given in the figure.

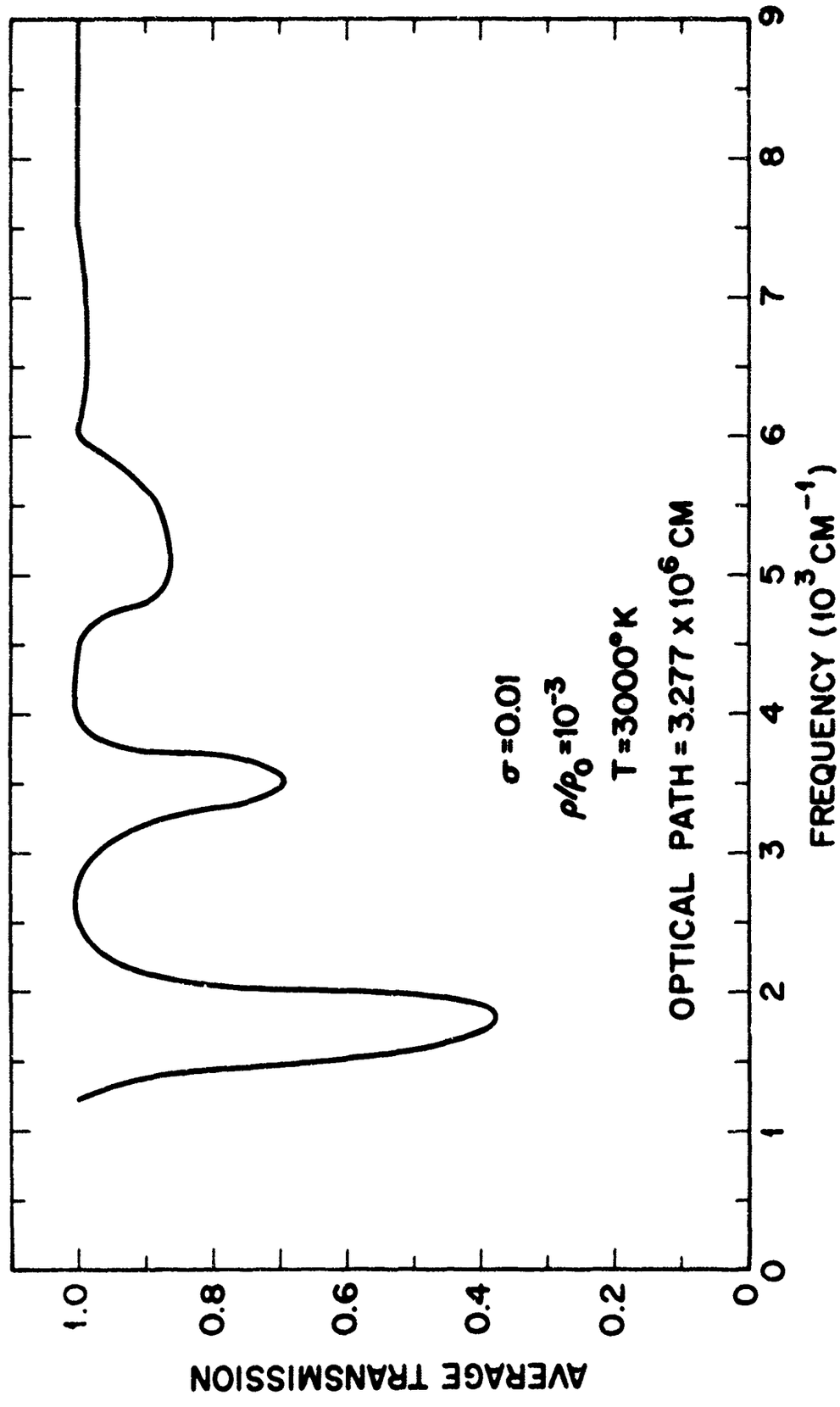

Fig. 46 Average transmission of optical radiation through a slab of heated air as a function of frequency contribution from vibration-rotation bands of nitric oxide. The temperature and optical path length are given in the figure.

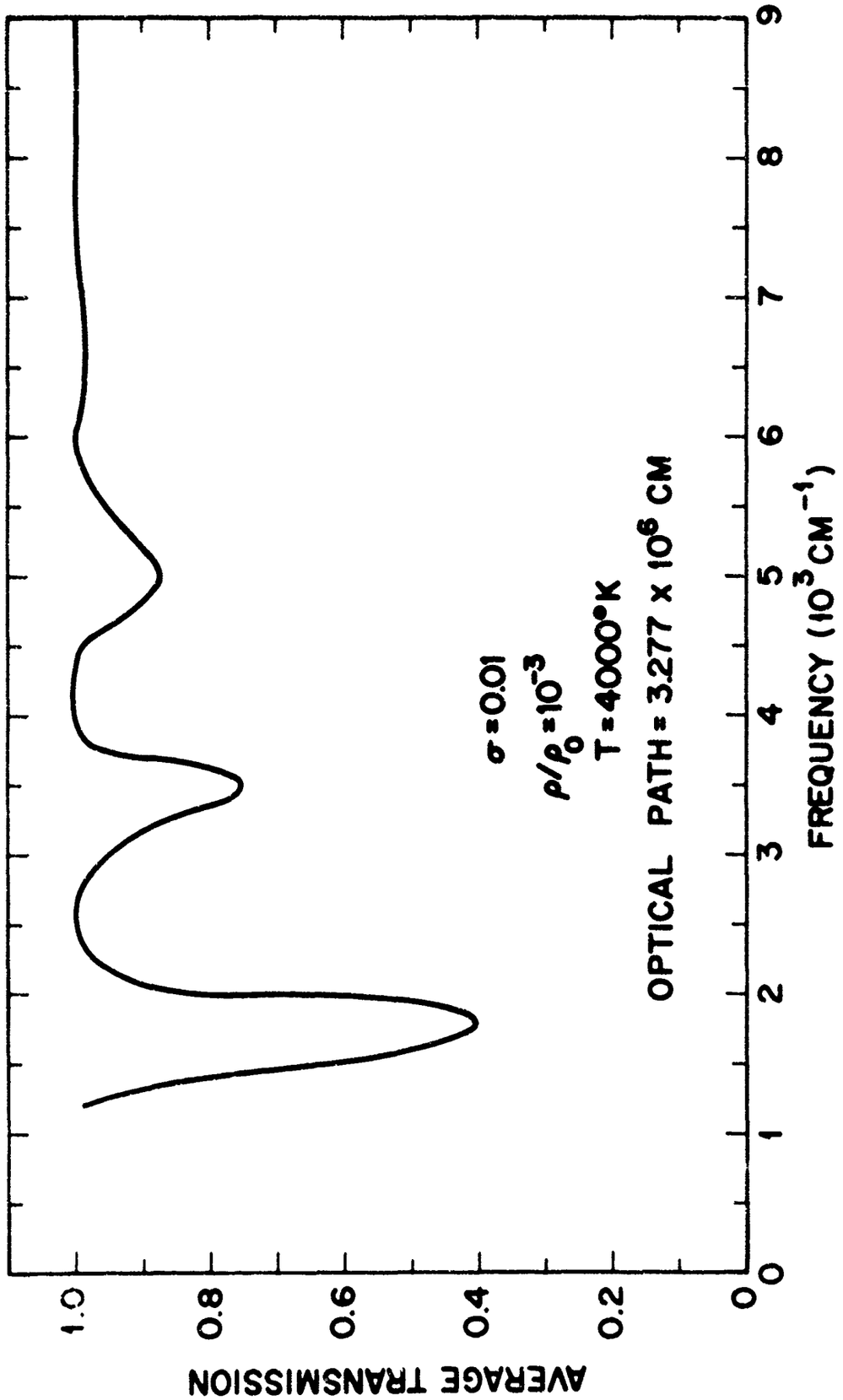

Fig. 47 Average transmission of optical radiation through a slab of heated air as a function of frequency: contribution from vibration-rotation bands of nitric oxide. The temperature and optical path length are given in the figure.

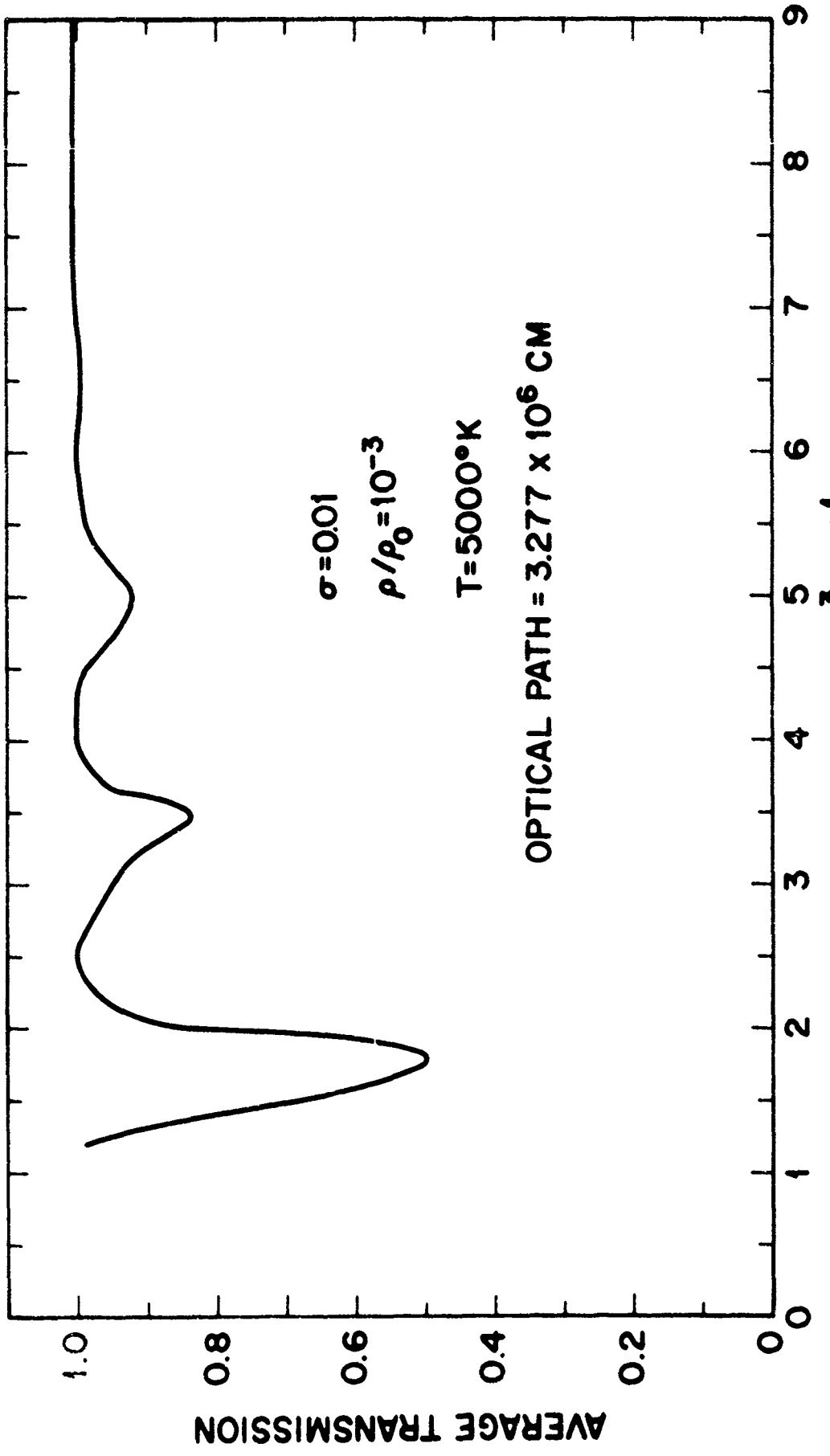

Fig. 48 Average transmission of optical radiation through a slab of heated air as a function of frequency: contribution from vibration-rotation bands of nitric oxide. The temperature and optical path length are given in the figure.

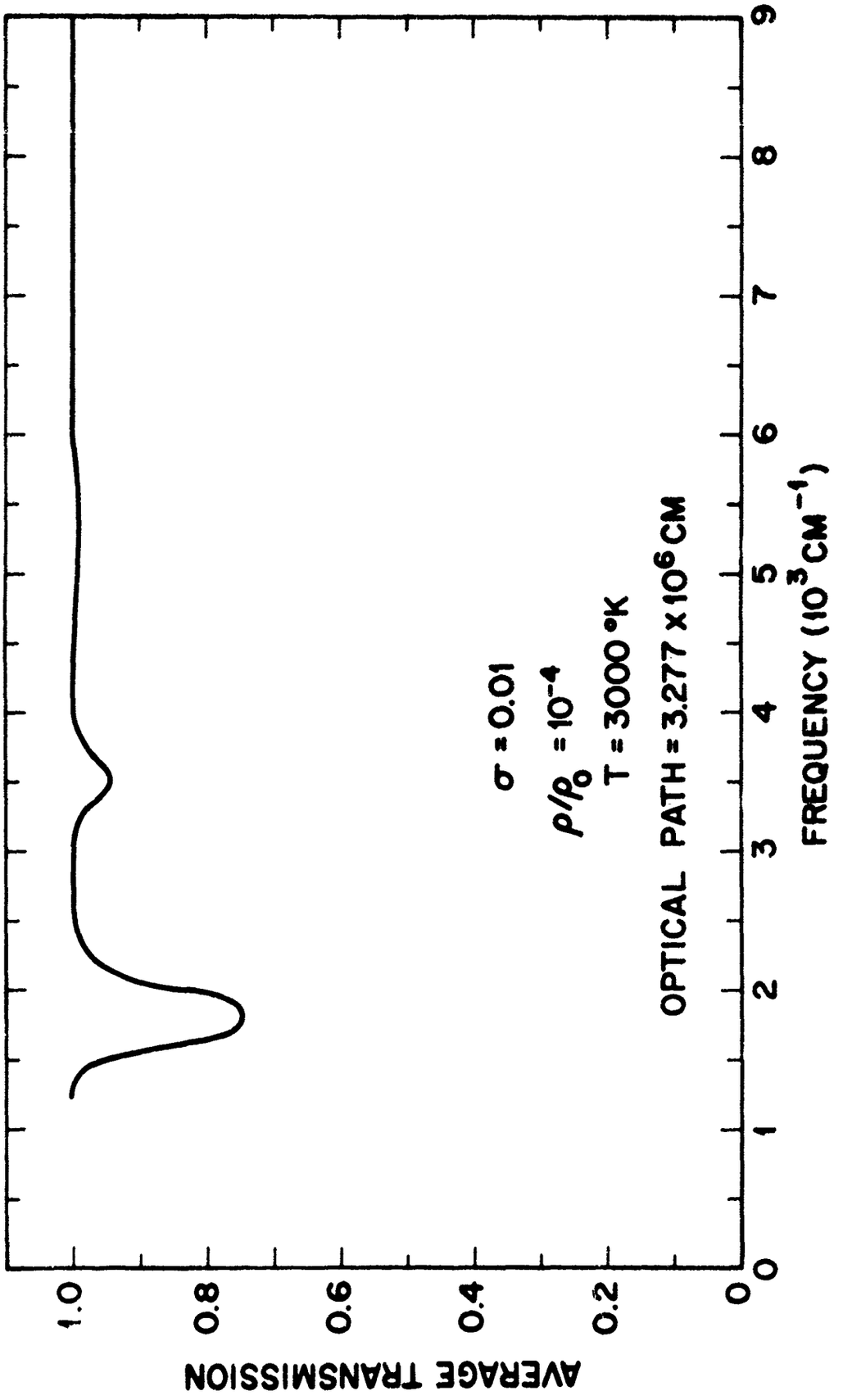

Fig. 49 Average transmission of optical radiation through a slab of heated air as a function of frequency: contribution from vibration-rotation bands of nitric oxide. The temperature and optical path length are given in the figure.

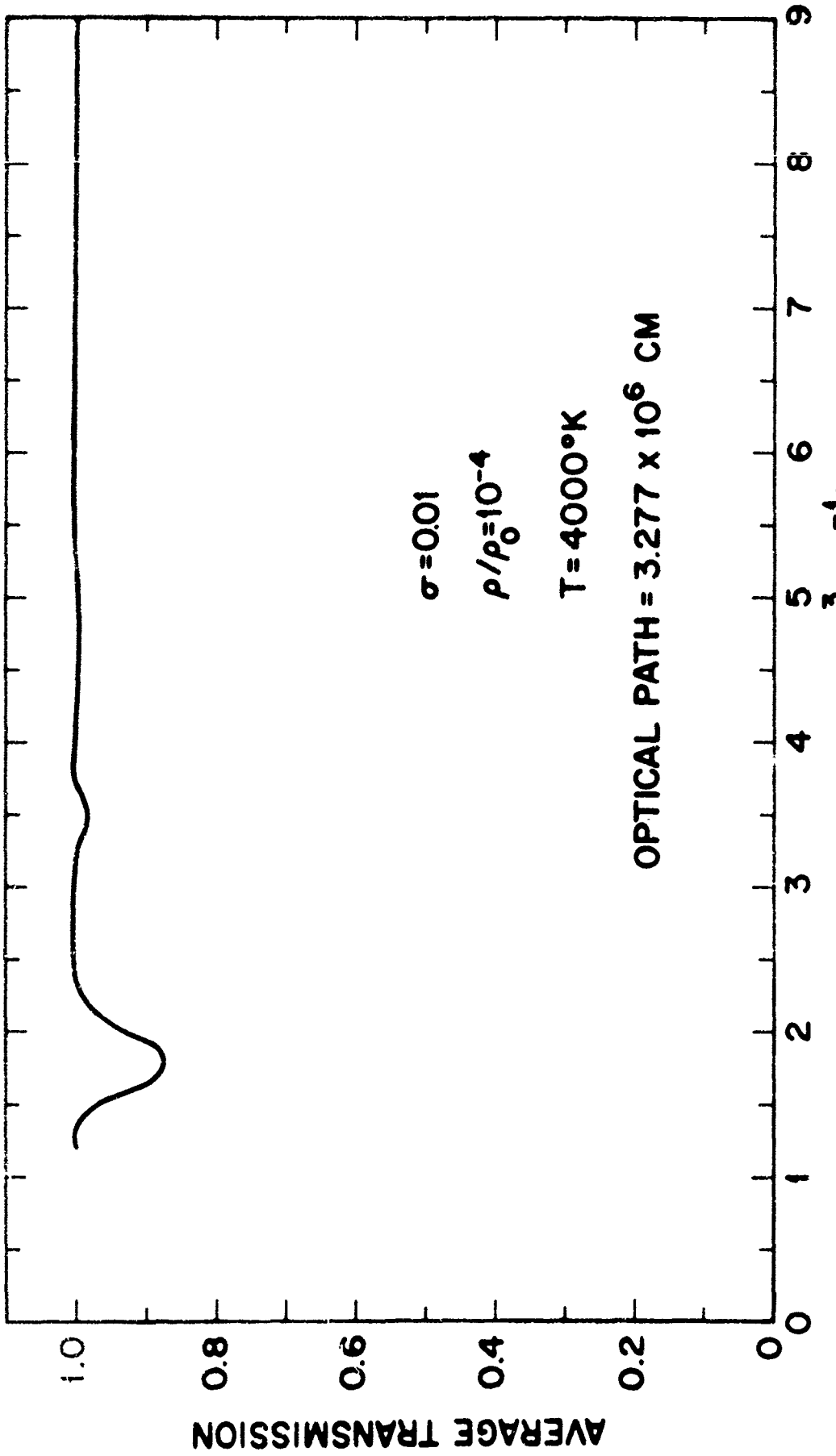

Fig. 50 Average transmission of optical radiation through a slab of heated air as a function of frequency: contribution from vibration-rotation bands of nitric oxide. The temperature and optical path length are given in the figure.

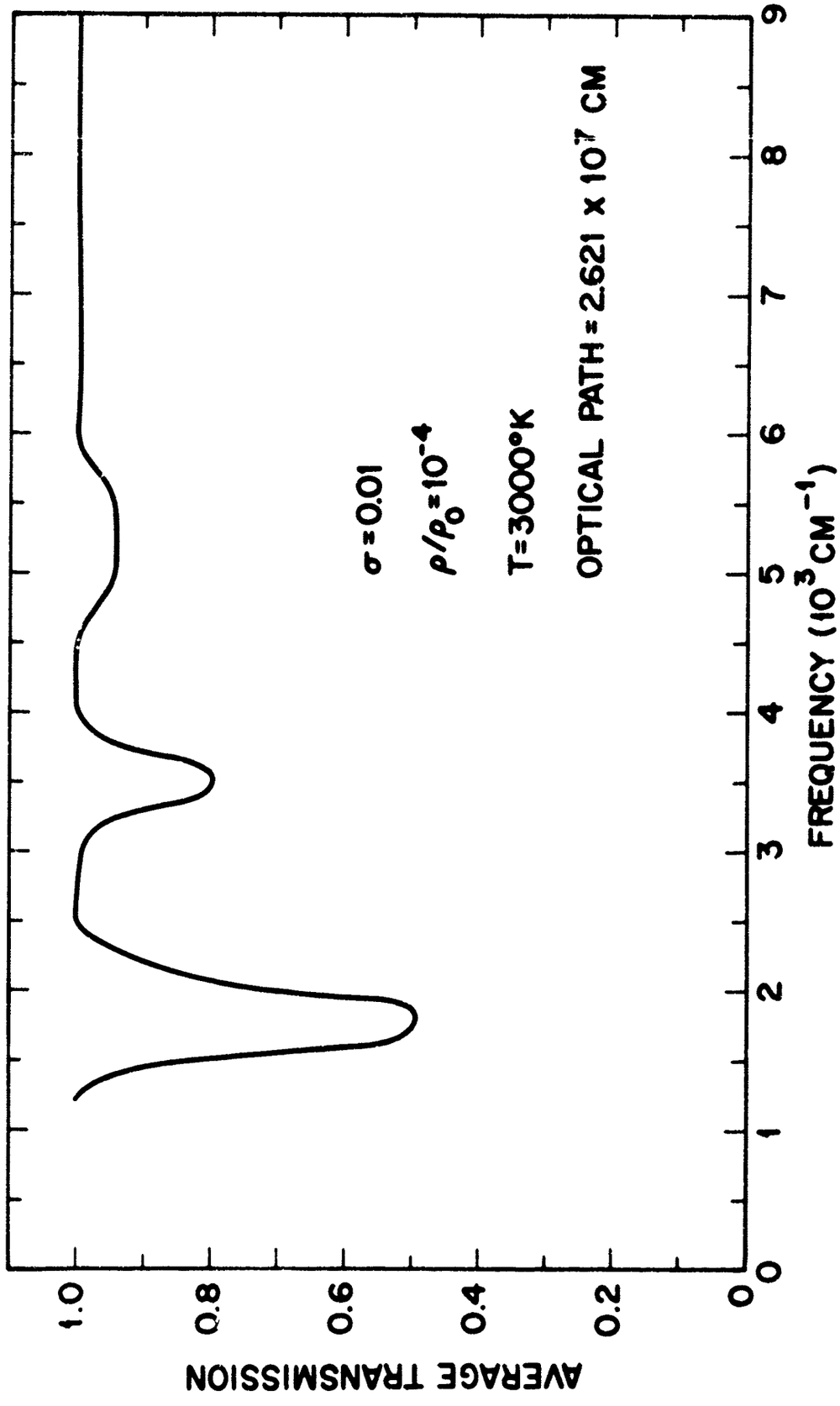

Fig. 51 Average transmission of optical radiation through a slab of heated air as a function of frequency: contribution from vibration-rotation bands of nitric oxide. The temperature and optical path length are given in the figure.

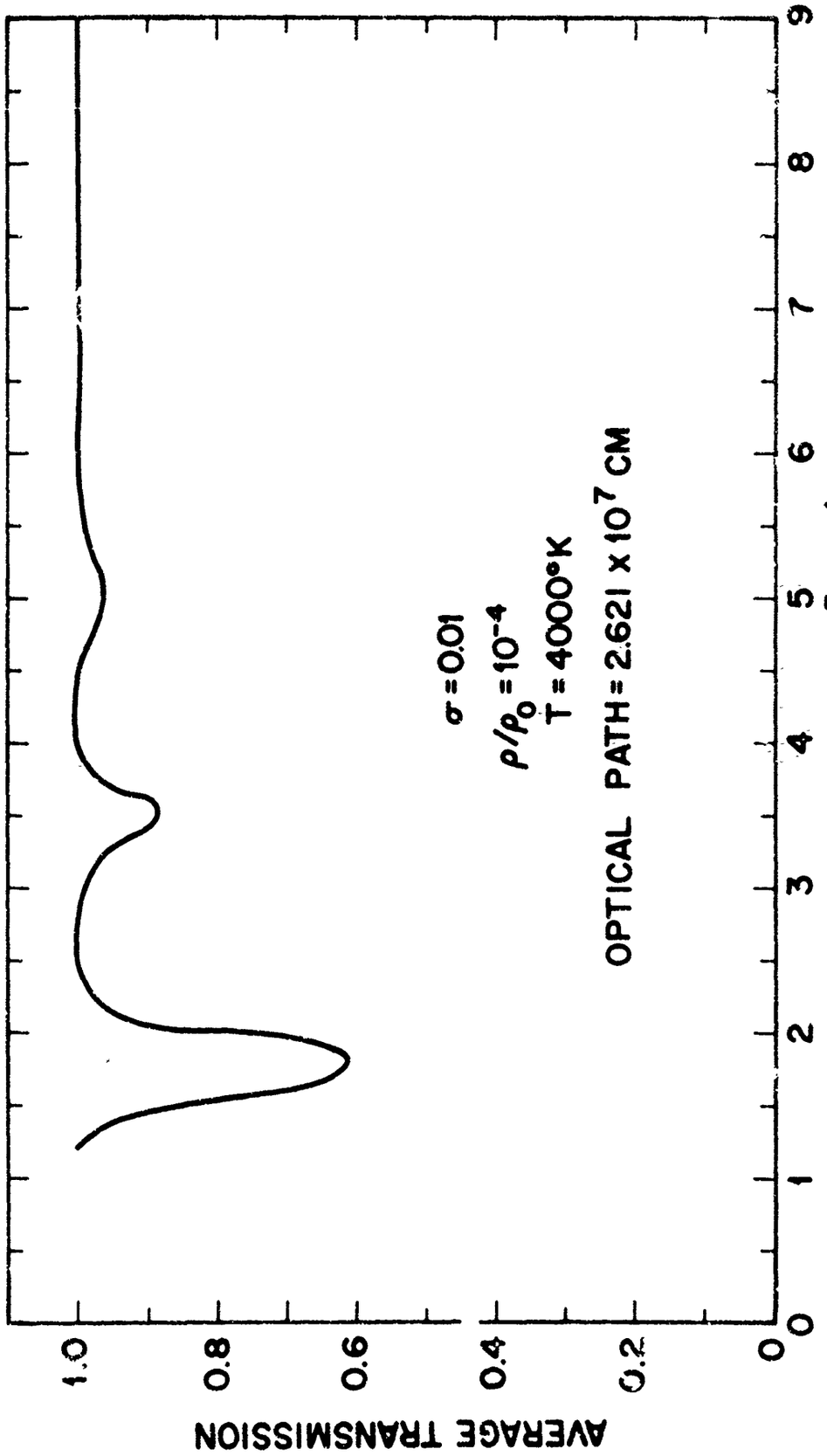

Fig. 52 Average transmission of optical radiation through a slab of heated air as a function of frequency: contribution from vibration-rotation bands of nitric oxide. The temperature and optical path length are given in the figure.